A genetic algorithm based model tree forest

Werner Van der Merwe
20076223

Thesis presented in partial fulfilment of the requirements for the degree of Master of Engineering (Industrial Engineering) in the Faculty of Engineering at Stellenbosch University

Supervisor: Prof. A.P. Engelbrecht

March 2022

Declaration

By submitting this thesis electronically, I declare that the entirety of the work contained therein is my own, original work, that I am the sole author thereof (save to the extent explicitly otherwise stated), that reproduction and publication thereof by Stellenbosch University will not infringe any third party rights and that I have not previously in its entirety or in part submitted it for obtaining any qualification.

Date: 18 November 2021

Abstract

Abstract

This thesis presents an ensemble approach that reduces the high variance error exhibited by model trees that comprise multivariate non-linear models and increases their overall robustness. The ensemble approach is conceptualised, tuned for, and evaluated against competing regression models on ten separate benchmarking datasets. The ensemble, referred to as the model tree forest (MTF), incorporates a hybrid genetic algorithm approach to construct structurally optimal polynomial expressions (GASOPE) within the leaf nodes of greedy induced model trees that form the base learners of the ensemble. Bootstrap aggregation, together with randomised splitting feature spaces during tree induction, sufficiently decorrelates the base learners within the ensemble, thereby reducing the variance error of MTF compared to that of a single model tree whilst retaining the favourable low bias error that model trees exhibit. The multivariate non-linear models that predicts the output enable MTF to produce approximations of highly non-linear data The addition of ensembling methods passively combat overfitting brought forth from the increased model complexity, compared to a previous implementation of GASOPE within a tree structure which is shown to exhibit overfitting in specific cases. MTF produced similar performance to a artificial feed-forward neural network and outperformed the M5 model tree, an ensemble of M5 model trees and support vector regression.

Opsomming

Hierdie tesis stel ’n groeperings metode voor wat die hoë variansie fout van modelbome, met hoër order uitset funksies, verminder. Die groeperings metode verhoog ook die robuustheid van die modelbome. Hierdie groepering metode word verwys na as “model tree forest”(MTF). MTF word volledig beskryf, verstel en evalueer teen ander regressie modelle op tien verskillende datastelle. MTF behels ’n genetiese algoritme wat optimale polinoom funksies binne die blaar nodes van die gierige geïnduseerede modelbome kweek. Die gebruik van “bootstrap aggregation”gesaamentlik met lukraak-bepaalde vertakkings gedurende die kweekingsproses van ’n enkele modelboom, verseker dat die varianse fout van MTF verlaag word. Terselfdetyd word die die gemiddelde afwykings fout van die modelbome, wat reeds baie laag is, laag gehou. Die polinoom funksies wat die skatting van MTF bepaal, laat toe dat die gesaamentlike model data, wat hoogs onliniêr is, goed naboots. Die polinoom funksies help ook om te keer dat die modelbome nie die datastel oorpas nie, wat andersins die geval sou wees as gevolg van die hoë kompleksiteit wat modelbome besit. MTF het gelykstaande resultate gelewer aan ’n neurale netwerk en beter resultate as die M5 model boom, groepering van M5 model bome en ondersteunende vektor regressie.

Acknowledgements

I would like to hereby acknowledge everyone who helped me throughout the past two years in writing this thesis. Professor Andries Engelbrecht, who provided me with guidance. My family and friends for their encouragement. The School for Data Science and Computational Thinking for supporting me. Without them this would not have been possible. Thank you.

Contents

List of Figures

List of Tables

Nomenclature

Variables and functions

A	intersection of two sets of term-coefficient mappings.
B	union of the exclusion between two sets of term-coefficient mappings.
c	model complexity.
c_s	ensemble pruning factor.
D	set of training instances comprising input features and target values.
$D(\cdot)$	euclidean distance between two vectors.
d	distance value.
$\boldsymbol{e}$	subset of polynomial orders.
f	given order within e.
$f_1, f_2, ..., f_i$	functions defining the output of node i.
g	given feature index from the vector of m inputs.
$g_i(\boldsymbol{x})$	predicted value of model tree i given the input vector $\boldsymbol{x}$.
G	number of generations.
h	uniformly distributed random number.
h_b	bandwidth parameter.
I	set of unique term-coefficient mappings.
i, j, k	generic counter variables/set indices.
$K_1(\cdot), K_2(\cdot)$	given kernel functions.
k_{nn}	number of nearest neighbours for evaluation.
m	number of input features.
N	set defining the children and split of a node.
n	number of instances within a given set.
n_l	number of base learners within an ensemble.
n_t	number of decision trees within an ensemble.
o	degree of the polynomial order for a given function.
P	set comprising a population of individuals.
p	maximum number of terms.

q	given instance.
R^2	fitness function of a given individual.
S	set defining the splitting feature and value.
s	split value.
s_c	specified numeric smoothing constant.
$s(\cdot)$	smoothing function.
$sd(D)$	standard deviation of the target values within set D.
T	set of unique variable-order pairs.
$Var(X, \boldsymbol{y})$	variance of a given model w.r.t the set X and target values $\boldsymbol{y}$.
$\boldsymbol{w}$	vector of weights.
w_m	real-valued polynomial coefficient of the m^{th} input feature.
X	set of instances.
$\boldsymbol{x_i}$	vector of input values of instance i.
y_i	target value of instance i.
y'_i	predicted value of instance i.
Z	set of nodes.
α	fuzzy parameter.
Δ_ϵ	expected error reduction.
ϵ	error criterion.
λ_j	whole-valued polynomial order of the input variable $x_j, j \in \{1, \ldots, m\}$.
$\mu(\cdot)$	Gaussian function.
$\rho(X)$	correlation with respect to the set X.
$\sigma^2(\boldsymbol{y})$	variance over the vector $\boldsymbol{y}$.

Acronyms and abbreviations

AG	additive groves
CART	classification and regression trees
CASP	physicochemical properties of protein tertiary structure dataset
GASOPE	genetic algorithm approach to evolve optimal polynomial expressions
GPMCC	genetic programming approach to extract symbolic rules from data sets with continuous-valued classes
GPR	Gaussian process regression
HTL	hybrid regression tree
LM	Leven-Marquardt
MAE	mean absolute error
MARS	multivariate adaptive regression spline
MSE	mean square error
MT	model tree forest base learner
MTE	Fuzzified M5 model tree ensemble
MTF	model tree forest
M5	piecewise linear model tree
M5E	bagged M5 model tree ensemble
NN	artificial feed-forward neural network
PLT	partial linear tree
ReLU	rectified linear unit
RF	random forest
RMSE	root mean square error
RMT	random model trees
SGD	stochastic gradient descent
SVR	support vector regression
UCI	University of California at Irvine

Chapter 1

Introduction

Machine learning, regarded as a subset of artificial intelligence, is quite an old research field. Many machine learning algorithms referred to in this thesis and still used to this day were first conceptualised in the late 1990s and early 2000s [5, 6, 19, 27]. Computers have since been able to produce increased computing power to allow for larger scale application of these algorithms. Furthermore, the available computing power continues to increase each year. With the increase in computing power comes the increase of interest in machine learning research and applications. More complex models can now be developed that utilise this increased computing power to better capture highly intricate patterns that are present in data. However, it is vital that the complexity of a model be finely tuned given the problem at hand, because an increase in complexity does not guarantee an increase in performance for all cases.

This chapter is outlined as follows. Section 1.1 provides further motivation for the research into model tree ensembles that comprise higher-order polynomial output function. Section 1.2 presents the research objectives of this thesis. The main contribution of this thesis is listed in Section 1.3. Finally, Section 1.4 presents the outline of this thesis.

1.1. Motivation

There are two different types of problems in machine learning that predictive models are tasked to solve, namely classification and regression problems. The former focuses on the prediction of a class label given a set of input features. The latter refers to the prediction of a target feature that takes on a numerical value from a set of input features, and is the focus of this thesis. A problem observed today is the size of data as well as the intricacy growing to a point where older predictive models, which where conceptualised long before data reached this point, may struggle to effectively predict the target feature. Moreover, the predictive models available today which are capable of modeling these non-linear relationships between input and target features within big data, such as artificial neural networks, suffer from a lack of opaqueness i.e. the models function as a black box model wherein the rules on which the model bases its prediction off of are unknown to the user. For these reasons, research on predictive models which are capable of modeling complex relationships between the input and target features within data, whilst providing transparency in its prediction, is a valuable commodity.

Aiming to address the above-mentioned problem, Engelbrecht and Potgieter conceptualised a genetic programming approach to extract symbolic rules (GPMCC) from regression problems [18].

A genetic algorithm approach to construct optimal polynomial expressions (GASOPE) was implemented during induction to evolve the output functions of GPMCC [17]. The advantages of GPMCC are the ability to adequately model the non-linear relationships between the input and target features in data, whilst the set of rules on which the model is based are visible. However, GPMCC was outperformed by a competing model tree on data with linear relationships between the input and target features [18]. GPMCC is a model tree comprising higher-order polynomial functions and therefore is likely to produce poor approximations of data with strictly linear relationships between input and target features. Furthermore, the computational cost of inducing GPMCC is large due to the genetic programming approach. Therefore, the application of GPMCC within an ensemble is not pursued and benefits of the use of GPMCC within an ensemble remain unknown. For decision trees, ensemble techniques significantly increase the robustness of the collective model [5,6]. Robustness refers to the ability of the model to produce good performance on training data as well as unseen data.

The majority of research on model tree ensembles are only focused on the M5 model tree, a model tree which utilises linear output functions to piecewise model non-linear relationships between input and output features [1,16,20]. The benefit of linear output functions are the reduced computational cost of their induction, which in turn allows for multiple model trees to be grown within an ensemble. Through the use of model trees as base learners, it was found that ensemble models were more robust than a single base learner [1,16,20]. For a complex regression model, such as GPMCC, robustness is a valuable aspect which may bring increased performance. Therefore, it is beneficial to investigate the feasibility of applying ensemble techniques to model trees comprising higher-order polynomial output functions to retain the increased accuracy whilst being robust.

This thesis utilises the increased computational power available today, to redesign the application of GASOPE within a model tree, allowing for the ensembling thereof. Through the use of an ensemble of model trees comprising higher-order output functions, the observed variance error is reduced while retaining the favourable low bias error these model trees offer. Compared to neural network, which is expected to produce similar performance, the model tree ensembles offer further benefits through its interpretability. The relationships between input and target features are available to the user to draw conclusions from.

The ensemble of model trees comprising higher-order output functions proposed in this thesis is referred to as model tree forest (MTF). For MTF to function to the best of its ability, it is essential that the architecture be optimised through the hyperparameters. Several questions arise when a decision tree is used as the base learner of an ensemble: What is the optimal size of the ensemble? How large should trees be allowed to grown? How can overfitting be prevented? Which type of data best suites the application of MTF? These questions are all answered through the empirical investigation and evaluation of model trees on a set of benchmarking datasets.

1.2. Research objectives

The main goal of this thesis is to thoroughly research, design and implement the use of a model tree comprising higher-order polynomial output function within an ensemble approach. To achieve the aforementioned goal, the following research objectives are defined:

- Provide an overview of existing decision tree and ensemble methods as well as how the ensembling of decision trees address the bias-variance tradeoff.
- Investigate the use of model trees comprising higher-order output functions in the current available literature as well as identify the ensemble methods used for model trees and the implications thereof.
- Redesign and implement the original of GASOPE with the improved computational power available today for the use within a model tree and ultimately an ensemble of model trees.
- Design and optimise the induction of computationally cost-effective model trees with higher-order polynomial output functions within an ensemble.
- Statistically test and compare the performance of MTF against other state-of-the-art regression models on a set of benchmarking problems.

1.3. Contributions

The main contributions of this thesis are:

1. A redesigned implementation of GASOPE which utilises the increased computational power now available.
2. The design and optimisation of decorrelated, bootstrap aggregated model trees that comprise higher-order polynomial output functions on a set of benchmarking problems.
3. The empirical evaluation and statistical testing of MTF against other state-of-the-art regression models on a set of benchmarking problems.
4. The finding that MTF is capable of producing competitive performance on both linear as well as non-linear problems, given that MTF is properly tuned for the problem at hand.
5. The finding that big data favours the use of deeper model trees within an ensemble, whereas small data favours the use of shallow model trees within an ensemble.
6. The finding that MTF produces similar accuracy to neural networks, outperforms support vector regression, M5 model trees as well as an M5 model tree ensemble and is outperformed only by random forest on a set of benchmarking problems.

1.4. Thesis outline

The remainder of this thesis is structured as follows:

- **Chapter 2** discusses the required information to thoroughly understand the implementation of decision trees and how predictive models address the bias-various tradeoff. Furthermore, existing implementations of model trees and model tree ensembles are discussed together with their shortcomings.

- **Chapter 3** presents the redesigned version of GASOPE and the statistical tests used to evaluate the performance of the redesigned GASOPE against other state-of-the-art regression techniques.

- **Chapter 4** discusses the entire induction algorithm of MTF and motivates the use of decorrelated model trees within a bootstrap aggregated ensemble. Thereafter, the optimisation of the hyperparameters of MTF is presented.

- **Chapter 5** presents and discusses the experimental results for MTF when compared to other state-of-the-art regression models on a set of benchmarking problems. Additionally, the statistical tests are performed on the results.

- **Chapter 6** concludes the thesis with a summary of all the findings and conclusions of each chapter. This chapter also provides avenues for possible future work.

The following appendices are provided to supplement the results summarised in the chapters:

- **Appendix A** lists the results in full of optimising each datasets for the maximum polynomial order hyperparameter.

- **Appendix B** lists the results in full of optimising each dataset for the maximum tree depth hyperparameter.

- **Appendix C** lists the results in full of optimising each dataset for the ensemble size hyperparameter.

- **Appendix D** presents alternative metrics of the results obtained by MTF as well as the competing models on each benchmarking dataset.

Chapter 2

Literature Review

This chapter presents the background of model trees and ensemble methods required to implement the model tree forest presented in the following chapters. There is no single conceptualised model tree, but many different implementations of the idea of a model tree. This is because any predictive machine learning model can be incorporated within the leaf nodes of a model tree. Model trees are a type of decision tree more commonly used for regression problems. Hence, decision trees are first discussed in this chapter. An understanding of the concept of the bias-variance tradeoff is necessary to motivate the use of decision trees in ensembles.

This chapter is structured as follows: Section 2.1 provides background of decision trees and discusses how decision trees are induced. The bias-variance tradeoff and two ensemble methods, *bagging* and *boosting*, are introduced and discussed in Section 2.2. Section 2.3 presents the differences between model tree and other decision trees as well as a general discussion on the performance of the piecewise linear model tree (M5). Two different model trees, hybrid regression tree (HTL) and a genetic program for mining continuous classes, which incorporate non-linear models at their leaf nodes are discussed in Section 2.4. Finally, two existing model tree ensembles, which incorporate M5 model trees, are introduced in Section 2.5

2.1. Decision trees

This section introduces the concept of decision trees in the context of machine learning. Section 2.1.1 discusses decision trees in the application as predictive models for classification and regression problems. Section 2.1.2 introduces the methodology of classification and regression trees (CART), conceptualised by Breiman et al. Finally, Section 2.1.3 discusses the induction process employed by CART to induce regression or classification trees.

2.1.1. Introduction to decision trees

Decision trees are tree-like predictive models used in machine learning on both classification or regression problems. Decision trees are induced on labelled datasets to model the relationship between input and output variables. The output variable represents the target value which the decision tree is tasked with predicting. Classification and regression applications of decision trees are characterised by their output variable type:

- classification trees are used to predict a categorical output, while

- regression trees predict a numerical output.

Categorical features are qualitative because they take on labelled values and numerical features are quantitative because they take on real values.

Decision trees were inspired by the *divide-and-conquer* paradigm, which entails recursively breaking an intricate problem down into smaller sub-problems which each can be solved more simply. A decision tree organises data recursively through a hierarchical representation of tests on input variables, giving the predictive model the appearance of a tree data structure. Each decision tree houses a series of tests in the nodes of the tree structure. Through each test data is divided through branch-like splits which represent the different outcomes of a test. Alternatively, decision trees are expressed as a collection of if-else statements to model decision boundaries in data.

Before the conception of decision trees, statistical techniques used for classification problems were developed with small datasets in mind [4]. Furthermore, the variables were all of the same type and the data was often assumed to be homogeneous, i.e. the same relationships between these variables held throughout the entirety of the decision space. For that reason, simple models that focused only on a few parameters to model the influence of a wide range of factors, made up the majority of conceptualised models at the time [4]. The application of these simple models to larger datasets, with the assumption that the data retains its homogeneous structure, is flawed.

Datasets are not only subject to being large, but complex as well. The complexity of data is influenced by the following: missing values, noise, outliers, high dimensionality, mixtures of data types, non-parametric distribution and non-homogeneity. Non-parametric distributed data refers to data which does not fit a known distribution. Non-homogeneous data refers to data where different relationships hold between variables within different parts of the decision space. *The curse of dimensionality* states the more features present, the higher the variance of the data points are. Hence, the data is sparser and more spread out. The dimensionality of data can be reduced. However the accompanying drawbacks are unfavourable. The drawbacks include the loss of data and a reduction in the ability to distinguish the influence of individual features. Most importantly, interpretability of data is significantly reduced with dimension reduction.

There was a need for a method in which the most important features of the data are accentuated, the background noise disregarded and the conclusions interpretable to the analyst [4], which brought rise to the conceptualisation of the decision tree. The defining characteristic of decision trees is its ability to not only produce satisfactory results but to also give the user thoughtful information and insight into the data. For example, for classification problems, a decision tree helps to uncover the predictive nature of a problem by helping the user to better understand how specific features contribute to the outcome that is being observed [4].

2.1.2. The CART algorithm

One of the earliest documented work on the theory of decision tree induction was published in 1984 [4];. Breiman et al. was inspired by the deficiencies of existing tree-structured classifiers at the time to develop an improved algorithm which provided a more flexible and accurate solution. Breiman et al. named the proposed decision tree induction algorithm as CART. CART induces a tree through a series of binary questions, which when answered sequentially, produces a solution to the problem at hand.

A simplistic classification tree is portrayed in Figure 2.1, capable of classifying an individual's gender based on two input features, namely weight and height. Nodes X_1 and X_3 each represents a test. Tests, also referred to as splits, comprise two parts: a feature on which the test is performed and a value indicating the decision boundary. Node X_1 is referred to as a *root* node because it is the starting node of the decision tree. Nodes X_2, X_4 and X_5 contain a label of the output class. A class label represents the majority class for the instances associated with the leaf node. These nodes are referred to as *leaf* nodes. Leaf nodes terminate all possible *paths* (sequences of nodes) that can be followed in the tree from the root node to any leaf node. *Neighbouring* leaf nodes refer to the adjacent leaf nodes at the end of every path, such as nodes X_2 and X_4 as well as nodes X_4 and X_5.

Each node of the decision tree encapsulates a subset of the dataset. The instances that make up the data subset of a node are characterised by the tests that lead up to the node. When combined, the data subsets that each leaf node of the decision tree denotes covers the entirety of the complete dataset. The *size* of a decision tree refers to the number of nodes it consists of. Finally, *depth* is the number of nodes in the longest path the tree contains. A decision tree is regarded as being *shallow* if its depth is small.

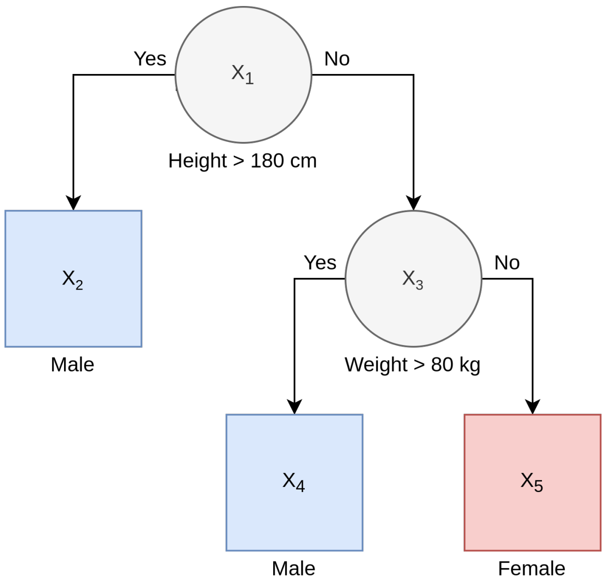

Figure 2.1: A hypothetical two-class tree-structured classifier.

2.1.3. CART's induction algorithm

CART induces a decision tree for classification, such as shown in Figure 2.1, from a set of labelled instances through three fundamental steps:

1. Determining the tests.

2. Evaluating stopping rules.
3. Assigning class labels to each leaf node.

Starting at the root node, step 1 is repeated for each subsequent node until step 2 is satisfied for each path in the decision tree. To construct a decision tree, each split is chosen to minimise the mixture of classes in the descendant nodes' subsets. A splitting function determines the feature as well as the value of a split; multiple splits are compared for a node by the splitting function. A metric often used to express the result of the splitting function is impurity. The larger the impurity the more heterogeneous the data subset is with respect to class distribution. CART produce a binary splits from the value of a single input feature only, i.e. a single split cannot house multiple rules or features. For that reason splits are always parallel to the decision space axes. CART allows input features to be both discrete and/or continuous.

At any node, the tree induction algorithm evaluates a total of $n_f \times n_i$ candidate splits, where n_f is the number of features and n_i the number of instances in the dataset. A split is evaluated on every feature and the corresponding feature value for each instance in the dataset. The best performing split is selected as the one split which minimises the impurity function. Therefore, the best performing split also maximises the reduction in heterogeneity.

Once a node is reached where no significant decrease in impurity is produced, the node is declared a leaf node. This is one example of a stopping rule, another is fixing the maximum depth of a decision tree. The class making up the majority of each leaf is assigned as the label of the leaf. The decision tree growing sequence, i.e. the induction algorithm, is thus completed.

In the application of CART's induction algorithm to regression problems, little changes. The induction algorithm proceeds to partition the dataset into subsets via a series of tests on the input features. However, a different form of impurity metric is incorporated. The expected reduction in either variance or absolute deviation of the instances that make up the data subset for each candidate split is calculated. Thereafter, the splitting function of regression trees maximises the reduction in either variance or absolute deviation. A change is also present in the leaf nodes; instead of predicting the class label of an instance, the decision tree now predicts a numerical value associated with a target feature. Recall a classification tree predicts a categorical value to define a target feature. The constant output value of a leaf node is calculated as the mean squared error of the numerical target values for all instances in the subset of data denoted by the path to the leaf node.

Fundamentally, the numerical variable predicted by the regression tree is a dependent variable based on a multitude of independent variables. The independent variables represent the input features and the dependent variable the target feature. The numerical values which represent the output in a regression tree are constant per leaf node. Subsequently, the regression tree models the relationship between the input and output variables through discrete piecewise approximation. Figure 2.2 illustrates the predicted constant values of a regression tree, induced on the values of $y = sin(x)$ for $x \in [0, 2\pi]$, with the target feature y being dependent on the input feature x.

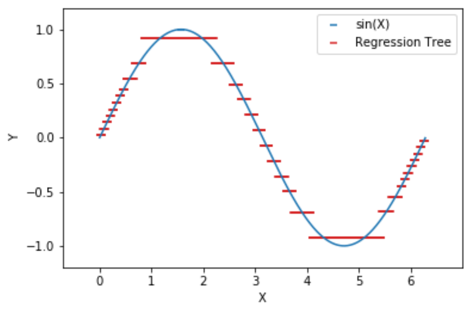

Figure 2.2: A regression tree's piecewise discrete approximation (red) of a continuous sinusoidal function (blue).

The advantages of the CART induction algorithm compared to other statistical models at the time of its conception include [4]:

1. The induction algorithm handles both categorical and/or numerical input as well as output data. A decision tree can thus be induced from a dataset containing mixed feature types.
2. Once induced, the application of a decision tree on new incoming data is computationally efficient and interpretable.
3. Decision trees exploit the conditional relationships between variables present in non-homogeneous data to better model the instances.
4. The most beneficial information required to interpret the relationships between input and output features are incorporated at split. Hence, automatic dimensionality reduction is effectively performed on the dataset.
5. CART showed to be quite robust when subjected to outliers and missclassified instance which are considered noise.

2.2. The bias-variance tradeoff

This section introduces the dilemma of the bias-variance tradeoff which is present in all predictive machine learning models. This section also introduces ensemble learning and aims to discuss how ensemble learning can be an effective way to mitigate the problems associated with the bias-variance tradeoff. Section 2.2.1 starts by discussing the bias-variance tradeoff and how it explains the tendency of a model to overfit or underfit. Next, Section 2.2.2 describes how the bias-variance tradeoff is specifically present in decision trees. Finally, Sections 2.2.3 and 2.2.4 introduces two popular ensemble methods and discusses how each addresses the bias-variance tradeoff.

2.2.1. Overfitting and underfitting

The tendency to overfit or underfit given data stems from the degree of inaccuracy present in machine learning models and is explained through the bias-variance dilemma. The bias-variance dilemma is a result of the problem to balance model complexity with the desire to have accurate models. Both bias and variance are degrees of prediction error present in the model, negatively affecting its prediction accuracy. Ideally, a machine learning model should exhibit perfect prediction accuracy, but perfect prediction accuracy is infeasible because models are exposed to unseen and often noisy data during testing. Therefore, during training, the focus is on minimising the prediction error, rather than trying to remove it altogether. To better explain how to mitigate the prediction error, the two components (bias and variance) must be examined.

Bias error is defined as the average difference in prediction a model makes from each target value. Variance error is defined as the amount of variability or spread a model is subject to when predicting the output of a given instance. Figure 2.3 illustrates the predicted output of three models as follows: the first model exhibits a high variance error, the second a high bias error and finally, the third has a balance of low bias as well as low variance error. Each model is trained on the same set of instances, shown in blue.

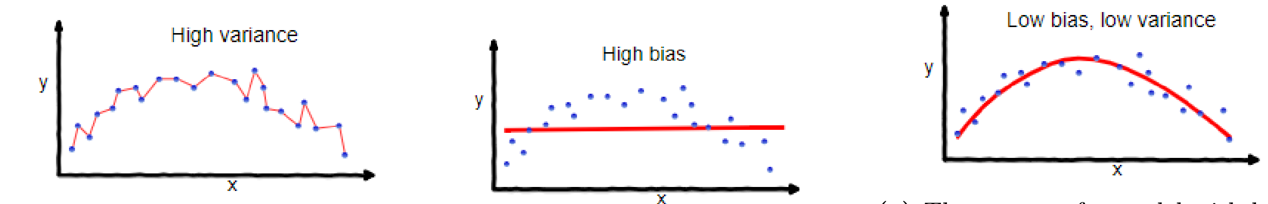

(a) An overly complex model's output.
(b) An overly simple model's output
(c) The output of a model with balanced complexity to the problem at hand.

Figure 2.3: Three separate models' predicted output (red) and target output (blue) of a simple regression problem with a one-dimensional input. Reproduced from [22].

Models that are simple in their composition, such as the model in Figure 2.3b, are incapable of capturing any intricate patterns in the training data. These models are referred to as simple models because the complexity of the output functions used to make predictions are low. Simple models do not have the discriminative ability to fit non-linear relationships within data. These models produce an oversimplified interpretation of the data. Testing overly simple models on unseen data results in a high bias error [14]. A model with high bias error *underfits* the training data, i.e. it cannot capture the complex relationships between the input space and target space within the data. Hence, a model that underfits will produce poor prediction accuracy on both training and unseen data.

In contrast, models that incorporate complex algorithms for output functions are more vulnerable to noise in the training data. During training, the overly complex output function causes the model to learn relationships within data that are a product of noise and not true to the nature of the data. Subsequently, a large variance error is present and the model *overfits* the training data, shown through the jagged output of in Figure 2.3a . Although the training of complex models may be low, such as the model in Figure 2.3a, the model performs poorly in terms of generalisation error [11]. An overly complex model fallaciously fits noisy patterns in the training data that are not associated with the desired output for all cases [14]. Although in the training data noise is actually associated with the target, the exact same associations do not always carry over to unseen data. Hence, poor generalisation accuracy is obtained, similar to models with large bias error. However, the training accuracy is speciously low.

Thus producing favourable prediction accuracy requires both bias and variance errors to be minimised. However, it is important to note that a model cannot simultaneously be less complex and more complex. Therefore, bias and variance, being respectively proportional to the complexity of a model, are error functions increasing in opposite directions. This tradeoff between bias and variance is portrayed in Figure 2.4. Models are designed with the strategy of minimising both components of the tradeoff simultaneously, thereby finding the point of optimal balance between the two errors.

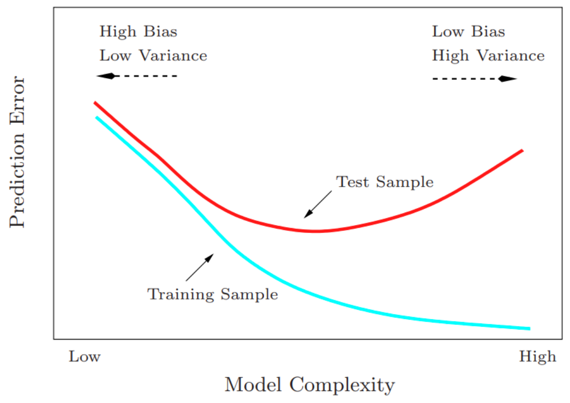

Figure 2.4: The change in a model's prediction error on the training set (red) and generalisation set (blue) as the complexity of the model is varied. Reproduced from [12].

2.2.2. How decision trees address the bias-variance tradeoff

Decision trees are classified as supervised learning models, because they are trained to map multiple input variables to an observed output variable. Unsupervised learning models are instead tasked with identifying patterns in unlabelled data to, for example, group the given data instances into homogeneous regions. In the case of a supervised learning model, the criteria used to assess prediction accuracy is both the training and test set errors. The ability of the model to generalise to unseen data is the most important of the two criteria [11].

When Breiman et al. started his initial work on decision trees, it was clear that arguably the biggest shortcoming was a product of the high variance present in decision trees [4]. Decision trees would often deliver satisfactory results on training sets, but generalised poorly on test sets. During induction, classification trees continuously optimise the classification boundaries by adding additional decision nodes. Hence, decision trees are prone to capturing noise in the training set the deeper the decision tree grows. This meant that trees were prone to overfitting and require something to remedy this.

The answer Breiman et al. put forth was a fundamental shift in focus. Instead of adjusting the stopping criterion to combat overfitting, the tree was induced with more lenient stopping rules and once fully grown, selectively *pruned*. Decision trees are not capped at a specific depth to ensure a thoroughly deep decision tree was induced. Classification trees are induced to comprise only homogeneous leaf nodes, i.e. all of the instances that a leaf node encapsulates is of the same class. Thereafter, pruning works as follows: starting at the leaf nodes and following the paths upwards into the tree, nodes are evaluated through cross-validation and the subtree below removed if warranted. Each node along the path is temporarily pruned to a leaf node and this temporary pruned decision tree's performance on unseen data is compared to that of the original unpruned decision tree. If the tree's prediction error is found to have decreased, the node remains pruned. Otherwise, the tree is reverted to its state before the node was pruned. Pruning showed to lower the variance in classification trees and significantly improve its performance with respect to generalisation [4]. Furthermore, less complex node sets are extracted from the data at hand.

As for regression trees, the tradeoff is more intricate. Because the induction step implements a stopping criterion based on the deviation over all target values within a node, regression trees are prone to overfitting. The stopping criterion is reached when the deviation of the target values is below a threshold. As a result, the tendency of a regression tree to overfit data is determined by the value of the threshold, i.e. the lower the value, the more likely it is that the regression tree is induced to overfit the data. However, the constant output value at a leaf node can be argued to underfit the subset of data denoted by the path to the leaf node. Figure 2.2 shows how poorly constant values fit the shape of a sinusoidal wave. This underfitting is only applicable to the subset of data though. If the regression tree is evaluated as a whole, a high variance error remains observed. Therefore regression trees are pruned similarly to classification trees to reduce the variance error.

2.2.3. Decision trees within an ensemble

An alternative method to pruning with the intent of minimising the variance of decision trees is the use of ensemble learning. The premise of ensemble learning is to develop multiple models in unison, which together produces a better result than the result an individual model is capable of producing.

One of the simplest decision tree ensemble methods is bootstrap aggregation, referred to as *bagging* [5]. Bagging is when several decision trees are induced in parallel, each on a subset of the training data. A subset is generated through random sampling of the dataset with replacement. Subsets of instances are always chosen from the entire dataset and the act of choosing an instance does not remove it from the dataset. For regression applied bagging, the final prediction of the ensemble is derived through averaging the predictions of each tree within the ensemble. In the case of classification, the majority vote is taken instead of the average predicted value. Note that this is simply the specific strategy bagging employs to predict the output.

The randomness in the data subsets on which the decision trees are induced contributes to minimising the variance of the collective model. The induced splits within decision trees are highly sensitive to changes in data because of the greedy induction algorithm, especially in the case of noisy data. A greedy algorithm is a heuristic approach that makes choices resulting in local optima, with the intentions of reaching an global optimum. As a result, the induction of decision trees on random subsets produces dissimilar decision trees. The total variation in the prediction a bagged ensemble produces for a given set of instances is decomposed into two terms and expressed as [14]

$$Var(X, \boldsymbol{y}) = \rho(X)\sigma^2(\boldsymbol{y}) + \frac{(1 - \rho(X))\sigma^2(\boldsymbol{y})}{n_l} \tag{2.1}$$

where ρ is the sampling correlation between the prediction of any two decision trees in the ensemble, σ^2 is the sampling variance over the target values of any single, randomly drawn, decision tree. n_l is the number of learners, in this case decision trees, in the ensemble. Finally, X represents a set of instances and $\boldsymbol{y}$ a vector of target values. The set of instances is assumed to be a set of independent and identically distributed random variables. Due to the sensitivity of splits and the injection of randomness in the tree induction algorithm, decision trees within the ensemble are divergent from one another, i.e. $\rho(X) < 1$. The more random effects are introduced, the more ρ tends to 0. Thereby, Equation 2.1 is reduced to only $\frac{\sigma^2(\boldsymbol{y})}{n_l}$. It is evident that as the number of decision trees in the ensemble is increased, the total variance decreases further. The variance of the ensemble is thus strictly less than the variance of an individual tree. Furthermore, combining randomised models does not affect the bias error [12]. Therefore, decision trees are ideal for bagging because they exhibit a very low bias individually. Bagged decision trees produce a model that is both low in bias and variance, improving its accuracy with respects to both training and generalisation significantly over that of a single tree.

Building on the success achieved by bagging, Breiman conceptualised the *random forest* method as an extension over bagging [6]. In a random forest, each tree is once again trained on a randomly selected subset of the data. The difference random forest incorporates is a change to the induction algorithm of the individual trees that make up the ensemble to strengthen random effects. A subset of input features is randomly selected at each node of the tree to determine the best split for that node. Hence, the splitting function only evaluates splits on the randomly selected features. The decision trees within the ensemble are further decorrelated as a result, decreasing the collective model's variance. Random forest has the benefit of performing well on higher dimensionality data, due to the dimension reduction-like induction algorithm [6]. Note that individual trees are left unpruned in a random forest. Therefore, each decision tree within the ensemble is *fully grown*, retaining the low bias of decision trees. Random forests were shown to outperform many competing classifiers whilst being robust to overfitting [6].

2.2.4. An alternative ensemble strategy for decision trees

In contrast to bagging is the *boosting* method. Boosting is fundamentally different from bagging; boosting employs a sequential learning strategy as opposed to the parallel induction of bagging. The models which make up a boosted ensemble are developed with a higher bias than variance in mind and are referred to as weak learners. A weak learner is only slightly better at predicting a target value than a random guess [12]. In the context of decision trees, an example strategy of inducing a high bias decision tree is a inducing a shallow tree, such as a decision stump that comprises a single split. Weak learners are incapable of individually modelling complex observed relationships. However, as a collective model, weak learners form a strong learner capable of adequately modelling more complicated patterns in data.

Boosting sequentially induces a weak learner on repeatedly modified versions of the data. Data is modified through weights that are assigned to each training instance. Weights represent the probability of an instance being chosen as part of a subset on which a weak learner is induced [15]. After each additional weak learner is added to the ensemble, larger weights are assigned to the instances which have the highest contribution to the prediction error. Each successive weak learner thereby prioritises improving the prediction error of the larger weighted instances. Through this sequential optimisation, the bias error of the collective model is reduced compared to that of a single weak learner. Once induction of the entire ensemble is complete, weights are assigned to the outputs of each weak learner based on their prediction error.

Bagging and boosting have fundamentally different approaches to addressing the bias-variance tradeoff. To conclude, boosting reduces bias with an already low variance whilst bagging reduces variance with an already low bias.

2.3. Model trees

This section discusses how model trees are an extension of regression trees conceptualised to produce increased performance on regression problems. The section is outlined as follows. Section 2.3.1 elaborates on the need that brought rise to the conceptualisation of model trees. The induction algorithm of the M5 model tree is described in Section 2.3.2. Section 2.3.3 discusses the first published performance results of the M5 model tree. The linear models which the M5' model tree incorporates is described in Section 2.3.4. Finally, Section 2.3.5 discusses the drawbacks associated with model trees that incorporate strictly linear models.

2.3.1. The limited capability of regression trees

The early work of Breiman et al. that improved the robustness of decision trees showed great success concerning the application of decision trees to classification problems [4]. However, the focus Breiman subsequently put on classification trees [5, 6] meant that regression applications of decision trees still left much to be desired. A big drawback of regression trees remained the discontinuous output it produced through the discrete approximation of the mapping between inputs and outputs of a regression problem, as illustrated in Figure 2.2. This meant that regression trees, developed through the CART algorithm, had limited capability of adequately predicting the target value for continuous target features.

Before the conception of model trees, problems where the predicted value took on a continuous numeric value favoured the use of learning techniques capable of producing continuous numerical predictions. Linear regression or neural networks are two example models capable of producing a continuous numerical output. However, no technique comes without its drawbacks and both linear regression and neural networks are no exception to this. Linear regression has limited capability because it imposes a linear relationship on data, whilst neural networks do not provide the user with an insight into the relationship of the data, due to its problem of opacity [27].

There was still a need for a learning model capable of performing non-linear regression and providing its user with insights into the relationship among descriptive features that results in specific predictions. M5 model trees were first developed by Quinlan in 1992 as an extension over the regression trees of Breiman et al. with the fundamental difference that the M5 model tree incorporated leaf nodes that are not limited to having a constant prediction value [19]. Model tree leaves can incorporate any multivariate model to better capture the patterns present in the training data. These multivariate models are used to predict a continuous target feature.

Figure 2.5 illustrates how a model tree, that comprises linear output models, approximates the continuous sinusoidal function $y = sin(x)$ for $x \in [0, 2\pi]$, as opposed to the regression tree in Figure 2.2. The use of linear models instead of constant values at the leaves allows a model tree to predict a numeric target value without producing discontinuities and thus better approximate the non-linear function. The linear models also allow profiling of the regression problem, i.e. describing the conditions on the input features that will result in a specific linear trend.

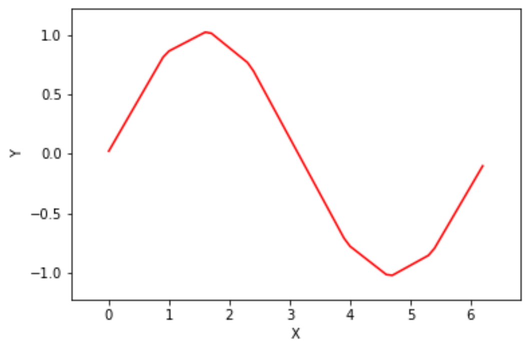

Figure 2.5: The continuous piecewise linear approximation of a sinusoidal wave using a model tree.

2.3.2. M5 model tree induction

The induction of an M5 model tree is quite similar to that of CART, with M5 model tree induction also employing a greedy approach. The first difference between the two methodologies is the splitting criterion used to evaluate a proposed split. Instead of selecting the split that maximises the reduction in variance or absolute deviation, the M5 induction algorithm selects the split which maximises an expected error reduction at a node, defined by [19]

$$\Delta_\epsilon = sd(D) - \sum_i \frac{|D_i|}{|D|} \times sd(D_i) \tag{2.2}$$

where D represents the set of training instances for the data in the node, and $sd(D)$ is the standard deviation of the target values in D. Every potential split is evaluated based on the subset of instances the split produces. D_i denotes the subset of instances that belong to outcome

i of a split and $sd(D_i)$ denotes the standard deviation of the target values in D_i. Therefore, the M5 induction algorithm chooses splits that are locally optimal for each node, similar to the induction of regression trees. After the model tree is induced, linear models are constructed for each node. The reason why linear models are constructed for non-leaf in addition to leaf nodes is to accommodate for *pruning*. The linear model of the parent node is required to calculate the alternate performance of the tree if that leaf node were to be pruned away.

A multivariate linear regression model, at any given node, is constructed with only the instances characterised within the splits of that node and its subtree nodes. Once the linear model is constructed, each parameter of the linear model is evaluated for simplification of the linear model. If the exclusion of a variable minimises the error of the linear model, it is removed. This means that all of the variables of a linear model can be removed, leaving only a constant behind. The process of variable reduction within a multivariate linear regression model is referred to as the simplification step.

Once a simplified linear model is constructed for each node, the tree is pruned by examining all non-leaf nodes as if they were leaf nodes, starting at the bottom of the tree. If the error of the final model is reduced by regarding the specified node as a leaf node, the subtree, of that node, is withdrawn from the model and the specified node pruned to a leaf node. The pruning step together with the simplification of the linear models at the nodes of the model tree helps to reduce the complexity of the final model, subsequently reducing its variance.

Smoothing is applied when the model is tasked with predicting a test instance. Discontinuities are prevented from forming between the linear models of adjacent leaf nodes. Smoothing adjusts the predicted values of the model tree as follows: starting at the leaf node, the predicted value is passed on along the path to the root node. At each node the predicted value is adjusted such that it better resembles each predicted value produced by the linear model of the next node on the path. The formula used to recursively adjust the predicted value, y'_i, at the i^{th} node along the path from the leaf node to the root is

$$s(y'_i) = \frac{ny'_{i-1} + s_c y'_i}{n + s_c} \tag{2.3}$$

where n is the number of training instances at the previous node along the path, y'_{i-1} is the adjusted prediction from the previous node, y'_i is the predicted value of node i, and s_c is the specified numeric smoothing constant. The i^{th} value of $s(\cdot)$, produced by the root node at the end of the path, is the predicted value of the model tree given a test instance.

2.3.3. Early M5 model tree performance

Quinlan compared the M5 model tree to MARS (multivariate adaptive regression spline), a popular regression model that is effective at modeling non-linear data, after the conception of the M5 model tree [19]. MARS is similar to M5 in that MARS is also non-parametric and utilises piecewise linear approximation. A non-parametric model has no preconceived notion regarding the number of parameters it is tasked with learning nor the distribution that the data follows. M5 and MARS produced similar accuracy results, but what set M5 apart from MARS was the computational requirement. The computational requirements of MARS grew aggressively with an increase in dimensionality, severely limiting its applicability. M5 was able to handle tasks with up to hundreds of input features, whereas MARS struggled past no more than twenty [19]. The results Quinlan published provided evidence that model trees are a viable choice for solving regression problems. Model trees also compare better to alternative regression techniques as opposed to regression trees which struggle to compete against linear regression models or neural networks.

2.3.4. The M5' model tree

Quinlan's work on the M5 model tree was not readily available and some design decisions, such as how missing values are handled, were not addressed. This prompted Wang and Witten to refine the induction steps to create the M5' model tree [27]. One important aspect of the M5' model tree is that it specifies the linear model implemented in a node. The linear model, named the $(m+1)$-parameter model, is denoted by [27]

$$w_0 + w_1x_1 + w_2x_2 + ... + w_mx_m \tag{2.4}$$

with x_m representing the m^{th} input feature, w_m the respective weight of that input feature in the linear model, and w_0 the bias term. Fundamentally, Equation (2.4) is a linear polynomial with weights that represents its coefficients. Through experimentation Wang and Witten deemed the simplification step of M5 compromising to the size of the model tree. Wang and Witten found that occasionally much smaller trees were obtained when all features were left in the linear models. Therefore the simplification step was omitted from the induction algorithm. The M5' model tree was shown to perform better than the original M5 tree on the standard datasets for which results where available [27]. For the remainder of this thesis, the M5' model tree is simply referred to as the M5 model tree.

2.3.5. Shortcomings of model trees comprising linear models

The M5 model has been shown to perform inadequately in comparison to other regression techniques on datasets that contain noisy patterns and highly non-linear relationships between its input and target features [1]. The susceptibility of the M5 model tree to initially overfit noisy data can be attributed to the already high variance produced by decision tree models, together with the increased complexity of a model tree compared to a regression tree. To combat this, the model tree is pruned after induction. However, excessively post-pruning a decision tree, with the intent of increasing its resilience to overfitting noisy patterns, limits the complexity of the model and in turn its ability to capture highly non-linear patterns. Post-pruning refers to pruning of the decision tree after it has been grown to overfit on the data, as opposed to stopping the growth of the tree prematurely to effectively prune it. Within the tree multiple leaf nodes, each with linear models, are pruned away and consequently the collection of linear models in the subtree are simplified into one. The remaining linear model is likely to underfit the data. This is referred to as over-pruning and has been shown to have negative affects on the performance of a model tree [1].

A study published in 2016 hypothesised that the reason for the inferior results produced by the M5 model tree on highly non-linear data is due to the limited capability piecewise linear functions have when trying to fit the training data [13]. Six quantitative water quality parameters were used in predicting the monthly chemical oxygen demand of a river. The relationship between these parameters is highly non-linear. A MARS model was able to achieve, on average, an accuracy of 19.1% better than the competing M5 model tree. It is important to note that Quinlan designed the M5 model tree with large datasets in mind, making it the preferred choice for problems with a large number of input parameters [19].

Quinlan recommended that the application of non-linear models at the leaf nodes of the M5 model tree be researched in order to improve the ability of the model tree to adequately capture highly non-linear patterns present in complex datasets [19]. Non-linear models for output functions would also allow for a model tree to be grown smaller, as a single non-linear model can approximate the same function which requires multiple linear models to approximate. The number of times the training data requires splitting is reduced, producing a smaller tree. Therefore, a decreased variance error is observed making the model tree less sensitive to noise and less prone to overfitting.

Careful consideration should be given to the increase in computational cost that comes with the implementation of non-linear models. A model has to justify its increased computation time with a clear and substantial improvement in its accuracy or even interpretability. Ockham's razor expresses the fallacy in expecting that the increase in complexity of a model will guarantee an improvement in its performance [3]. More often than not, a simpler approach is the favoured solution to a problem. These factors are hypothesised as contributing to the lack of abundant research on model trees that incorporate non-linear models.

2.4. Non-linear solutions

This section discusses two existing model tree approaches that incorporate non-linear models within their leaf nodes. Section 2.4.1 discusses how the non-linear model, present in partial linear trees (PLT), is broken down and the performance thereof examined. Next, Section 2.4.2 discusses a model tree which is induced via a genetic programming approach.

2.4.1. Kernel regression

Torgo developed the hybrid regression tree that, amongst other proposed models, incorporated kernel regression at its leaf nodes [26]. A kernel function empowers a linear model to interpret the relationships between the instances as non-linear by mapping the instances to a higher-dimensional feature space. Feature space refers to the m dimensions through which the data is defined, excluding the target feature. The kernel regression that HTL incorporates is known as a lazy learner. Lazy learners only generalizes the training data once a prediction must be made and never before. For this reason, lazy learners are also a popular choice for models where the training data is regularly updated.

The HTL structure is induced using the CART algorithm of selecting splits that minimizes the mean square error (MSE)

$$MSE = \frac{1}{n}\sum_{i=1}^{n}(y_i - y_i')^2 \tag{2.5}$$

where n is the number of instances over which the MSE is computed, y_i is the actual target value of the i^{th} instance, and y_i' is the predicted value for the instance. The predicted value for each instance is chosen as the average target value in the subtree where the split is proposed. Effectively, the deviation is being calculated; Equation (2.5) is showcased this way to emphasise the potential of interchanging y_i with the kernel regression prediction. Torgo states that using the calculations of kernel regression to determine the MSE for each proposed split within the tree structure is computationally too expensive and therefore opts to use the CART algorithm to induce the tree structure instead [26]. After the splits have been determined, a kernel regression model within the leaf node is thereafter employed to calculate y_i' when making predictions. The use of kernel functions gives rise to the hybrid nature of HTL.

The kernel regression model comprises a nearest neighbours model and a Gaussian kernel function. The kernel regression model calculates predictions using only the training instances most similar to a given query. The similarity is based on a distance metric between two instances. The Gaussian kernel function increases the influence (based on the distance metric) neighbours have on the prediction the nearer they are to the instance in the feature space. Given the instance $\boldsymbol{q}$, the prediction is calculated using the following function [26]:

$$y'(\boldsymbol{q}) = \frac{1}{K_1(\boldsymbol{q})}\sum_{i=1}^{k_{nn}} y_i \times K_2\left(\frac{D(\boldsymbol{x_i}, \boldsymbol{q})}{h_b}\right) \tag{2.6}$$

with

$$K_1(\boldsymbol{q}) = \sum_{i=1}^{k_{nn}} K\left(\frac{D(\boldsymbol{x_i}, \boldsymbol{q})}{h_b}\right) \tag{2.7}$$

and

$$K_2(d) = e^{-d^2} \tag{2.8}$$

where $D(\cdot)$ is a distance function between two vectors, h_b is the bandwidth parameter, and $\boldsymbol{x}_i$ is a vector of input features with target value y_i for the i^{th} training instance. The number of nearest neighbours is indicated by k_{nn}. Only the training instances that fall into the same leaf node as $\boldsymbol{q}$ are evaluated as a potential nearest neighbours.

HTL is computationally more expensive than other tree models, because the nearest neighbours have to be re-evaluated for each query. Equation (2.6) portrays how the computational complexity grows as the value of k increases due to the added terms in both the kernel function and the encapsulated distance function. For experimentation, Torgo chose $k_{nn} = 3$ without specifying the reasoning behind that choice [26].

The performance of HTL was evaluated on eleven different benchmarking datasets. Torgo concluded that, compared to linear models, the use of kernel regression models at the HTL leaf nodes resulted in significantly better performance for most cases and never significantly worse. One dataset was considered an exception which Torgo claimed is biased towards linear models. Although Torgo mentioned the M5 model tree incorporating similar linear models to the linear HTL variant, Torgo did not compare the performance of HTL directly to that of M5 [26].

HTL was further improved on by imposing the kernel regression model, described by Equation (2.6), on the linear model in Equation (2.4) [24]. The resulting model now incorporates the weight vector of Equation (2.4), $\boldsymbol{w}$, and is described by the equation

$$y'(\boldsymbol{q}) = \boldsymbol{w}\boldsymbol{q} - \frac{1}{K_2}\sum_{i}^{k_{nn}} \epsilon_i \times K_1\left(\frac{D(\boldsymbol{x_i}, \boldsymbol{q})}{h}\right) \tag{2.9}$$

where e_i is the error of the linear model calculated as $\epsilon_i = \boldsymbol{w}\boldsymbol{x_i} - y_i$. The vector $\boldsymbol{w}$ is a set of weights that represent the coefficients of a linear polynomial, equivalently expressed in Equation (2.4). For a set of n training instances $\{(\boldsymbol{x_1}, y_1), \ldots, (\boldsymbol{x_n}, y_n)\}$, the weights of $\boldsymbol{w}$ are calculated by minimising a least squares error criterion:

$$\epsilon = \sum_{i=1}^{n} (y_i - \boldsymbol{w}\boldsymbol{x_i})^2 \tag{2.10}$$

This adaption of HTL was referred to as the partial linear tree (PLT) [24]. PLT was designed with the goal of maintaining the accuracy of linear models while improving its comprehensibility of non-linear patterns [24]. PLT was compared to MARS as well as a commercial version of M5 on 12 separate benchmarking datasets.. The commercial version of M5, namely Cubist, also incorporates linear models. PLT produced highly competitive results, though Torgo described the use of PLT as being computationally heavy for the same reasons HTL is considered computationally expensive [24].

Torgo recommended further research be done on the use of an alternative splitting criterion when inducing the tree structure. PLT did not change the procedure that HTL follows, which is the same as the standard CART algorithm of selecting splits that minimise deviation over the target value of the training instances. A criterion which incorporates the models used at the leaf nodes, such as the one used in M5, can improve the fit of the models in leaf nodes to be more accurate. However, this also increases the computation time and therefore demands careful consideration.

2.4.2. Higher-order polynomial regression

Another approach to modelling non-linear data is through the use of higher-order polynomial expressions, rather than piecewise linear polynomials. However, the estimation of the structure of a multivariate polynomial as well as its parameters is a time consuming task. A multivariate polynomial function incorporating all possible terms is expressed as [17]:

$$f(\boldsymbol{x}) = \sum_{\tau=0,\Sigma_{j=1}^{m}\lambda_j=\tau}^{o} \left(w_{(\lambda_1,\lambda_2,\ldots,\lambda_m)} \prod_{i=1}^{m} x_i^{\lambda_i} \right) \tag{2.11}$$

where m is the number of input features, o is the degree of the polynomial order and $w_{(\lambda_1,\lambda_2,\ldots,\lambda_m)}$ the polynomial coefficients, i.e. the weights when used as a regression model. For a third order polynomial describing a ten-dimensional feature space, there are 286 terms in total. Terms, also referred to as monomials, can also be excluded to change the characteristics of the polynomial function. Subsequently, there are 2^{286} different possible combinations of monomials for a third order, ten-dimensional polynomial function. Even with the coefficients already estimated, iteratively testing all 2^{286} possible monomials on a set of instances is already computationally demanding. Genetic algorithms, however, can be implemented to perform these tasks that are otherwise considered computationally too expensive [17].

A genetic algorithm is a heuristic search method that models aspects of natural selection mechanisms to evolve an optimal solution from multiple candidates [8]. "Survival of the fittest" is simulated across numerous generations, each generation having multiple candidate solutions, referred to as individuals [20]. The fitness function of a genetic algorithm dictates which individuals represent better solutions in the problem domain [18]. Only the individuals deemed fit are allowed to reproduce or to survive to the next generation. The genetic algorithm thereby optimises the fitness function to produce a globally optimal solution.

Potgieter and Engelbrecht developed a genetic algorithm capable of evolving polynomial expressions that are structurally optimal whilst providing favourable accuracy [17]. Potgieter and Engelbrecht defined optimality as the shortest polynomial with the best possible function approximation. GASOPE was evaluated by approximating several non-linear functions. GASOPE was shown to be significantly faster than a neural network approach, whilst producing comparable results [17]. Note that GASOPE is regarded as a polynomial regression model in the context of this paper.

Building on the success of GASOPE, Potgieter and Engelbrecht employed GASOPE to evolve the models used at the leaf nodes of a model tree. The proposed model tree, labelled GPMCC, made use of a genetic program to evolve a tree structure [18]. Hitherto discussed decision trees all employed greedy approaches to induce a decision tree structure. A greedy approach can be problematic because it is susceptible to becoming stuck in locally optimal solutions. The problem is attributed to the short-sighted nature of a greedy approach. Genetic approaches to inducing the structure of a decision tree outperform greedy approaches in the size of the induced tree, but at the expense of computational cost [2, 18]. The advantage a genetic approaches exhibits over greedy approaches is due to the search for a globally optimal solution as opposed to iteratively favouring solutions that yield local optima.

The genetic heuristic of GPMCC initialises multiple tree candidates by recursively adding nodes to each individual, until a maximum depth. At each node, the feature on which to split and the splitting value were randomly selected upon initialisation. The remaining operators ensured that only the optimal splits are maintained through the generations. Specialised mutation and crossover operators were introduced. Mutation ensures that new genetic material, utilising domain-specific knowledge, is injected into the population of candidate decision trees. The crossover operator was used to splice together two candidates to produce new candidate decision trees for the following generation. The fitness function incorporates the complexity of a candidate tree, in terms of the size and number of polynomial terms within all the leaf nodes, as well as the difference in the predicted and actual output of an instance. Thereby, the fitness functions can minimise both the prediction error as well as the structure of the candidate solution.

GPMCC was compared to Cubist on 13 benchmarking/artificial datasets producing significantly smaller tree structures, whilst being competitive with the accuracy of its predictions. For the majority of datasets, the order of the polynomials produced by GASOPE at the leaf nodes of GPMCC never exceeded three. This meant that cubic surfaces were sufficient in describing the non-linear relationships within these datasets. A disadvantage of GPMCC is the speed at which the genetic algorithm induces a model tree. Potgieter and Engelbrecht attributed the slow computational speed to the recursive procedures that perform fitness evaluation, crossover, and mutation of genetic candidates [18].

2.5. Model tree ensembles

Model tree ensembles are discussed in this final section of the chapter. Model tree ensemble research is not widespread and the computational cost associated with model tree ensembles is hypothesised as the main factor contributing to the lack of research. Section 2.5.1 motivates the reason why further research into model tree ensembles can be beneficial and introduces two successful ensembles based on the M5 model tree. Section 2.5.2 discusses the performance of random model trees (RMT). Finally, model tree ensemble (MTE) is examined in Section 2.5.3.

2.5.1. M5 ensembles

The challenges of developing ensembles of model trees are the increased computational cost and the difficulty of interpreting the models [20]. The increased interpretation difficulty is due to the increased number of learners as well as the injection of randomness into the selection of splits. One of the advantages decision trees have over competing supervised learning techniques is the interpretability that decision trees exhibits. Decision trees not only produce adequate performance, but also gives insight into the relationships between the input and output features for a given problem. The performance increase of ensembling decision trees has to be adequate to justify the loss of interpretability. Due to the added complexity of polynomial output function, model trees exhibit an even greater variance error and lower bias error than regression trees. Ensemble methods have proven effective in minimizing the variance error of model trees [20]. The right choice of ensemble method that comprises model trees is critical to producing an effective ensemble model. There are various approaches to ensemble modelling, those applicable in the context of this thesis were discussed in Section 2.2.

Aleksovski [1] and Pfahringer [16] are two of the few who have applied ensemble methods to model trees for regression problems, with each author incorporating a unique approach. The common denominator between the approaches these authors employed was the use of the M5 model tree as the base learner. Each of the model tree ensemble approaches discussed here also incorporates an aspect of randomness in the induction step. The authors referenced the success Breiman achieved with random forests as justification for the injection of randomness into RMT and MTE. Incorporation of randomness into an ensemble increases the decorrelation present between the base learners that comprise the ensemble, allowing for greater prediction accuracy [6] as proven by Equation (2.1).

Both Aleksovski and Pfahringer opted to only incorporate model trees that comprise linear models. To the best knowledge of the Author of this thesis, there is no research published yet on ensembles of model trees that comprise non-linear models.

2.5.2. Pfahringer's random model trees

Pfahringer modified the M5 algorithm to grow balanced trees within an ensemble, largely based on Breiman's random forest with little deviation other than the use of model trees as base learners [16]. Balanced trees are defined as trees incorporating the same number of instances in each leaf node. Pfahringer developed balanced trees by always selecting the median of a feature as the split value .

Pfahringer did not directly compare RMT to a single M5 tree. Instead, RMT was compared to a simple linear regression model, Gaussian process regression (GPR) and additive groves[1] (AG) [16]. At the time, GPR and AG were considered competing state-of-the-art regression methods. RMT outperformed both GPR and AG in terms of computational efficiency, whilst having competitive predictive accuracy [16].

2.5.3. Aleksovski's model tree ensembles

Aleksovski was tasked with developing models for dynamic systems, for which data was not evenly distributed in the feature space [1]. Aleksovski, therefore, opted not to incorporate balanced trees for base learners to avoid poor approximations of the data [1]. Aleksovski's approach to growing a model tree within an ensemble included three key features: randomised splitting features, *fuzzification*, and ensemble pruning.

The induction process of MTE is based on bagging, meaning that subsets of randomly selected features with replacement are created for each tree in the ensemble. Subsets of features are always chosen from the entire pool of available features and the act of choosing a feature does not remove it from this pool. The standard induction of M5 follows on each subset, i.e. growth that favours a reduction in standard deviation and pruning nodes to reduce prediction error.

[1]Additive groves is an ensemble of bagged additive regression trees which are iteratively trained.

MTE omits the smoothing process that M5 incorporated and instead uses fuzzification to prevent the discontinuities that each split within the model tree introduced. Aleksovski stated that the smoothing procedure of M5 produces poor performing models, and fuzzification is used instead to combat this [1]. Fuzzification removes discontinuities from the prediction of a model by creating a smooth transition between two local models. Splits are transformed into fuzzy splits via the implementation of a sigmoid function. For a tree comprising a single split, the prediction $y'(\boldsymbol{x})$ of a given instance is accordingly calculated as

$$y'(\boldsymbol{x}) = \mu(x_j, s, \alpha) f_1(\boldsymbol{x}) + \mu(x_j, s, \alpha) f_2(\boldsymbol{x}) \tag{2.12}$$

with

$$\mu(x_j, s, \alpha) = \frac{1}{1 + e^{-\alpha(x_j - s)}} \tag{2.13}$$

where, f_1 and f_2 are the linear models of two adjacent leaf nodes separated by a split on the j^{th} feature with split value s. Finally, α is a fuzzy parameter calculated using cross-validation. It is important to note that Aleksovski did not incorporate fuzzification into the induction of the tree structure because it showed to decrease the efficiency of the M5 algorithm due to the added computational cost it demanded [1].

Once the ensemble is fully grown, i.e. a specified number of learners have been induced on the dataset, the ensemble is pruned as a whole via a greedy selection procedure. As is the case with individual tree pruning, the generalisation error of MTE is evaluated both with and without each tree in the ensemble. In the case of individual tree pruning, nodes are removed. If a particular tree contributes to an increase in the prediction error, it is removed from the ensemble. The prediction of MTE is calculated through the uniformly weighted average of the predictions each tree within the ensemble makes.

MTE performed competitively against other state-of-the-art methods, including neural networks, in terms of its prediction error, whilst having the advantage of being quite robust to noise. Aleksovski described the MTE as being resilient to data that exhibited up to 20% noise. This resilience to noise is contributed to injection of randomness in the induction of MTE and helped MTE to produce a low variance error [1].

2.6. Conclusion

This chapter aimed to provide background information about how decision trees and ensemble methods thereof each address the bias-variance dilemma. Furthermore, this chapter investigated existing model tree methods and the application of model trees within an ensemble. It is evident that the application of model trees comprising higher-order polynomial output function as the base learners within an ensemble model is under researched. There are studies conducted on model trees comprising linear output functions within an ensemble which confirms the advantages ensemble techniques have. The advantages are a successful reduction in the variance errors to improve the robustness to overfitting and overall performance over the base learner. Model trees comprising higher-order polynomial output functions have been shown to outperform their linear output function counterparts. Consequently, further research into the application of model trees with higher-order polynomial output functions as the base learner of an ensemble is required.

Chapter 3

Genetic algorithm to evolve structurally optimal polynomial expressions

This chapter discusses the genetic algorithm to evolve structurally optimal polynomial expressions. Potgieter and Engelbrecht incorporated GASOPE in the leaves of the GPMCC model tree. Since the conception of GASOPE, computational limitations has lessened. Therefore, changes from the original implementation have been made. The model tree forest proposed in this paper employs an adaption of GASOPE in the leaf nodes of the model trees that make up the ensemble. The adaption of GASOPE was developed from the ground up. The complete genetic algorithm and all the deviations from the original are discussed with pseudo code in Section 3.1. The adaption GASOPE is evaluated and compared to the original results obtained by Potgieter and Engelbrecht in Section 3.2. Furthermore, in the final section GASOPE is evaluated on higher dimensional problems against other regression models.

3.1. Adapting the genetic algorithm

This section discusses the original implementation of GASOPE as well as the adaption. Section 3.1.1 discusses the original implementation of GASOPE and a drawback that was identified by Potgieter and Engelbrecht. The remaining sections each discuss the adapted genetic algorithm. Section 3.1.2 discusses the representation of an individual in the genetic algorithm. Section 3.1.3 illustrates the initialisation of an individual. Sections 3.1.4 and 3.1.5 illustrate the mutation and crossover operators of the genetic algorithm respectively. Section 3.1.6 introduces discrete least-squares approximation, used to produce the coefficients of an individual. Section 3.1.7 discusses the fitness function employed by the genetic algorithm to rank individuals. Finally, Section 3.1.8 discusses the entire genetic algorithm used by GASOPE to evolve a population of individuals for a given dataset.

3.1.1. Original implementation of the genetic algorithm

The original implementation of GASOPE was heavily influenced by the computational limitations at the time and developed with techniques to minimise computational cost [17]. The algorithm consists of a three-stage process:

1. Clustering of the training instances,
2. the genetic algorithm to evolve a structurally optimal polynomial expression and
3. a hall-of-fame to combat the drawback clustering causes.

The clustering stage draws a clustered random sample of training instances where each cluster represents a collection of homogeneous training instances. The clustering stage is implemented to minimise the number of training instances to iterate over for evolving each individual in every generation. Clustering significantly reduced the time taken for the genetic algorithm to evolve the final individual, without reducing the accuracy of the genetic algorithm [17]. Potgieter and Engelbrecht acknowledged that due to the aspect of randomness injected into the clustering stage, the data subset of a given generation may not inherit a true representation of the entire dataset [17]. In turn, an individual may be evolved that does not present the true nature of the dataset, particularly for extremely noisy datasets [17]. A hall-of-fame was incorporated to ensure that the clustering stage does not hinder the accuracy of GASOPE. The hall-of-fame is a set of individuals that performed the best for each generation of the genetic algorithm. Each generation the training instances differed, due to the clustering stage. Subsequently, the individual that performs best on the last generation does not necessarily perform the best of all individuals on the entire dataset but only on a sample of the dataset. Therefore, once the maximum number of generations is reached, the individual that performed best over all generations is chosen from the hall-of-fame, as opposed to the individual that performed best in the last generation.

Compared to when GASOPE was first conceptualised, computational limitations are now more lenient. Consequently, the new version of GASOPE developed in this chapter and used in MTF, does not require the same three-stage process to minimise computational demand. Instead, the dataset in its entirety is utilised, ensuring the best individual is evolved through each of the generations of the genetic algorithm. The clustering stage and therefore the hall-of-fame stage are dropped in the adaption of GASOPE. Therefore, an in-depth discussion of the clustering and hall-of-fame stages are omitted from this chapter because these two stages are no longer applicable to the evolution of higher-order polynomial functions. The removal of the clustering stage is the crucial difference between the original version of GASOPE and the adaption of GASOPE because it utilises an increased computational budget available at the time of writing this thesis. The adaptation of GASOPE follows the same representation, genetic operators and fitness function as the original implementation of GASOPE. Any aspects from the original genetic algorithm that differ due to the increased computational budget are clearly indicated under the corresponding section.

3.1.2. Representation

Each individual in the population is a representation of a multivariate higher-order polynomial function which is evolved to best fit the given data. Any given individual is made up of a set, I, of unique term-coefficient mappings that collectively represent Equation (2.11). For an individual that incorporates p terms, I is expressed as:

$$I = \{(t_0 \rightarrow w_0), ..., (t_p \rightarrow w_p)\} \tag{3.1}$$

where $w_i, i \in \{0, \ldots, p-1\}$ is the real-valued coefficient for the corresponding term t_i. Each term in the set I comprises, consists of m unique variable-order pairs to form a set T, where m is strictly equal to the number of input variables in the dataset. Therefore, a set of variable-order pairs, that represent any single term in the polynomial function, is expressed as:

$$T = \{(x_1 \rightarrow \lambda_1), ..., (x_m \rightarrow \lambda_m)\} \tag{3.2}$$

where λ_j is the whole-valued polynomial order of the respective input variable $x_j, j \in \{1, \ldots, m\}$.

3.1.3. Initialisation

Algorithm 1 describes how each individual in the population is initialised. The initialisation algorithm is illustrated in Figure 3.1. Random variable-order pairs are repeatedly selected for each term-coefficient mapping. To help promote the growth of smaller sized polynomials, the polynomial orders for a term are randomly selected without replacement from all available order up to the maximum polynomial order. This results in a set of variable-order pairs that do not strictly include every available polynomial order (all remaining input variables within the set T are assigned a polynomial order of zero). The maximum number of terms, p, as well as the maximum polynomial order, o, are both user-specified parameters. Increasing either p or o increases the computational cost of the genetic algorithm. This is because for each additional term an additional coefficient is estimated for fitness calculations. In the case of the maximum polynomial order, an additional is computed for each increment of o.

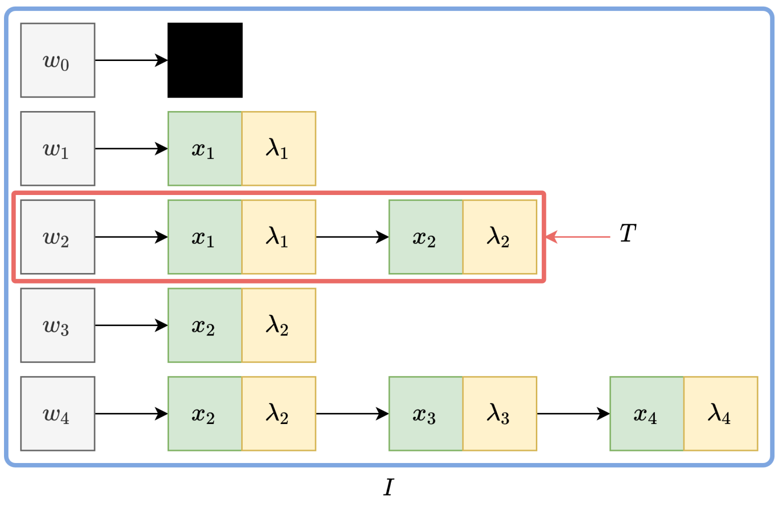

Figure 3.1: Illustration of the GASOPE initialisation algorithm, adapted from [17].

Algorithm 1: Pseudo-code for the initialisation of an individual.

```
Set $I = \{\}$
while $|I| < p$ do
    Set $T = \{\}$
    Select $\boldsymbol{e} \in \{1, \dots, o\}$ as random integers up to the maximum polynomial order $o$.
    while $|\boldsymbol{e}| > 0$ do
        Select $f$ to be a random order within $\boldsymbol{e}$
        Select $g$ randomly from $\{1, 2, ..., m\}$
        if $|T| < |T \cup \{(g \to f)\}|$ then
            $\boldsymbol{e} \coloneqq \boldsymbol{e}\{f\}$, i.e. remove $f$ from the available orders
            Set $T = T \cup \{g \to f\}$
        end
    end
    Set $I = I \cup \{T \to 0\}$ as illustrated in Figure 3.1
end
```

It is important to note that the coefficients of an individual cannot be estimated until the polynomial structure is fixed. Therefore, during initialisation, each coefficient is assigned the preliminary value of one. Furthermore, when an empty set of variable-order pairs is initialised, all input variables are assigned a polynomial order of zero.

3.1.4. Mutation operators

The mutation operators randomly inject new genetic material into selected individuals of the population. The mutation operators ensure that the search space is better explored by the genetic algorithm. Thereby, the probability of the algorithm producing a local optimum solution is reduced. Each operator aims to optimise the structure of the polynomial by either making adjustments to variable-order pairs or an entire term-coefficient mapping. The four, equally probable, mutation operators are shrink, expand, perturb and reinitialise.

The first mutation operator, *shrink*, is simple in its execution and is responsible for decreasing the size of the polynomial structure of an individual. One term-coefficient pair is arbitrarily selected from the set I and removed. The shrink operator is described in Algorithm 2.

Algorithm 2: Pseudo-code for performing the shrink operator on an individual.

```
Select $T \in I$ randomly from the set of terms $I$
Set $I = I/\{T\}$ as illustrated in Figure 3.2
```

Figure 3.2 illustrates the shrink operator. A set of variable-order pairs T is randomly selected and removed from the set of term-coefficient mappings I, as indicated by the red arrow in Figure 3.2.

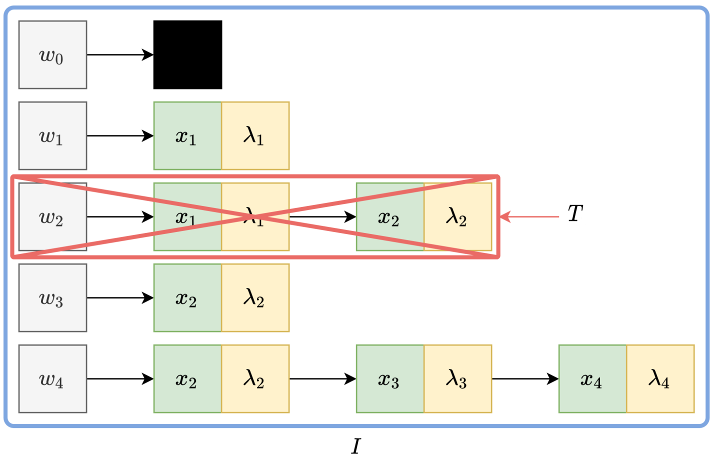

Figure 3.2: Illustration of the GASOPE shrink algorithm, adapted from [17].

The second operator, *expand*, is responsible for increasing the size of the polynomial structure of an individual. The expand operator adds a new term-coefficient mapping to the set I as described in Algorithm 3. Expand is illustrated in Figure 3.3 through the insertion of a new variable-order pair, indicated by the red arrow, into the term-coefficient mapping. In comparison to the original implementation, the expand operator is executed on an individual even if the individual already contains or exceeds the maximum number of allowed terms p. The removal of a maximum term threshold allows for larger polynomial structures to be explored, if the increase in accuracy justifies it. For this reason, polynomials that incorporate a structure too large should be adequately penalised during fitness calculations to prevent individuals from evolving polynomial structures that may compromise the computational cost of the genetic algorithm.

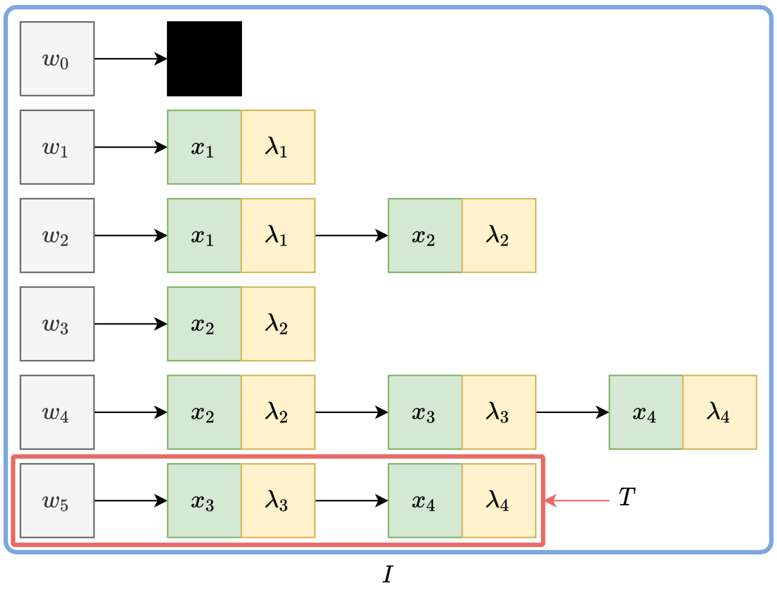

Figure 3.3: Illustration of the GASOPE expand algorithm, adapted from [17].

Algorithm 3: Pseudo-code for performing the expand operator on an individual.

```
Set $T = \{\}$
Select $\boldsymbol{e} \in \{0, \ldots, o\}$ as random integers up to the maximum polynomial order $o$
while $|\boldsymbol{e}| > 0$ do
    Select $f$ to be a random order within $\boldsymbol{e}$
    Select $g$ randomly from $\{1, 2, ..., m\}$
    if $|T| < |T \cup \{(g \rightarrow f)\}|$ then
        $\boldsymbol{e} := \boldsymbol{e}/\{f\}$, i.e. remove $f$ from the available orders
        Set $T = T \cup \{g \rightarrow f\}$
    end
end
Set $I = I \cup \{T \rightarrow 0\}$ as illustrated in Figure 3.3
```

The third mutation operator, *perturb*, is focused on altering a randomly selected variable-order pair $\{x_m \rightarrow \lambda_m\}$ within another randomly selected term T in the set of term-coefficient mappings I. When perturb is performed on an individual, one of three possible adjustments are made: a new variable-order pair is added to the term, an existing variable-order pair is removed from the term or an existing variable-order pair is adjusted. This process is described in Algorithm 4 and illustrated in Figure 3.4. A change in the perturb operator from the original implementation of GASOPE is introduced. When a variable-order pair is either adjusted or added, the available orders $\boldsymbol{e}$ remains unchanged. Previously, once a order was randomly selected, it was removed from $\boldsymbol{e}$. The change is implemented to increase the diversity of variable-order pairs that are introduced through mutation.

Algorithm 4: Pseudo-code for performing the perturb operator on an individual.

```
Select $T \in I$ randomly from the set of terms in $I$
Select $\boldsymbol{e} \in \{0, \ldots, o\}$ as random integers up to a maximum polynomial order $o$
Select $g$ randomly from $\{1, 2, ..., m\}$
Select $h$ randomly from a uniform distribution over $[0, 1]$
if $h < 0.333$ then
    Set $T = T/\{g \rightarrow \lambda\}$ where $\lambda > 0$, i.e. remove the $g^{th}$ variable-order pair present in
      $T$, as portrayed by the crossed out variable-order pair in Figure 3.4
else if $h < 0.666$ then
    Select $f$ to be a random order within $\boldsymbol{e}$.
    Set $T = T \cup \{g \rightarrow f\}$ as portrayed by the entirely circled variable-order pair in
      Figure 3.4
else
    Set $T = T/\{g \rightarrow \lambda\}$ where $\lambda > 0$
    Select $f$ to be a random order within $\boldsymbol{e}$
    Set $T = T \cup \{g \rightarrow f\}$ as portrayed by the partially circled order of the variable-order
      pair in Figure 3.4
end
```

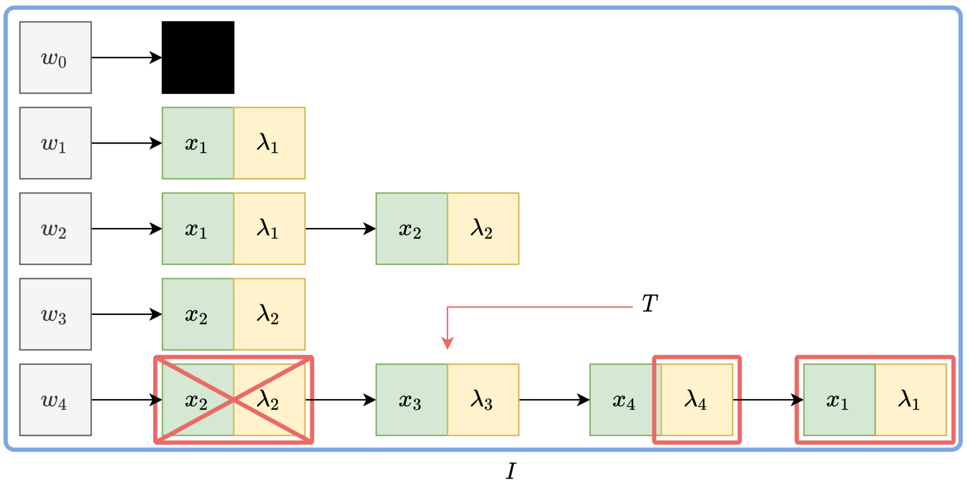

Figure 3.4: Illustration of the GASOPE perturb algorithm, adapted from [17]. Each of the three variable-order pairs marked by the red square describe a peturb operation.

The fourth and final mutation operator, *reinitialise*, is simply a re-invocation of Algorithm 1, already discussed in Section 3.1.3. The purpose of the reinitialise operator is to introduce new, random genetic material into the pool of candidate solutions.

3.1.5. Crossover operator

The crossover operator recombines favourable genetic material from one generation of individuals to produce the offspring candidates of the next generation. Consequently, the favourable genetic material is transferred over to the next generation. The crossover operator serves to aid the genetic algorithm. The crossover operator produces new individuals from the top-ranked genetic material to promote positive exploration of the search space. When the crossover operator is called two of the best performing individuals are randomly selected and their term-coefficient mappings evaluated before a new individual is evolved which retains some of their genetic makeup. Any term-coefficient mappings simultaneously present in both individuals have a larger probability of being transferred over to the newly evolved individual. The probability of a mutual or non-mutual term-coefficient mapping being passed on from parent to offspring is determined by a user-specified parameter, namely selection ratio. The selection ratio represents the probability of offspring retaining the inclusive and exclusive term-coefficient mappings. Potgieter and Engelbrecht found that a selection ratio of 80%:20% resulted in newly generated individuals roughly equalling the length of its longer parent [17]. Consequently, inclusive terms between parents have an 80% chance of being passed on and exclusive terms have a 20% chance.

Algorithm 5 describes how the selection ratio is implemented in the crossover operator to evolve a new individual and Figure 3.5 presents the crossover operator. Only one change exists from the original implementation of GASOPE. Newly generated individuals may now exceed the maximum number of terms. The increased computational budget allows for the exploration of candidate solutions with larger polynomial structures. It is worth noting that a larger polynomial structure requires a significant improvement in accuracy to justify any increased computational cost.

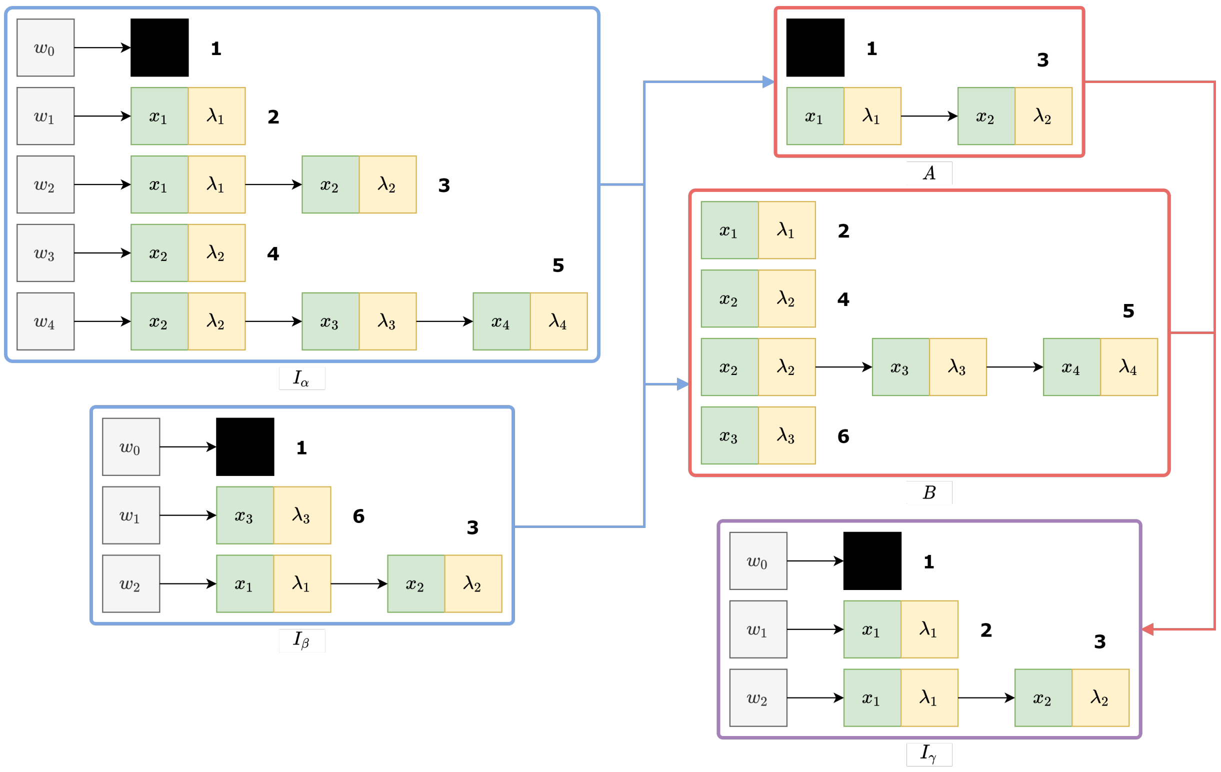

Figure 3.5: Illustration of the GASOPE crossover algorithm, adapted from [17].

Algorithm 5: Pseudo-code for performing crossover between two individuals.

```
Set $I_\alpha = \{\}$, i.e. a new, empty term-coefficient set (individual)
Select $I_\beta, I_\gamma \in P$ as two unique, randomly chosen individuals from a given population
Set $A = I_\beta \cap I_\gamma$, i.e. the intersection of the term-coefficient mappings
Let $B = (I_\beta / I_\gamma) \cup (I_\gamma / I_\beta)$ be the union of the exclusion
for each term-coefficient mapping ($T_A$) in $A$ do
    Select $h$ randomly from a uniform distribution over $[0, 1]$
    if $h < 0.8$ then
        Set $I_\alpha = I_\alpha \cup \{T_A\}$.
    end
end
for each term-coefficient mapping ($T_B$) in $B$ do
    Select $h$ randomly from a uniform distribution over $[0, 1]$
    if $h < 0.2$ then
        Set $I_\alpha = I_\alpha \cup \{T_B\}$.
    end
end
```

3.1.6. Discrete least-squares approximation

With every generation an individual is evaluated to be structurally optimal through two phases. In the first phase, the terms (which encapsulate variable-order pairs) of the polynomial function are evolved with the crossover operator and possibly mutated. In the second phase, the coefficients are approximated using discrete least-squares approximation to complete a set of term-coefficient mappings of an individual. Discrete least-squares approximation for a arbitrary set of n data points $\{(\boldsymbol{x_1}, y_1), \ldots, (\boldsymbol{x_n}, y_n)\}$, minimises the least squares error:

$$\epsilon = \sum_{i=1}^{n} (y_i - y_i')^2 \tag{3.3}$$

where y_i' is the predicted output of the polynomial function of an individual, for the i^{th} instance. The predicted output is described by the equation (similar to Equation (2.11))

$$y_i' = \sum_{\tau=0, \Sigma_{j=1}^{m} \lambda_j = \tau}^{o} \left(w_{(\lambda_1, \lambda_2, \ldots, \lambda_m)} \prod_{k=1}^{m} x_{i,k}^{\lambda_k} \right) \tag{3.4}$$

where m represents the number of input variables and o the maximum polynomial order. Equation (3.4) allows for the representation of an arbitrary individual as

$$y_i' = w_{(0,0)} + w_{(1,0)} x_{i,1} + w_{(0,1)} x_{i,2} + w_{(1,1)} x_{i,1} x_{i,2} + w_{(2,0)} x_{i,1}^2 + w_{(0,2)} x_{i,2}^2 \tag{3.5}$$

for $m = 2$ and $o = 2$. The vector of coefficients, $\boldsymbol{w}$, of the polynomial function are determined by solving the linear system:

$$\boldsymbol{y} \approx \boldsymbol{X}\boldsymbol{w} \tag{3.6}$$

where $\boldsymbol{w}^{\mathrm{T}} = \begin{bmatrix} w_0 & w_1 & \cdots & w_p \end{bmatrix}$ for a polynomial incorporating p terms, which is rewritten as

$$\left(\boldsymbol{X}^{\mathrm{T}}\boldsymbol{X}\right)\boldsymbol{w} = \boldsymbol{X}^{\mathrm{T}}\boldsymbol{y} \tag{3.7}$$

There is no exact solution to Equation (3.7). In the case of a univariate function, matrix $\boldsymbol{X}$ may be of the form

$$\boldsymbol{X} = \begin{bmatrix} 1 & x_1 & x_1^2 & \cdots & x_1^o \\ 1 & x_2 & x_2^2 & \cdots & x_2^o \\ \vdots & \vdots & \vdots & & \vdots \\ 1 & x_n & x_n^2 & \cdots & x_n^o \end{bmatrix} \tag{3.8}$$

and vector $\boldsymbol{y}^{\mathrm{T}} = \begin{bmatrix} y_0 & y_1 & \cdots & y_n \end{bmatrix}$. Matrix X has no universally set form and is adapted to correspond with the set of variable-order pairs present in any given individual.

The coefficients of an individual are estimated by solving the above-mentioned linear system as follows. Matrix $\boldsymbol{X}$ in Equation (3.8) is first populated from left to right using the combination of terms that each term-coefficient mapping of an individual represents. With vector $\boldsymbol{y}$ containing the target output for each pattern, the linear system in Equation (3.7) is reduced, producing vector $\boldsymbol{w}$ which is populated with the coefficient of each term-coefficient mapping. Thus, the evolution of an individual for a single generation is concluded. After the term-coefficient mappings are estimated successfully, the fitness of the individual is calculated.

3.1.7. Fitness calculation

The fitness function determines the rank of each individual in the population. The fitness function serves to guide the genetic algorithm into favourable search space with each generation. This rank is determined by how well the individual solves the problem at hand. In the case of GASOPE the fitness function is maximised. Therefore, the individual with the highest scoring fitness is ranked first. Each generation, individuals with the lowest fitness scores are replaced preventing the genetic algorithm from exploring poor solutions. The fitness function of GASOPE penalises individuals with polynomials that are not structurally optimal and well-fitted function approximations. The fitness function of a given individual is defined as [17]:

$$R^2 = 1 - \frac{\sum_{i=1}^{n} (y_i - y_i')^2}{\sum_{i=1}^{n} (y_i - \bar{y})^2} \cdot \frac{n-1}{n-c} \tag{3.9}$$

where n is the number of instances in the dataset, y_i is the target output, and y_i' is the output predicted by individual I for instance i. The model complexity c is,

$$c = \sum_{i=1}^{|I|} \sum_{j=1}^{|T_i|} \lambda_{i,j} \tag{3.10}$$

where $\lambda_{i,j}$ is the order of a variable-order pair within a term-coefficient mapping T_i of individual I. Thereby, c penalises an individual based on the number of multiplications needed to calculate the predicted output. The c variable in the fitness function is crucial in ensuring the genetic algorithms develops solutions that are structurally optimal both in the number of terms and their orders.

3.1.8. The complete genetic algorithm

Algorithm 6 presents the complete procedure executed by the genetic algorithm to evolve a structurally optimal polynomial function from a given training dataset. The genetic algorithm starts with a randomly initialised population of individuals P. For each generation, each individual within the population is subjected to least-squares approximation producing the set of coefficients needed to perform fitness calculations. Once the fitness of each individual is calculated, the population is ranked accordingly.

Algorithm 6: Complete genetic algorithm for evolving polynomials. Adapted from [17].

```
Let $i = 0$ be the generation counter
Initialise a population $P_i$ of $n_j$ individuals:
  $P_i = \{I_j | j = 1, ..., n_j\}$
Set $n_m$ = mutation rate$\times n_j$
Set $n_c$ = crossover rate$\times n_j$
while $i < G$, where $G$ is the maximum number of generations do
    for each individual $I_j$ in $P_i$ do
        Perform least square optimisation to determine the coefficients of $I_j$
        Calculate the fitness of $I_j$ from Equation (3.9)
    end
    Let $P_i' \subset P_i$ be the top $x\%$ of the individuals selected for elitism
    $P_{i+1} := P_i'$
    Let $P_i'' \subset P_i$ be the top $y\%$ of the individuals selected for crossover
    while $|P_{i+1}| < (n_j - n_c - n_m)$ do
        Select two unique individuals $I_\alpha$ and $I_\beta$ randomly from $P_i''$
        Perform crossover between $I_\alpha$ and $I_\beta$ to produce $I_\gamma$
        $P_{i+1} := P_{i+1} \cup \{I_\gamma\}$
    end
    Let $k = 0$ be the mutation counter.
    while $k < n_m$ do
        Duplicate a randomly selected individual as $I_\delta$ from $P_{i+1}$
        Perform a randomly chosen mutation operator on $I_\delta$
        $P_{i+1} := P_{i+1} \cup \{I_\delta\}$
        $k := k + 1$
    end
    $P_i := P_{i+1}$
end
```

An elite few of the top-ranked individuals survives to partially form the population of the following generation. The top-ranked individuals survive to the next generation without any alterations to their polynomial structure. The number of individuals selected for elitism is specified by the user-controlled parameter, the elitism rate. From the top-ranked individuals, two unique individuals are randomly selected for crossover. Parent selection and crossover is repeated to populate the remainder of the population for the next generation The number of individuals selected for crossover is specified by the user-controlled parameter, crossover rate.

Once the population of the following generation is fully populated, mutation is performed. Specified by the user-controlled parameter, mutation rate, several randomly selected individuals are mutated. Because GASOPE does not incorporates a hall of fame, the best-performing individual from any given generation is no longer saved into an separate set. Only the best performing individual from the **final** generation is of importance. Consequently, the mutation operator may select the best-performing individual of a generation to be mutated and possibly cause the best candidate solution to be lost during evolution. To prevent the ideal candidate from being lost a duplicate of the individual selected for mutation is stored in the population prior to mutation. After the maximum number of generations has passed, the highest ranked individual is presented as the optimal polynomial.

3.2. Evaluation of the adapted genetic algorithm

This section focuses on tuning as well as evaluating the predictive accuracy of GASOPE. Section 3.2.1 presents the experimental procedure followed and the accuracy of adapted GASOPE compared to originally recorded results of Potgieter and Engelbrecht [17]. The hyperparameters of GASOPE are tuned in section 3.2.2 specifically for a multi-dimensional dataset. Finally, GASOPE is compared in section 3.2.3 with other regression models and the results obtained by GPMCC on a dataset incorporating nine input features. The evaluation of GASOPE against other regression models follows a requires experimental procedure.

3.2.1. Experimental procedure and results

A set of functions was used to evaluate the predictive accuracy of GASOPE on unseen data. Table 3.1 lists these four functions with their function definitions. All functions are injected with uniformly generated noise over the interval $[-1, 1]$. A total of 12 000 instances are created for each function to make up a dataset. From these 12 000, 10 000 are allocated for the training set, 1 000 for the validation set and 1 000 for the test set. All tests were repeated 100 times with the dataset being shuffled for each.

Table 3.1: Function definitions on which GASOPE is tested.

Name	Function
h_1	$h(x_0) = \sin(x_0); x_0 \in [0, 2\pi]$
h_2	$h(x_0, x_1) = \sin(x_0) + \sin(x_1); \{x_0, x_1\} \in [0, 2\pi]$
h_3	$h(x_0) = x_0^5 - 5x_0^3 + 4x_0; x_0 \in [-2, 2]$
h_4	$h(x_0, x_1) = x_0^5 - 5x_0^3 + 4x_0 + x_1^5 - 5x_1^3 + 4x_1; \{x_0, x_1\} \in [-2, 2]$

The hyperparameters of adapted GASOPE are chosen to equal the values first specified by Potgieter and Engelbrecht [17]. The hyperparameters values that were used are shown in Table 3.2.

Table 3.3 lists the results achieved by GASOPE in [17] on the same functions, together with the results obtained from the adaptation of GASOPE.

Predictive performance was measured using the average mean square error on the test set over the 100 test runs, with σ_{MSE} indicating the standard deviation. The statistical significance of the results could not be evaluated, however from observation there are no notably large discrepancies. It is clear from the results shown in Table 3.3 that the alterations implemented in

Table 3.2: Chosen values for the hyperparameters of GASOPE.

Hyperparameter	Value
Elite	0.1
Mutation rate	0.1
Crossover rate	0.2
Maximum terms	20
Maximum order	5
Population size	100
Generations	30

Table 3.3: The accuracy of GASOPE compared to the original from [17].

Function	Model	$\overline{MSE}$	σ_{MSE}
h_1	Original Gasope	0.343135	0.001644
	Gasope	0.332955	0.009163
h_2	Original Gasope	0.345282	0.001698
	Gasope	0.330054	0.009625
h_3	Original Gasope	0.339414	0.001765
	Gasope	0.334083	0.009059
h_4	Original Gasope	0.332791	0.001935
	Gasope	0.342808	0.007728

the adapted version of GASOPE did not compromise its predictive accuracy. However, further testing on multi-dimensional data is required to verify this.

It is unclear if the hyperparameter values listed in Table 3.2 are indeed the optimal values for adapted GASOPE. The hyperparameter values of GASOPE were initially chosen "based on numerous experimental runs" [17]. Therefore, before further testing of adapted GASOPE, the hyperparameters require tuning.

3.2.2. Tuning the genetic algorithm for multi-dimensional problems

Shortcomings of the original evaluation of GASOPE include the lack of multi-dimensional datasets and motivation for the choice of hyperparameters. The choice of hyperparameter values, listed in Table 3.2, for GASOPE was applicable on only one- and two-dimensional functions as listed in Table 3.1.

To ensure adapted GASOPE is the optimal model to employ at the leaves of MTF, it is first tuned and evaluated on a multi-dimensional problem. There are many openly available datasets from the UCI Machine Learning Repository[1]. The Abalone dataset is chosen because the results

[1]https://archive.ics.uci.edu/ml/datasets.php

GPMCC previously produced on this dataset were not as favourable [18]. It is hypothesised that The appropriate tuning of GASOPE's hyperparameters as well as the newly implemented changes can improve the performance of GASOPE on the Abalone dataset.

Evaluation of the predictive accuracy of GASOPE on the dataset is done for 30 independent runs. For each run, the dataset is split into a training set, validation set, and test set in an 80%:10%:10% split. Tuning makes use of the training and validation set. The first three hyperparameters that require optimisation are:

1. Population size,
2. the number of generations evolved for and
3. the maximum number of terms of an individual.

The computational expense for the above-mentioned hyperparameters requires critically evaluation during tuning. Furthermore, each of the three hyperparameter negatively influences the computational cost of GASOPE as its value is increased. The reason for this, is each hyperparameter increases the number of computations required to evolve an optimal polynomial.

To find the point where a further increase in population sizes causes the error metric to converge, GASOPE with population size varying from 10 to 60 in increments of five were evolved. Figure 3.6 illustrates the validation set RMSE for each instance of GASOPE with varying population size. From the box plots in Figure 3.6 that portray the RMSE distribution over the 30 independent , it is clear that for very small population sizes the RMSE value tends to fluctuate more. The smallest population size that produced consistently low RMSE values was that of 30 individuals. Figure 3.7 shows how the average training set RMSE decreases with each generation that is evolved for. Population sizes smaller than 30 resulted in a significantly increased average training set RMSE. Once the populations size is increased above 30, both the training set RMSE as well as validation set RMSE converges.

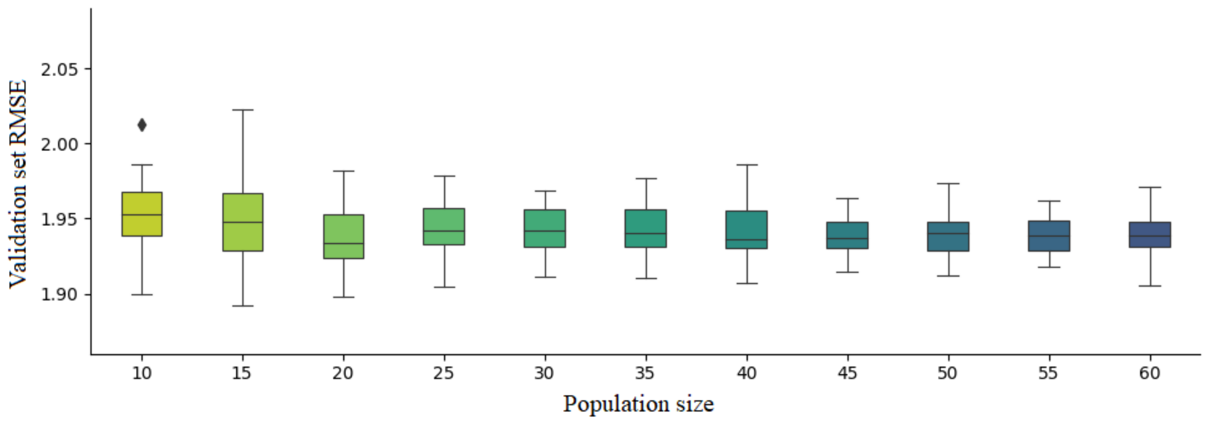

Figure 3.6: RMSE on the Abalone validation set for GASOPE models with varying number of individuals within the population.

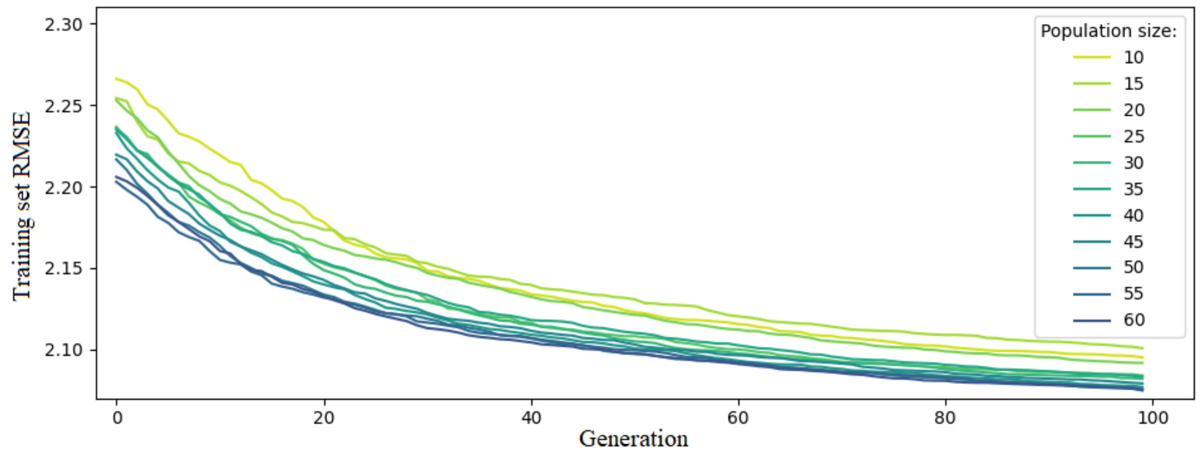

Figure 3.7: RMSE on the Abalone training set for each generation of GASOPE models with varying number of individuals.

The next hyperparameter which heavily influences computational costs is the number of generations GASOPE evolves a population of individuals for. Figure 3.8 provides the box plots of 30 independent RMSE scores of the best polynomial evolved using GASOPE for generations varying from 10 to 200 in increments of 10. As the number of generations increased, the RMSE values tend to decrease as well as fluctuate less. However, this tendency starts dropping off after 100 generations and the RMSE converges.

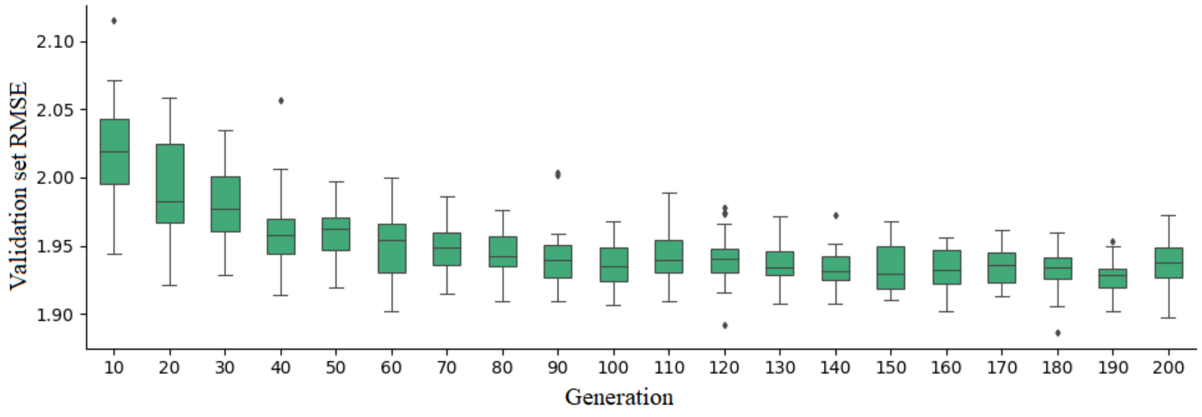

Figure 3.8: RMSE GASOPE with a population size of 30 produced on the Abalone validation set over each generation for 30 repeated runs.

Next, the maximum number of terms hyperparameter is discussed. The maximum number of terms has the largest contribution to the computational cost associated with evolving an optimal polynomial. Therefore, the maximum number of terms is chosen as small as possible without compromising the performance of GASOPE whilst also large enough to ensure that the initial search space is adequately covered. From the implementation of GASOPE in GPMCC, a value of 10 for the maximum number of terms was found to produce sufficient results in multi-dimensional problems and the best performing individual was found to often comprise less than 10 terms [18]. Note that the maximum number of terms hyperparameter parameter is only applicable to the initialisation of an individual.

The next hyperparameter for discussion, maximum polynomial order, is considered unique to each case GASOPE is applied to. Allowing polynomials to incorporate large polynomial orders when the dataset itself does not exhibit highly non-linear tendencies results in GASOPE imposing non-linear relationships that are not necessarily prevalent in the data. Despite the fitness function penalising larger polynomial orders more severely, there is still a need to tune the maximum polynomial order per problem. As discussed in the Section 2.2, if a model is too complex in its composition for the data at hand, it will increase the variance error and subsequently overfit the data. The Abalone dataset is quite linear but GASOPE within GPMCC evolved polynomials orders up to a value of four [17]. Limiting the maximum polynomial order of GASOPE to a value smaller than four may produce improved results. However, an order too small is will prevent GASOPE from adequately capturing any non-linear relationships in the dataset. To analyze the effect that the maximum polynomial order has on the performance of GASOPE in the case of the Abalone dataset, three different instances of GASOPE are further tuned and compared. Each instance is evolved with a respective maximum polynomial order, o, set to 1, 2 and 3. For each of the three GASOPE instances, the remaining hyperparameters that require optimisation are:

- Crossover rate
- Mutation rate
- Elitism rate

Bayesian optimisation is applied on the validation set for the tuning of the remaining hyperparameters of GASOPE. Bayesian optimisation is a tuning method used to determine the hyperparameter values that minimise a given objective function. Bayesian optimisation is used to build probabilistic models of the function mappings between hyperparameter values and the objective function. Bayesian optimisation used the RMSE on the validation set as the error metric that forms the objective function. Although Bayesian optimisation is not as exhaustive as a gridsearch, it is less time-consuming for large parameter spaces [23]. Table 3.4 lists the final hyperparameter values obtained from Bayesian optimisation for each GASOPE instance.

Table 3.4: GASOPE hyperparameters obtained through Bayesian optimisation.

Hyperparameter	GASOPE with $o = 1$	GASOPE with $o = 1$	GASOPE with $o = 1$
Elitism rate	0.15	0.3	0.25
Mutation rate	0.3	0.2	0.3
Crossover rate	0.3	0.2	0.2
Maximum terms	10	10	10
Population size	30	30	30
Generations	100	100	100

3.2.3. Evaluation against other regression models

For the comparison of the prediction accuracy of adapted GASOPE on a higher-dimensional problem, competing regression models are also trained and evaluated on a test set of the Abalone dataset. The regression models are a support vector regression (SVR) model, incorporating a Gaussian kernel function, as well as a simple linear regression model, used by M5 at its leaf nodes. GPMCC, which utilises GASOPE, was evaluated on the same higher dimensional problem and therefore also serves as an adequate comparison for adapted GASOPE [18]. The experimental procedure of the evaluation follows.

For the linear regression model there are no hyperparameters to tune. For the SVR model, two hyperparameters are tuned with Bayesian optimisation. The SVR hyperparameters are the *gamma* and C values. Gamma represents the coefficient of the Gaussian kernel function and C a regularisation parameter. The purpose of these variables are superfluous to the experimental procedure and therefore not further discussed.

To evaluate the accuracy of a model, the results of 30 independent runs are recorded. Recall that the Abalone dataset was split into a training, validation and test set. Here the training and test sets are used. For all models, excluding GPMCC, both RMSE and MAE values with their standard deviations, σ, are used for evaluation. Note that RMSE is considered a more robust estimation of the performance of a model because it penalises larger errors more severely [7]. For each run the five models that are compared are ranked according to their RMSE and MAE errors respectively. The average ranking is thereafter used to test the statistical significance of the results.

The Friedman test [21], is a non-parametric statistical test to detect significant differences between the performance of the models. The null-hypothesis is that all models are equal in their performance based on the results. In the event that the null-hypothesis is rejected, a post-hoc test is performed. A post-hoc test is a statistical test performed to further distinguish the results. In this case, the post-hoc test shows which models are statistically dissimilar in accuracy. The post-hoc pairwise test used is the Bonferroni-Dunn test [9], because it is best suited for comparisons of several methods with a control method (in this case, the linear regression model serves as control). A statistical tests, a significance level of 5% is used. The significance level is the probability of rejecting the null-hypothesis, given that it is true.

Table 3.5 presents the results obtained for each model together with the results GPMCC obtained on the Abalone dataset [18]. SVR is scored the lowest MAE and average rank amongst all models. GASOPE with a maximum polynomial order of two achieved the lowest RMSE and second best average ranking. The null-hypothesis was rejected and the post-hoc test performed to show which algorithms are statistically dissimilar.

Table 3.5: Comparison of different GASOPE instances on Abalone.

Model	$\overline{RMSE}$	σ_{RMSE}	$\overline{MAE}$	σ_{MAE}	Average Rank
GPMCC	n/a	n/a	1.6051	0.0156	n/a
GASOPE with $o = 1$	2.159098	0.082020	1.531867	0.052391	3.875
GASOPE with $o = 2$	2.125721	0.084797	1.480717	0.055245	2.033
GASOPE with $o = 3$	2.142215	0.080056	1.497536	0.055468	2.783
SVR with Gaussian Kernel	2.136233	0.086790	1.434549	0.053255	1.733
Linear Regression	2.162230	0.080725	1.544813	0.053264	4.575

Figure 3.9 presents the critical difference diagram summarising the results of the post-hoc test. A critical difference diagram indicates the average rank of each method and connects those that are not statistically different. It is evident from Figure 3.9 that the results of SVR and GASOPE with $o = 2$ are statistically equivalent. The linear regression and GASOPE with $o = 1$ are also considered statistically similar. This is expected, because GASOPE with $o = 1$ produces a polynomial with an equal order to linear regression. Thereby, the two models have a similar discriminative ability. GASOPE with $o = 3$ is shown producing statistically worse results than both SVR and GASOPE with $o = 2$, confirming that imposing higher order relationships on data that is not necessarily of such sort will impact the accuracy of GASOPE negatively. However, GASOPE with $o = 3$ is ranked better than GASOPE with $o = 1$, showing that a maximum polynomial order to small is also detrimental to the accuracy of GASOPE.

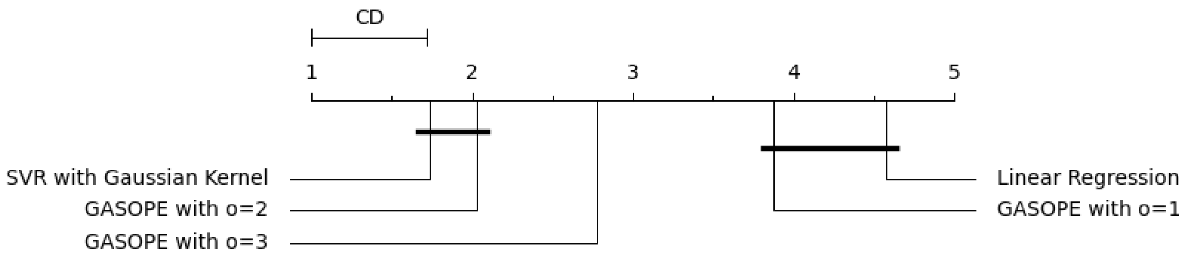

Figure 3.9: Criticial difference diagram for the results obtained in Table 3.5.

3.3. Conclusion

This chapter investigated the original implementation of GASOPE and defined the proposed changes that are required for the use of GASOPE with increased computational power. After testing, it is evident that the changes brought into GASOPE produced improved results when compared to its original implementation within GPMCC. In the case of the Abalone dataset, GPMCC clearly overfitted the data. The results GASOPE produced were adequate to justify implementing it in the leaf nodes of MTF, which will be further discussed in the following chapter. MTF can prove to produce more robust results by being able to not only adapt to highly non-linear data, but linear data as well.

To prevent future instances of MTF from overfitting data, careful consideration should be given to the maximum polynomial order value. There is no universal maximum polynomial order value that will result in the optimal polynomial being evolved for all cases. Although GASOPE already has systems in place to penalise overly complex polynomials, in some cases the fitness function alone cannot prevent overly complex polynomials from being evolved. Through testing it was found that leaving the maximum polynomial order too large, would result in the population of individuals being flooded by overly complex polynomials during initialisation. The fitness function as well as crossover and mutation operators cannot escape these local optima resulted by overly complex solutions. Therefore, the maximum polynomial order hyperparameter should be carefully chosen for each unique dataset. Doing so ensures that the initial search space is close enough to the globally optimal solution.

Chapter 4

Model Tree Forest

The model tree forest induction algorithm proposed in this thesis is presented and discussed in this chapter. MTF consists of a random forest (RF) inspired tree induction algorithm with GASOPE applied to evolve optimal multivariate polynomial functions for each leaf node within a given tree of the ensemble. Furthermore, the hyperparameters of MTF are listed and tuned for on a collection of datasets obtained from the UCI Machine Learning Repository as well as artificially generated data. Firstly, Section 4.1 discusses the RF inspirations implemented to help combat the high variance associated with MTF and presents pseudo code to describe the MTF induction algorithm. Next, Section 4.2 showcases the hyperparameter tuning of MTF as well as the steps that were taken to combat initially unfavourable results. Finally, Section 4.3 concludes the results of the tuning of MTF.

4.1. The conceptualisation of model tree forest

This section presents the methodology of model tree forest. The steps taken to ensure the base learner model trees within MTF are sufficiently decorrelated, similarly to the trees within RF, are motivated and listed in Section 4.1.1. Section 4.1.2 thereafter discusses the considerations of successfully applying these steps as well as the reasoning behind the omission of solutions that have been presented in previous research. Finally, Section 4.1.3 presents the complete pseudo code of the MTF induction algorithm.

4.1.1. Inspirations from existing ensemble methods

As discussed in Chapter 2, model trees have a greater intrinsic ability to approximate continuous non-linear data compared to the simpler regression trees found in RFs. This is due to the polynomials that are employed to produce the output of a model tree for a given sample as opposed to the singular output value in the leaf nodes of a regression tree. The cost of employing polynomials, specifically higher-order polynomials, is a significant increase in the observed variance error. However, it has been shown in Equation (2.1) that the variance error can be effectively reduced through the use of an ensemble of decorrelated trees. RF extends the idea of decorrelating trees by introducing randomly selected subsets of splits during the induction of a single tree. Therefore, RF inspired induction steps are implemented in MTF to help reduce the expected high variance error that MTF inherits from both GASOPE and its decision tree architecture.

The base learners of MTF, which together form an ensemble, are referred to as model trees (MT). In the case of RF for regression problems, the base learners are regression trees. Regression trees and model trees both employ a divide-and-conquer induction approach to recursively split the training data using a set of rules. The rules are referred to as the splitting functions and are obtained using a greedy search approach. During the induction of a decision tree, several splits are proposed and evaluated using a chosen criterion, for the M5 model tree this criterion is standard deviation reduction. Standard deviation reduction Δ_ϵ is calculated as (refer to Section 2.3.2)

$$\Delta_\epsilon = sd(D) - \sum_i \frac{|D_i|}{|D|} \times sd(D_i) \tag{4.1}$$

where D is the set of training instances for the data within a node, and $sd(D)$ is the standard deviation of the target values in D. D_i denotes the subset of instances that belong to outcome i of a split and $sd(D_i)$ the standard deviation of the target values in D_i. MT employs the same splitting function as in Equation (2.2). Recursive splitting of the training set contributes to the high variance error, because a decision tree tends to overfit the training data through each additional split. The greedy search approach to decision tree induction is what RFs, MTFs and similar M5 ensembles have in common in their base learners.

What differentiates the base learners of MTF from more traditional model trees, such as the M5 model tree, is the use of GASOPE to evolve higher-order polynomials to describe the mapping between the input and output features for all of the instances within a leaf node. For the M5 model tree, a simpler linear model is employed, described by the following equation:

$$y'(\boldsymbol{x}) = w_0 + w_1 x_1 + w_2 x_2 + ... + w_m x_m \tag{4.2}$$

where x_m represents the m^{th} input feature, w_m its respective weight, and w_0 the bias term. In contrast to Equation (4.2), MTF generates higher-order polynomial of the form

$$f(\boldsymbol{x}) = \sum_{\tau=0, \Sigma_{j=1}^{m} \lambda_j = \tau}^{o} \left(w_{(\lambda_1, \lambda_2, ..., \lambda_m)} \prod_{i=1}^{m} x_i^{\lambda_i} \right) \tag{4.3}$$

where m is the dimensionality of the feature space, o is the degree of the polynomial order and $w_{(\lambda_1, \lambda_2, ..., \lambda_m)}$ is the weight of each term. For a regression tree, employed by RF, Equations (4.2) and (4.3) are simply replaced by a constant value in the leaf nodes. The increased complexity of linear models and higher-order polynomials used to produce the output of a model tree leads to a significant increase in variance error. Therefore, the high variance error of MTF is attributed to two factors:

1. The decision tree structure of the base learners that comprise MTF.
2. The higher-order polynomials evolved via GASOPE in the leaf nodes of MT.

In turn, these two factors together also result in a low bias error.

Techniques similar to RF in MTF, may retain a more favourable bias error, whilst keeping the variance error low enough to not degrade the performance of MTF. A previous approach employed to combat high variance error was the introduction of base learner pruning. However, for RF base learner pruning is omitted because RF introduced new methods to reduce variance. Pruning prohibits a decision tree from exhibiting the advantageous low bias error associated with decision trees. Both RF and MTF employ a bagging approach, discussed in Section 2.2.3, to ensembling. For RF, each tree in a bagged ensemble is induced on a subset of the training set equal to two-thirds of the original training set size. Recall that a high variance error of bagged decision tree ensembles can be reduced through decorrelation of the base learners within the ensemble, because

$$Var(X, \boldsymbol{y}) = \rho(X)\sigma^2(\boldsymbol{y}) + \frac{(1-\rho(X))\sigma^2(\boldsymbol{y})}{n_l} \tag{4.4}$$

where ρ is the sampling correlation between the prediction of any two decision trees in the ensemble and σ^2 is the sampling variance over the target values of any single, randomly drawn, decision tree. n_t is the number of decision trees in the ensemble, X represents a set of instances and $\boldsymbol{y}$ the vector of target values. It is clear from Equation (4.4) that increasing the number of decision trees in the ensemble will effectively reduce the variance error.

To further decorrelate trees within the ensemble, RF induces the splits of base learner decision trees on subsets of the input feature space. The splitting function, shown Equation (4.1), randomly draws a specified number of input features from those available and computes the proposed splits only on this subset of input features. The split within the subset of features which maximises the reduction in error criterion Δ_ϵ is selected Thereby, RF can both minimise bias and variance errors through the induction of numerous, fully-grown, decorrelated decision trees as base learners. The random feature space selection process is implemented in MTF to further reduce the high variance error of MTF. The only factor limiting the ensemble size of MTF is the computational cost of inducing large numbers of model trees in serial.

As discussed in Section 2.5.3 Aleksovski includes a greedy ensemble pruning step to optimise M5E. Trees that do not contribute to the accuracy of the ensemble are removed, thereby aiming to produce a more accurate model of the training data. The contribution of an individual tree is evaluated through the performance of the ensemble both with and without the tree at hand. The same greedy optimisation step implemented in M5E is employed in MTF.

4.1.2. Steps taken to ensure model tree forest is robust and computationally efficient

MTF attempts to not only perform well on complex, highly non-linear data but simpler data as well. The previous chapter showed that GASOPE, if correctly tuned, can generalise adequately to data comprising linear mappings between the input and output features. MTF, which incorporates GASOPE, also requires fine-tuning of its hyperparameters before being applied to a regression problem. To ensure MTF produces favourable results for both linear and non-linear cases, its robustness must be addressed.

Previously discussed approaches to increasing the robustness of a decision tree model were pruning and smoothing. Pruning was addressed in the previous section and omitted because the ensemble structure of MTF replaces the need for pruning. Smoothing is applied in decision trees, such as the M5 model tree, to minimise the discontinuities that are formed between the output of adjacent leaf nodes. The M5 model tree incorporates a smoothing function that is applied from the leaf node up the path to the root node, each time altering the final output based on the output of a given node on the path. This method of smoothing is previously described through Equation (2.3) in Section 2.3.2. Aleksovski's MTE, that comprised an ensemble of M5 model trees, improved on the smoothing process of the original M5 model tree through the use of fuzzification [1]. Fuzzification, as previously discussed in Section 2.5.3, employed Equation (2.12) to smooth the output of neighbouring leaf nodes through the use of a sigmoid function. As opposed to smoothing, which requires each node in the tree to encapsulate an output function, fuzzification only requires the leaf nodes of a decision tree to constitute an output function. This would allow for a lower computational cost, however, the computational cost is still prevalent. Aleksovski concluded that the modifications introduced to the original M5 model tree, including fuzzification, did not yield conclusive results [1]. Furthermore, smoothing and fuzzification were both applied to model trees that incorporated linear models. Linear models are more likely to produce discontinuities as opposed to non-linear models.

For MTF, computational cost is a major dictator in the freedom to which the model is allowed to increase in its complexity. All parameters and aspects of the induction algorithm of MTF should be designed to minimise computational cost. Therefore, the added computational cost of implementing smoothing, fuzzification, or a similar process into MTF, which utilises non-linear polynomials, is detrimental to its performance. This fact holds especially in the case of smoothing for which an output function is induced for each node within the model tree, not only the leaf nodes. By omitting the smoothing step, MTF is given an increased computational budget for the induction of the base learner model trees.

In the unlikely event that a polynomial evolved using GASOPE produces a poor approximation of the given data, MTF employs a baseline linear model comparison step in its induction algorithm. The baseline linear model comparison step evaluates the performance of the higher-order polynomial for a given leaf node against a simpler linear model and if the linear model is found to outperform the higher-order polynomial, the linear model is instead used to model the output for the given leaf node.

In the case where a model tree is induced that significantly decreases the accuracy of the ensemble, MTF includes an ensemble pruning step to ensure the accuracy of the final ensemble is not negatively effected. MTF calculates a vector of predicted outputs, $\boldsymbol{y'}$, for a given set of instances, X, as the uniformly weighted average over the predictions of each model tree within the ensemble:

$$\boldsymbol{y'}(X) = \frac{1}{n_t} \sum_{i=1}^{n_t} g_i(X) \tag{4.5}$$

where $\boldsymbol{y}'_i(X)$ denotes the predicted value of the i^{th} model tree within the ensemble, given the set X. The number of base learners within the ensemble is denoted by n_t. Ensemble pruning is implement as follows: the size of the ensemble is reduced by omitting, one by one, each base learner model tree from the output calculation described in Equation (4.5). If the validation set error metric of the ensemble model is improved with the omission of the base learner which is being evaluated, the base learner is permanently removed from the final ensemble. The addition of the baseline linear model comparison step together with ensemble pruning increases the robustness of MTF, ensuring MTF performs adequately on unseen data.

4.1.3. Pseudo code

In this section, the pseudo code that describes the induction of each MT as well as MTF is presented. The induction algorithm of a single MT is described in Algorithm 7.

Algorithm 7: Pseudo-code for MT induction.

```
Initialise root node, $N_0$.
Given the training set $D_t$ with $n$ instances,
initialise an empty set of nodes $Z = \{\}$
Let $Z = Z \cup N_0$
Call Grow($N_0, D_t$)

**Grow** ($N_i, D_i$):
**if** *stopping criteria is met* **then**
    Label $N_i$ a leaf node
    Parse $D_i$ to GASOPE
    Save the returned output function in $N_i$
**else**
    Select $\{g_1, g_2, .., g_n\}$ as a random subset of feature indexes from $D_i$
    Initialise $S = \{g_1, s_1\}$
    **for** $j = 1, .., n$ **do**
        **for** $k = 1, .., l$ **do**
            Select sample value $s_k$ from $D_i$
            Let $S' = \{g_j, s_k\}$
            Compute $SDR(S')$
            **if** $SDR(S') < SDR(S)$ **then** $S = S'$
        **end**
    **end**
    Initialise left child node, $N_L$, and right child node, $N_R$
    Split $D_i$ into $D_L$ and $D_R$ according to $S$
    $Z = Z \cup \{N_L, N_R\}$
    Grow( $N_L, TS_L$ )
    Grow( $N_R, TS_R$ )
**end**
```

The MT induction algorithm is described in Algorithm 8

Algorithm 8: Pseudo-code for MTF induction.

```
initialise empty ensemble array, $E = []$
Given the training set $D_t$
and the validation set $D_v$
while stopping criterion is not met do
    Randomly sample with replacement from $D_t$ to produce $D_\gamma$
    Call MT induction algorithm and parse $D_\gamma$
    Insert the returned MT into $E$
end

Compute a baseline $MSE$ on $D_v$
for $i$ = 1 to $|E|$ do
    Prune $MT_i$ from $E$
    Compute $MSE'$ on validation set
    if $MSE \times c_s > MSE'$ then reinsert $MT_i$ into $E$
end
```

A single MTF model comprises multiple MT base learners and a single MT further comprises multiple higher-order polynomial output functions evolved through GASOPE. Therefore, the MTF induction algorithm consists of three nested induction stages:

1. evolving polynomials with GASOPE,
2. MT induction and
3. MTF induction.

The MT induction algorithm incorporates a recursive node splitting function. Starting at the root node, multiple candidate splits are evaluated and unless stopping criteria are met, the best split is chosen. The best split maximises the reduction in standard deviation over the target values of the instances characterised by the split. For MTF the stopping criteria are either when a maximum tree depth is met, or when the number of instances on which to split is smaller than twice the minimum number of leaf instances. The latter is to prevent one of the children nodes from having less instances than the minimum number of leaf instances. Thereafter, each child node is evaluated for further splitting. Once stopping criteria for a node are met, the node is labelled a leaf node and the recursive splitting function continued on the remaining nodes. All splits that together define the decision tree structure of each MT is stored in a recursive set.

The i^{th} node, N_i, within a decision tree is described by the following set:

$$N_i = \{S, N_L, N_R, f_i(\boldsymbol{x})\} \tag{4.6}$$

where S is a set describing the splitting conditions for node N_i. N_L and N_R are the left and right children nodes of N_i and $f_i(\boldsymbol{x})$ is the function evolved by GASOPE defining the output of N_i for a given input vector $\boldsymbol{x}$. In the case of a leaf node S, N_L and N_R are left void, whilst

$f_i(\boldsymbol{x})$ is defined. For any other node, the opposite is true, i.e. only the $f_i(\boldsymbol{x})$ parameter is void, whilst S, N_L and N_R are defined. A split is defined through the set of two parameters:

$$S = \{g, s\} \tag{4.7}$$

where g is the index of the input feature on which to split and s is the value of the split. In a dataset with 10 features and 100 instances there are $10 \times 100 = 1,000$ possible splits initially. Evaluating a proposed split through Equation (4.1) returns a value that represents the standard deviation reduction (SDR) of the proposed split. The optimal split for a given dataset is computed by iterating through each feature as well as the corresponding sample value and calculating the SDR of the proposed split. The split with the highest SDR is selected as the optimal split. For MTF, splits are computed on a random subset of the feature space to decorrelate the base learners within MTF.

The induction of MT for a given path is halted when stopping criteria are met. Once stopping criteria are met, the applicable node is labelled a leaf node and the data within the leaf node. The data subset associated with a leaf node is determined through the splits on the path from the root node to the leaf node. GASOPE evolves the output function that is stored in the leaf node. Thereafter, GASOPE compares the evolved polynomial to the baseline linear function. The accuracy of both functions are compared through the MSE scores on the training data within the leaf node. Finally, the function which minimises the MSE is returned by GASOPE.

When MTF induces an entire forest of model trees, Algorithm 7 is executed on several bootstrapped subsamples of the training set. Each bootstrap subset is selected with replacement. Once the stopping criterion is met, the induction phase concludes. For MTF the only stopping criterion is the maximum ensemble size.

After the first phase follows the ensemble pruning phase. At the start of the ensemble pruning phase, a baseline MSE is calculated on the validation set. MTF employs a greedy pruning step where each MT in the ensemble is individually omitted from the ensemble and the MSE on a validation set thereafter calculated. If the MSE with the respective tree omitted is significantly smaller than the baseline MSE, the tree is permanently pruned from the ensemble. For an increase in MSE to be regarded as significant, the MSE must have increased with at least a factor of c_s, where $c_s = 1 + \frac{1}{|E|}$. Here $|E|$ refers to the ensemble size. The value of c_s was chosen such that MTs must increase the MSE of the ensemble by a factor greater than their weight within the ensemble. For example, an ensemble comprising 20 MTs requires that a single MT increase the MSE score with more than 5% to justify pruning it away.

Figure 4.1 illustrates the complete MTF induction algorithm. Figure 4.2 illustrates the bagging process employed by MTF to induce the base learners and produce an output from the ensemble.

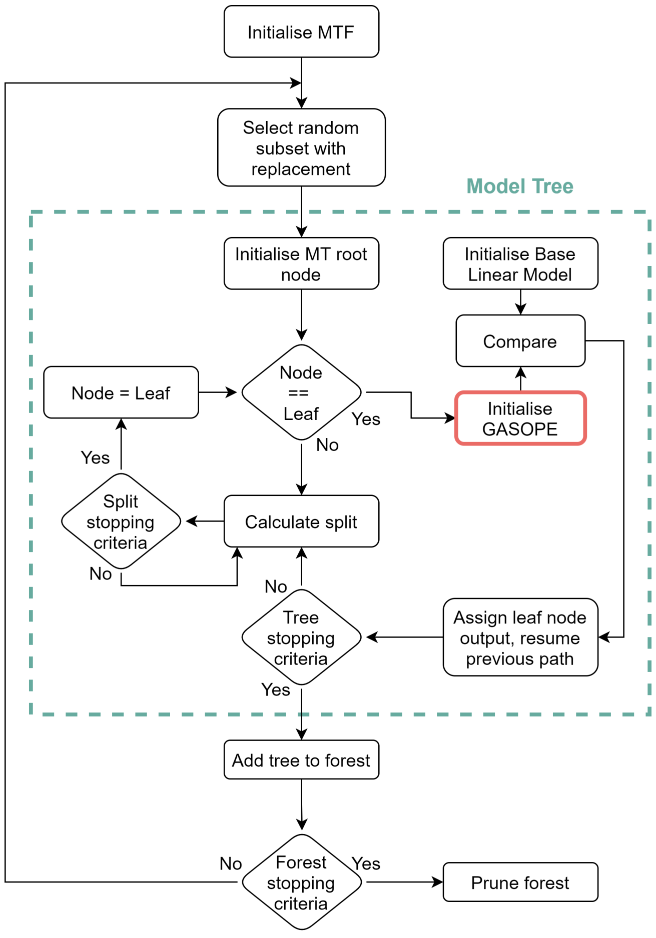

Figure 4.1: Illustration of the MTF induction algorithm.

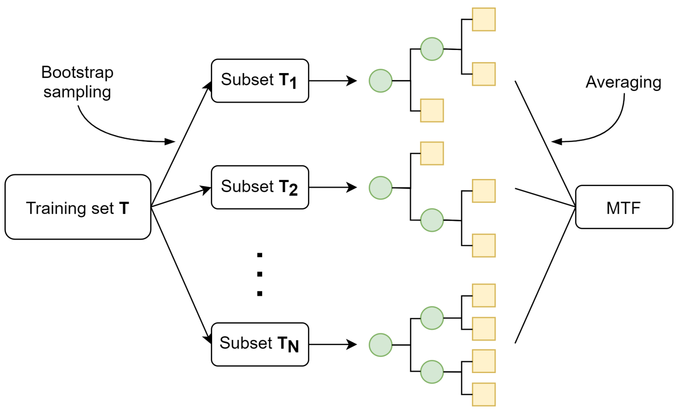

Figure 4.2: Illustration of the MTF bagging and output calculation.

4.2. Hyperparamater tuning

This section discusses the tuning of all hyperparameters applicable to MTF. The hyperparameters are listed and the experimental procedure to follow for the tuning thereof is discussed in Section 4.2.1. Next, Section 4.2.2 analyses the linearity of each dataset on which the accuracy of MTF is evaluated to tune the maximum polynomial order parameter. Section 4.2.3 presents the tuning of the maximum tree depth of the base learners of MTF as well as the analysis of computational costs associated with the induction of MT. Finally, Section 4.2.4 presents the tuning of the final hyperparameter of MTF, namely ensemble size.

4.2.1. Experimental procedure

The GASOPE hyperparameters were previously tuned for in Section 3.2. However, as stated, careful consideration should be given in choosing the maximum polynomial order for a given problem. For each unique dataset on which MTF is applied, an analysis of the best performing maximum polynomial order is first performed. The remaining parameters of MTF are:

1. Number of splitting features,
2. minimum number of leaf instances,
3. maximum depth and
4. ensemble size.

During the conceptualisation of random forest, Breiman proposed the number of splitting features for each node equal $\log_2(m+1)$ where m is the dimensionality of the feature space [6]. This value was approximated to $\sqrt{m}$ for classification problems and $m/3$ for regression problems. Therefore, a value of $m/3$ was chosen for the number of splitting features for MTF.

The next hyperparameter, minimum number of leaf instances, is dependant on the least-squares algorithm. The Python package used to implement least-squares approximation in GASOPE, SciPy, incorporates the Leven-Marquardt (LM) algorithm to solve the non-linear least-squares problem, previously described through Equation (3.7). The prerequisite for the implementation of the LM algorithm is that the number of training instances is greater than the number of coefficients to solve for. Therefore, the minimum number of leaf instances should always be at least greater than the number of features in the dataset. In the case of GASOPE, the number of leaf instances should be greater than the number of terms used, specifically, 10. However, the polynomials describing a given individual are given the freedom of exceeding the number 10, if doing so results in increased fitness. In most cases, it is rare for the polynomial to grow substantially beyond 10 as the fitness function, described in Equation (3.9), punishes individuals with increased terms. In conclusion, a value of 20 is assigned to the minimum number of leaf instances to accommodate for an increase in polynomial terms. It is worth noting that minimising the value for the minimum number of leaf instances allows for an increased number of evaluated splits during training.

To tune the remaining applicable hyperparameters, ten datasets each with a unique composition are selected from the UCI Machine Learning Repository and the L. Torgo Repository [25]. Six of the datasets were present in the testing of GPMCC. The additional four datasets are chosen to expose MTF to big data problems. The ten datasets are listed in Table 4.1 with their attributes.

Table 4.1: Benchmark datasets used for tuning of MTF.

Dataset	Number of features (N = Nominal, C = Continuous)	Number of instances
Abalone	1N 7C	4,177
Auto-MPG	3N 4C	398
Boston housing	0N 13C	506
California housing	0N 8C	20,460
CASP	0N 9C	45,730
Elevators	0N 18C	16,559
Friedman artificial domain	0N 10C	40,768
Machine CPU	0N 6C	209
MV artificial domain	3N 7C	40,768
Servo	4N 0C	167

The hyperparameters that require individual tuning for each dataset are maximum polynomial order, maximum depth and ensemble size. From these hyperparameters, it is clear that computational cost heavily influences the optimal chosen value. For each hyperparameter, increasing its value increases the computational cost of MTF. For the maximum depth as well as maximum polynomial order, an increased value also increases the complexity of a given base learner and thereby contributes to an increased variance error. Although increasing the ensemble size helps reduce this variance error, it also significantly increases the computational cost for each additional base learner that is induced. Therefore, it is beneficial to tune maximum polynomial order and maximum depth first.

Each of the three hyperparameters is associated with different stages of MTF. The maximum polynomial order applies to GASOPE, maximum depth to MT and the ensemble size to MTF as a whole. Therefore, the hyperparameters may be tuned for individually, eliminating the need for a grid search based tuning approach.

4.2.2. Maximum polynomial order

For maximum polynomial order, values of one, two and three are compared. Maximum polynomial order tuning serves as an estimation of the non-linearity of a dataset. By inducing GASOPE models of one, two and three maximum polynomial order on the entire training set and comparing the results on a generalisation set, the linearity of the dataset is effectively estimated. The polynomial order of the best performing GASOPE instance is thereafter chosen as the maximum polynomial order for MTF.

The error metric used to evaluate the performance of GASOPE for a given maximum polynomial order value on a specific dataset is MSE as described in Equation (2.5). For each given hyperparameter value and dataset, GASOPE is trained on a training set and the MSE is calculated on a generalisation set for 30 independent runs. The training set and generalisation set are split 80:20. Figure 4.3 shows across the following pages the MSE GASOPE scored on the generalisation set for each dataset for a varying maximum polynomial order.

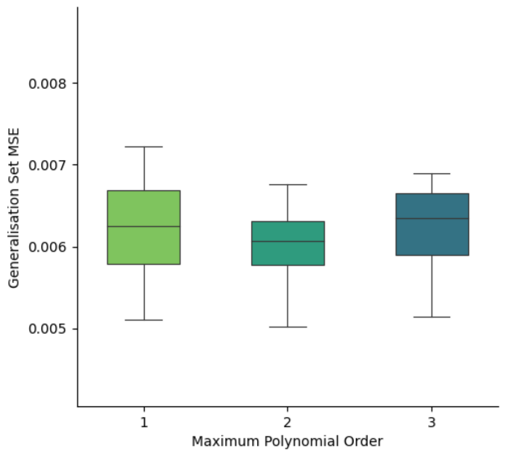

(a) Abalone

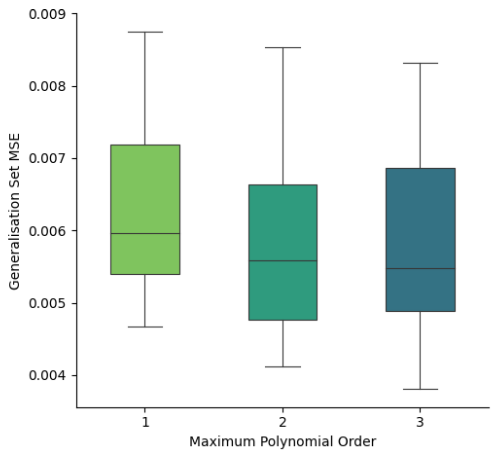

(b) Auto-MPG

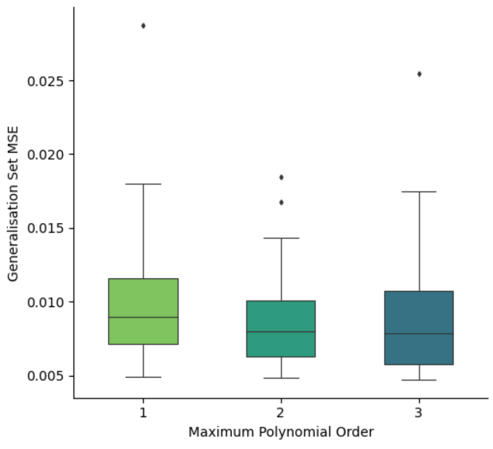

(c) Boston housing

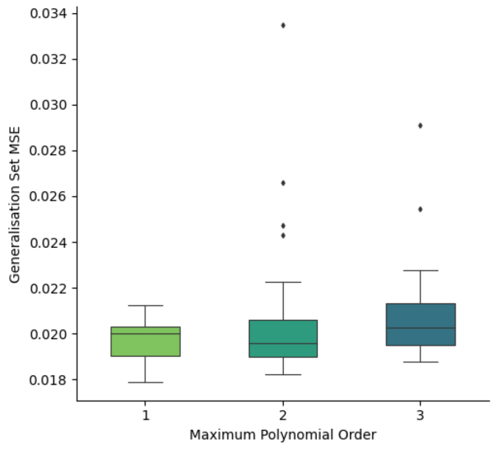

(d) California housing

Figure 4.3: MSE of GASOPE for varying degrees of maximum polynomial order on the benchmarking datasets.

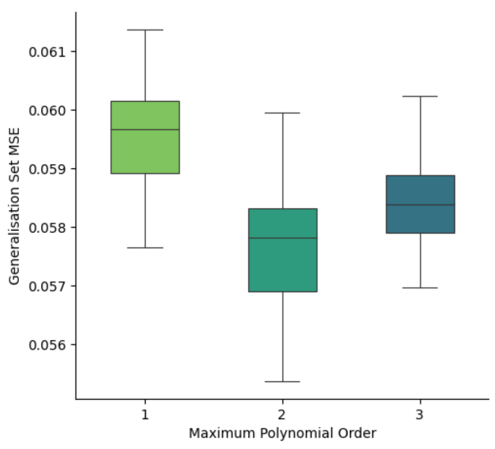

(e) CASP

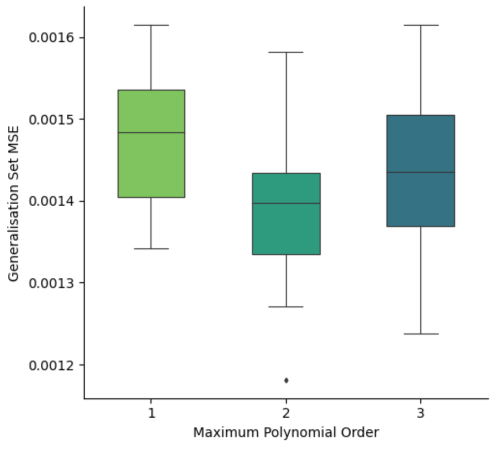

(f) Elevators

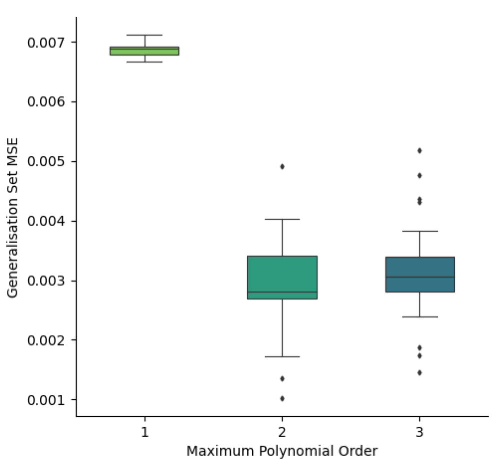

(g) Friedman artificial domain

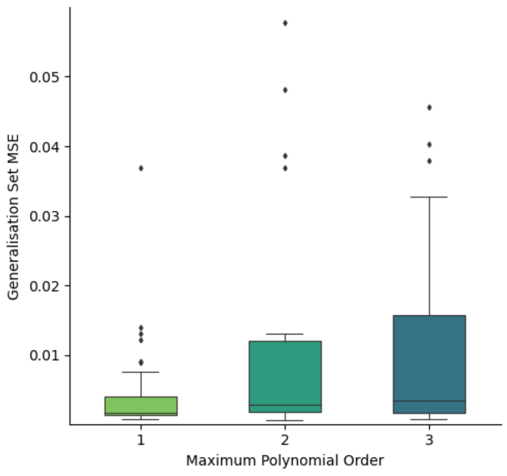

(h) Machine CPU

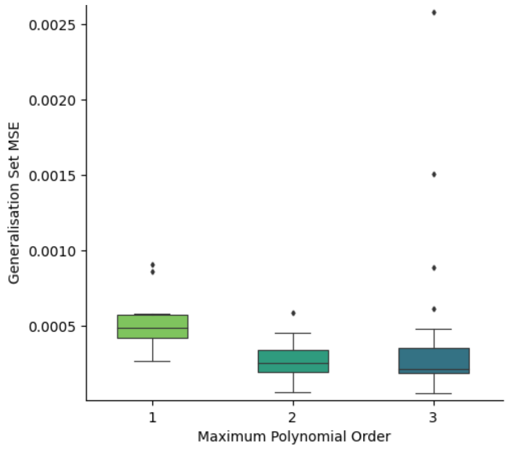

(i) MV artificial domain

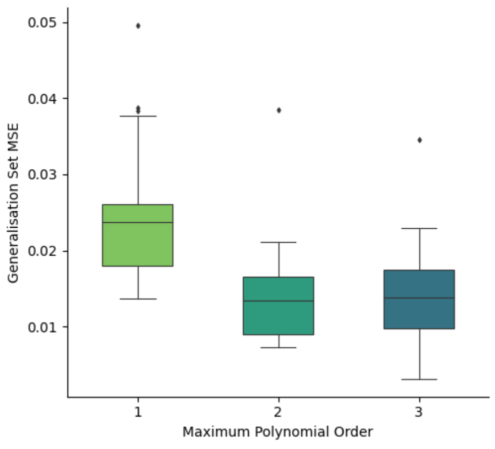

(j) Servo

Figure 4.3: (continued)

The maximum polynomial order that produced the lowest MSE for each dataset is chosen as the final parameter value. For the majority of datasets, a value of two resulted in the lowest MSE. Only the Machine CPU dataset favoured a maximum polynomial order of one. This shows that the datasets chosen for the testing of MTF are all non-linear except for the Machine CPU dataset. However, the minority of datasets are highly non-linear, because only three of the ten datasets favours a maximum polynomial order of three.

It is worth noting that assigning a maximum polynomial order higher than the favourable value is not fatal to the performance of the algorithm because the fitness function of GASOPE penalises higher-order functions that do not significantly improve the error metric when compared to a lower-order function. For the cases where there is little discrepancy between the MSE for maximum polynomial orders values of one and two, two is chosen as the preferred value. Two is also chosen due to the base linear models that are used as a fallback if the output function evolved through GASOPE performs poorly on the given set of data instances.

Appendix A lists the values portrayed in Figure 4.3 in full. Additionally, the average computational time of each dataset is listed.

4.2.3. Maximum model tree depth

The maximum depth of MT has a large influence on the computational cost as well as the variance error of MTF. The larger a decision tree is grown, the more likely it is to overfit the training set. In conjunction, the larger a decision tree is grown, the higher the number of leaf nodes are. For MTF, each additional leaf node present in MT requires a polynomial be evolved on the data characterised by the leaf node. It is therefore beneficial for the MTF induction algorithm to cap the depth of MT at a specific value, to combat high computational costs. An unintended consequence of limiting the depth is a further reduction in the variance error of MTF. In the case of traditional regression trees, prematurely limiting the depth of the tree results in a significant increase in bias error. However, with MTF this increase is minimal due to the already complex composition of GASOPE.

The error metric used to evaluate the performance of the base learners within MTF, for a given maximum depth on a specific dataset is MSE. For each given hyperparameter value and dataset, MT is trained on a training set and the MSE is calculated on a generalisation set for 30 independent runs. The training set and generalisation set are split 80:20. The computed MSE on the generalisation set is shown for each dataset in Figure 4.4 across the following pages.

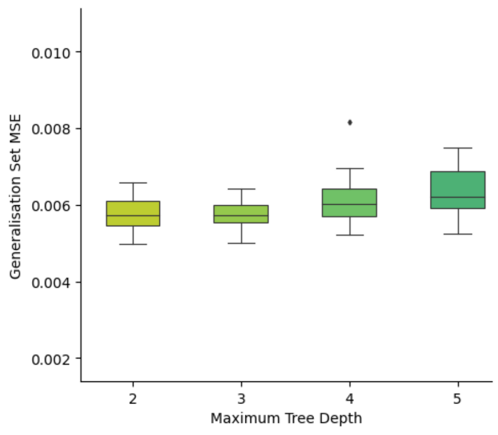

(a) Abalone

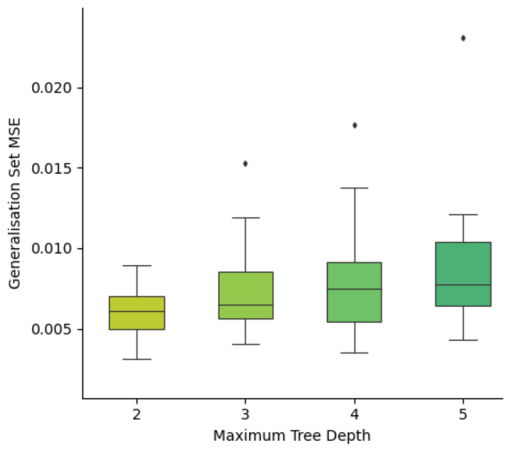

(b) Auto-MPG

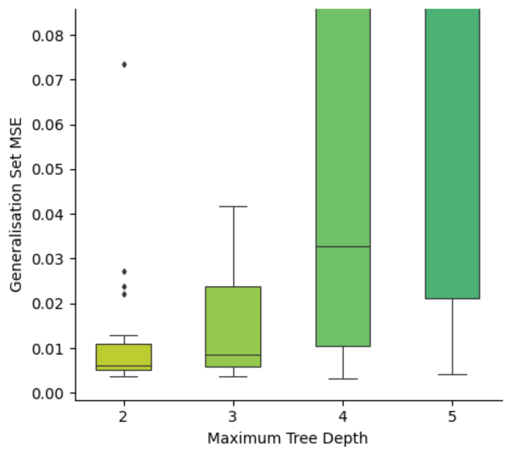

(c) Boston housing

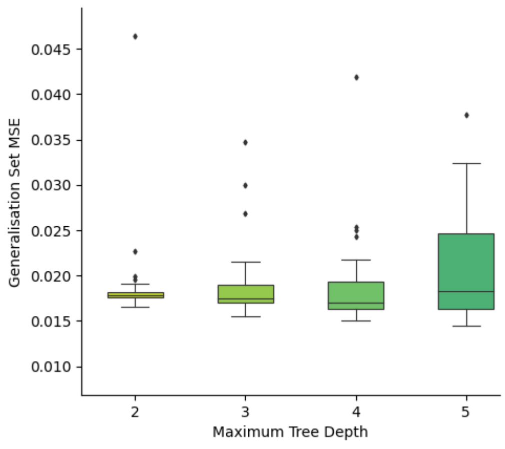

(d) California housing

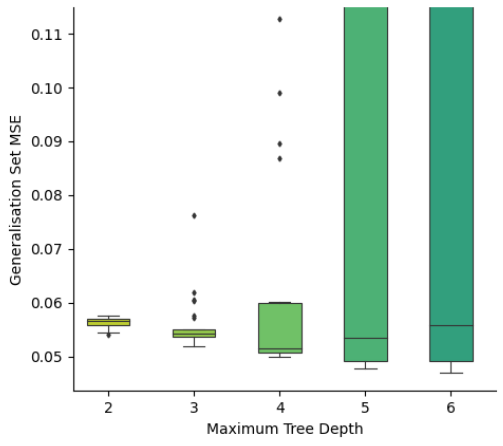

(e) CASP

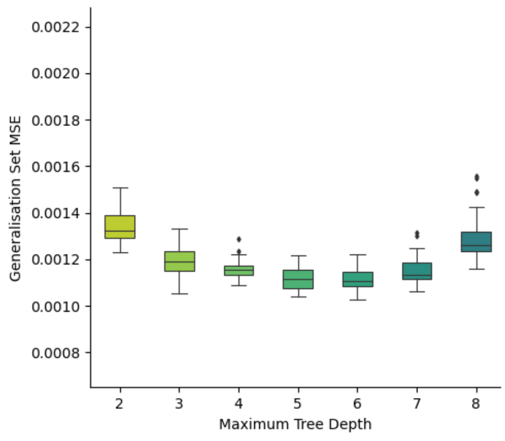

(f) Elevators

Figure 4.4: MSE of MT for varying degrees of maximum tree depth on the benchmarking datasets.

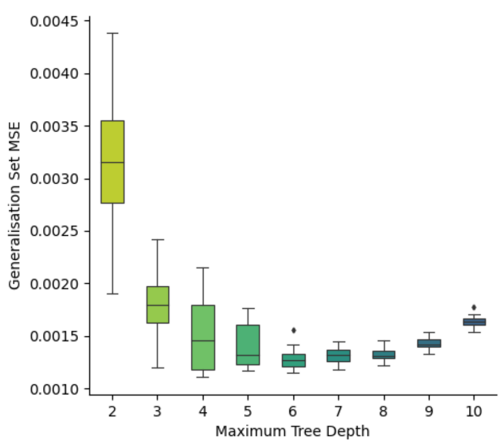

(g) Friedman artificial domain

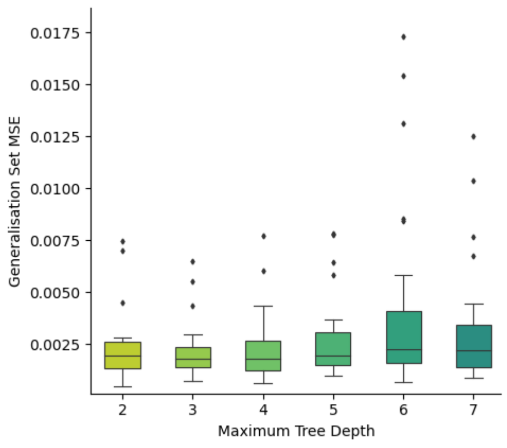

(h) Machine CPU

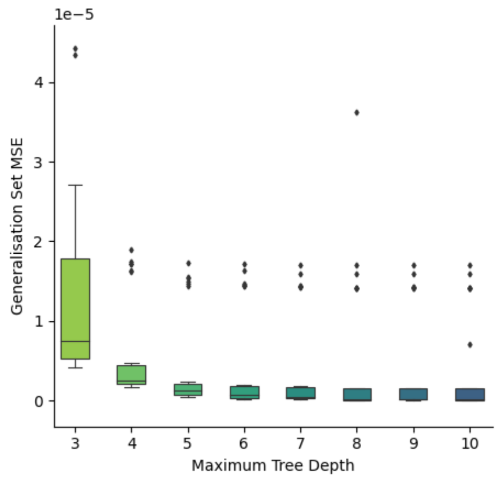

(i) MV artificial domain

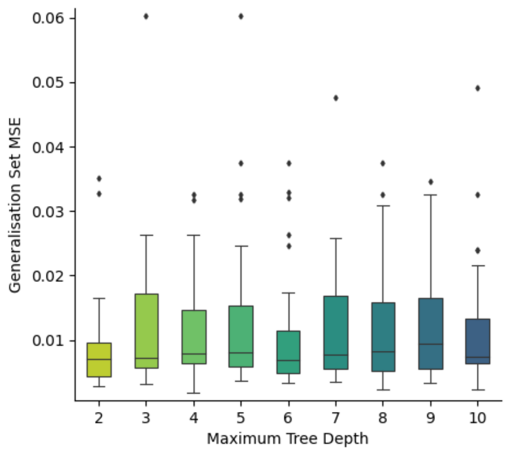

(j) Servo

Figure 4.4: (continued)

For a single model tree, there is an optimal maximum depth that produces the best performing MSE on the generalisation set. This value differs depending on the data given to the induction algorithm. Allowing trees to grow beyond this value would increase the MSE for a single model tree, however, if multiple model trees are bagged in an ensemble the increase in MSE is reduced. It is still favourable to limit the depth of a single model tree to help reduce the computational cost and allow for more trees to be induced in the ensemble.

For illustrative purposes severe outlier results are omitted in the boxplots of Figure 4.4. Tables B.1 through B.10 in Appendix B show the complete results. Linear base models were enabled in these results to ensure the model trees were tuned appropriately. Tests were also run where linear base models were disabled to show the difference in the tuning results. These alternative results are shown in Appendix B. Incorporating linear base models brought more consistency to the results.

Figure 4.5 shows across the following pages how the computational cost increased in execution time as the maximum depth of the model tree is increased . In smaller datasets, the execution time is shown to plateau off after a given value. This is explained through the minimum number of leaf instances value that prohibit the remainder of the dataset to be split on further during the induction process. For example, in Figure 4.5b beyond a maximum tree depth value of six, the execution time no longer increases. Each time a model tree was induced on the dataset, the number of instances in a node with a depth of six is smaller than twice the minimum number of leaf instances, prohibiting the node from being split on further by the induction algorithm. For larger datasets, such as Abalone and California Housing, the execution time can be seen growing exponentially, confirming the need to keep the tree depth and consequently computational cost at a minimum.

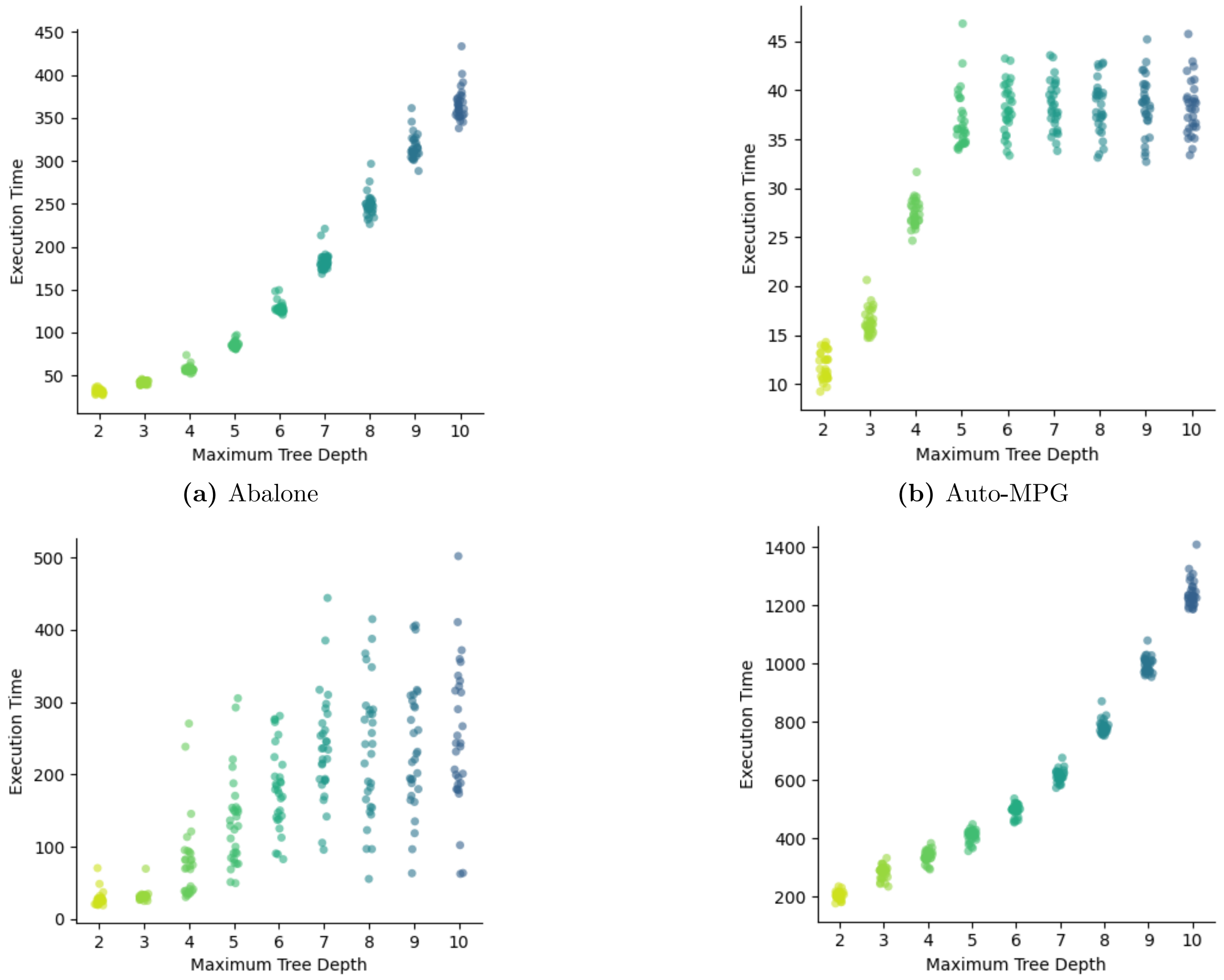

(a) Abalone

(b) Auto-MPG

(c) Boston housing

(d) California housing

Figure 4.5: The computational cost of MT for varying degrees of tree depth on the benchmarking datasets.

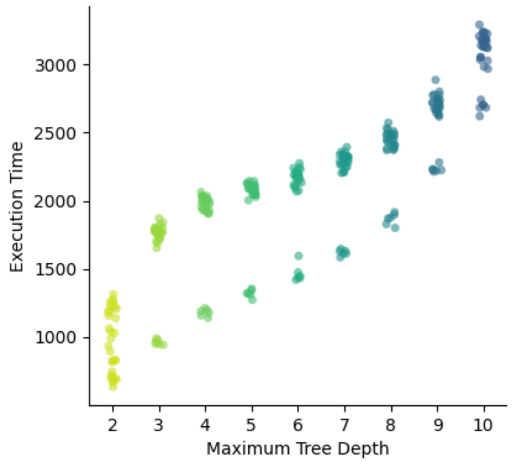

(e) CASP

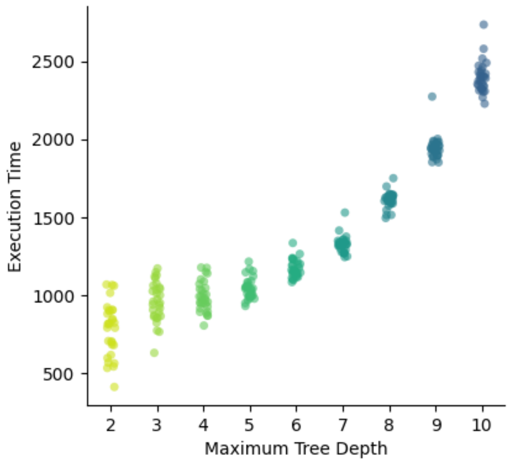

(f) Elevators

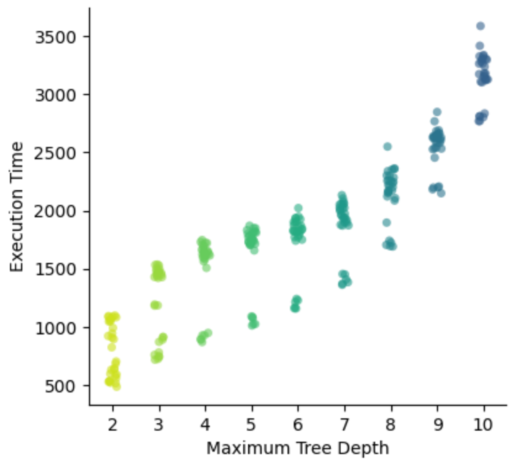

(g) Friedman artificial domain

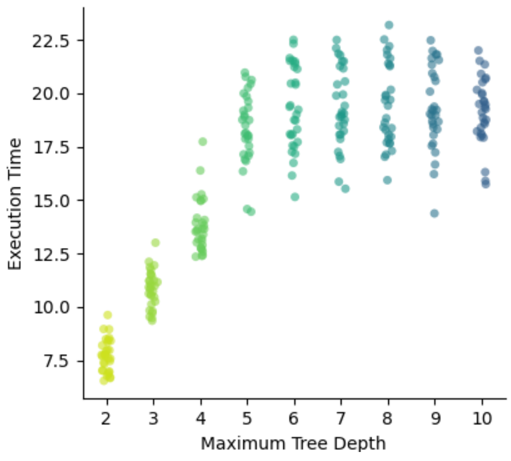

(h) Machine CPU

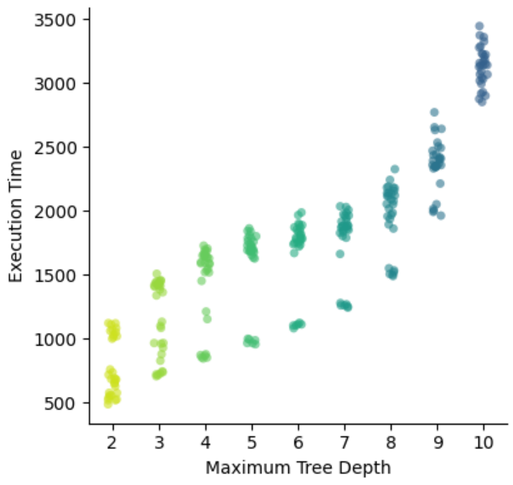

(i) MV artificial domain

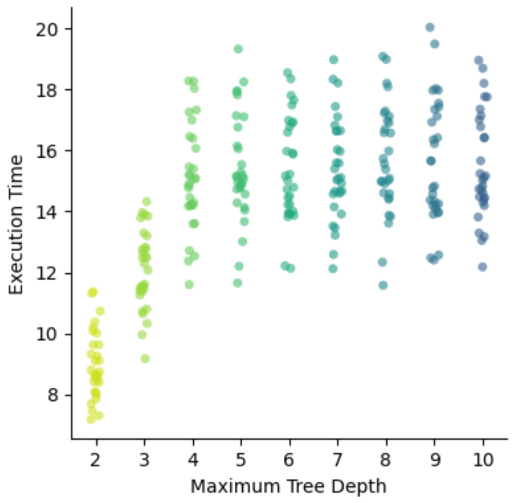

(j) Servo

Figure 4.5: (continued)

4.2.4. Ensemble size

The error metric used to evaluate the performance of MTF for a given set of hyperparameter values on a specific dataset is MSE. For each given hyperparameter value and dataset, MTF is trained on a testing set, pruned using the validation set and the MSE is calculated on a test set for 30 repeated runs. The training set, validation set and test set are split 80:10:10.

The MSE scored by MTF on the test set for each consecutively added model tree in the ensemble is portrayed in Figures 4.6 through 4.15. For smaller datasets where computational expenses are more lenient, the ensemble is grown beyond 30. The results are shown in full in Appendix B.

Take note of the high offset observed in the MSE for the minority of the 30 runs, shown through outliers. This effect can be clearly observed in Figures 4.7 and 4.8 This is due to one or two model trees in the ensemble performing exceptionally poor and biasing the average prediction significantly enough to compromise the ensemble as a whole. As the ensemble is increased, the effective weight such a tree has on the ensemble decreases, however with each additionally induced model tree there is the risk of adding another poorly performing tree. Furthermore, the computational costs associated with growing ensembles large enough to reduce this effect is quite high. It is for this reason that ensemble pruning is implemented in MTF as opposed to increasing the ensemble size. Ensemble pruning is performed via the validation set and retroactively in the induction algorithm of MTF.

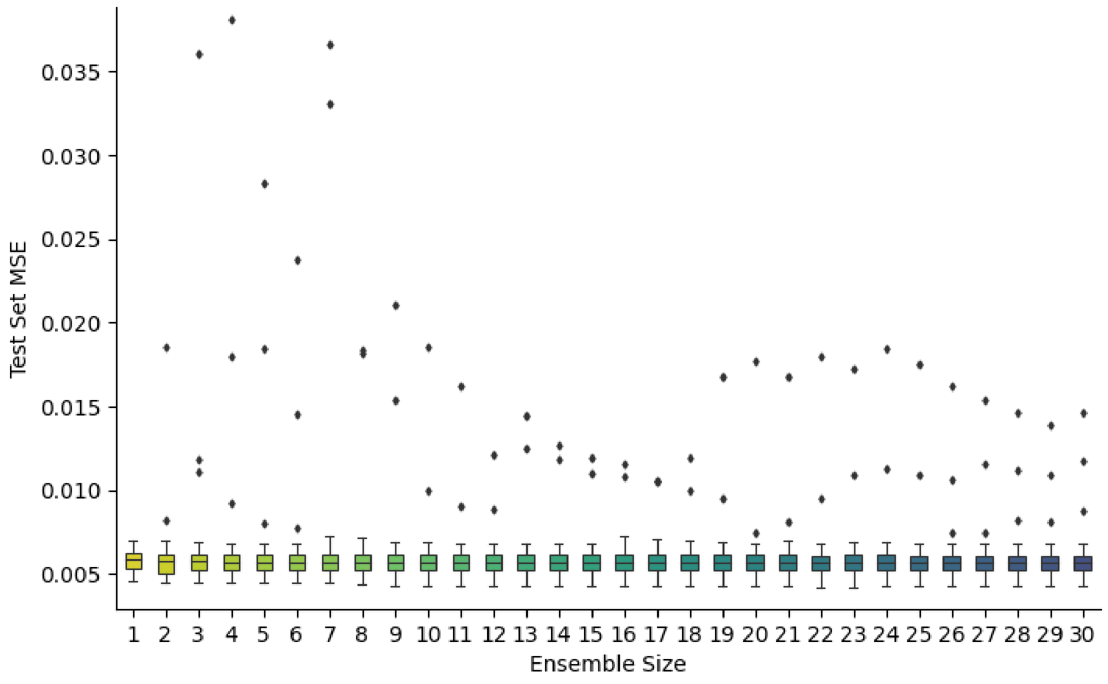

Figure 4.6: Abalone: MSE vs ensemble size of MTF.

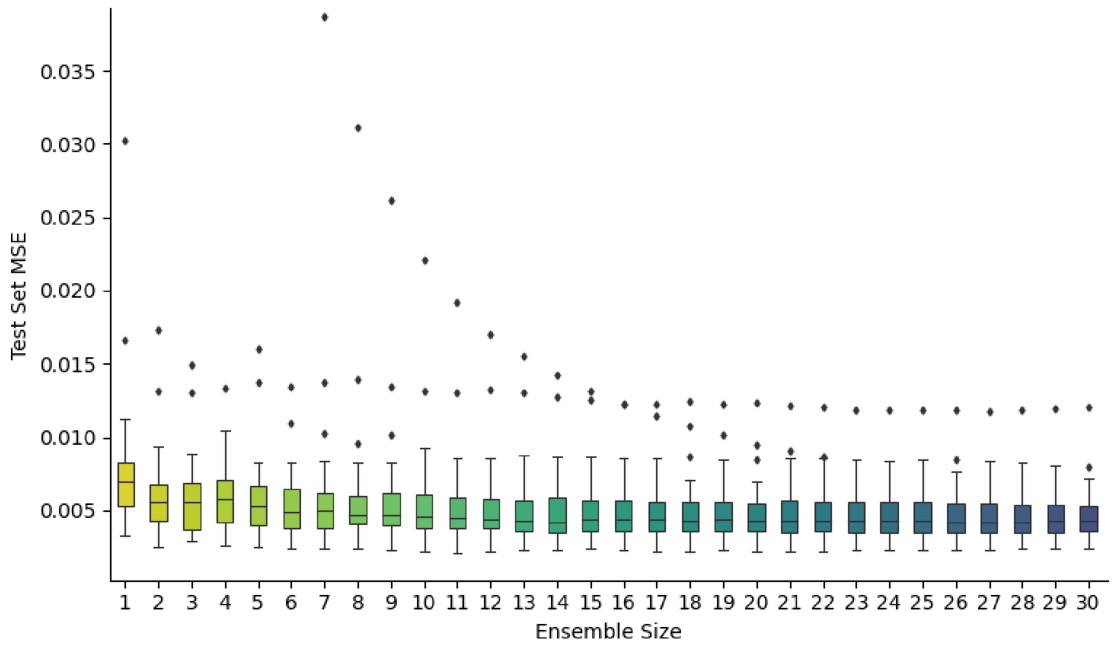

Figure 4.7: Auto-MPG: MSE vs ensemble size of MTF.

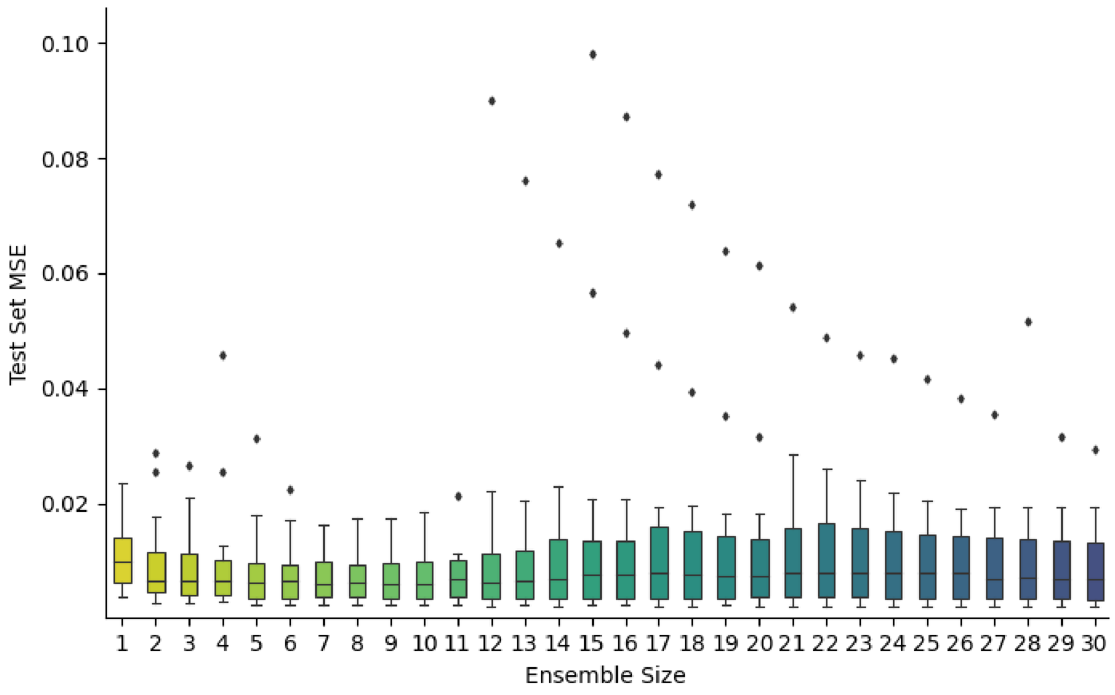

Figure 4.8: Boston Housing: MSE vs ensemble size of MTF.

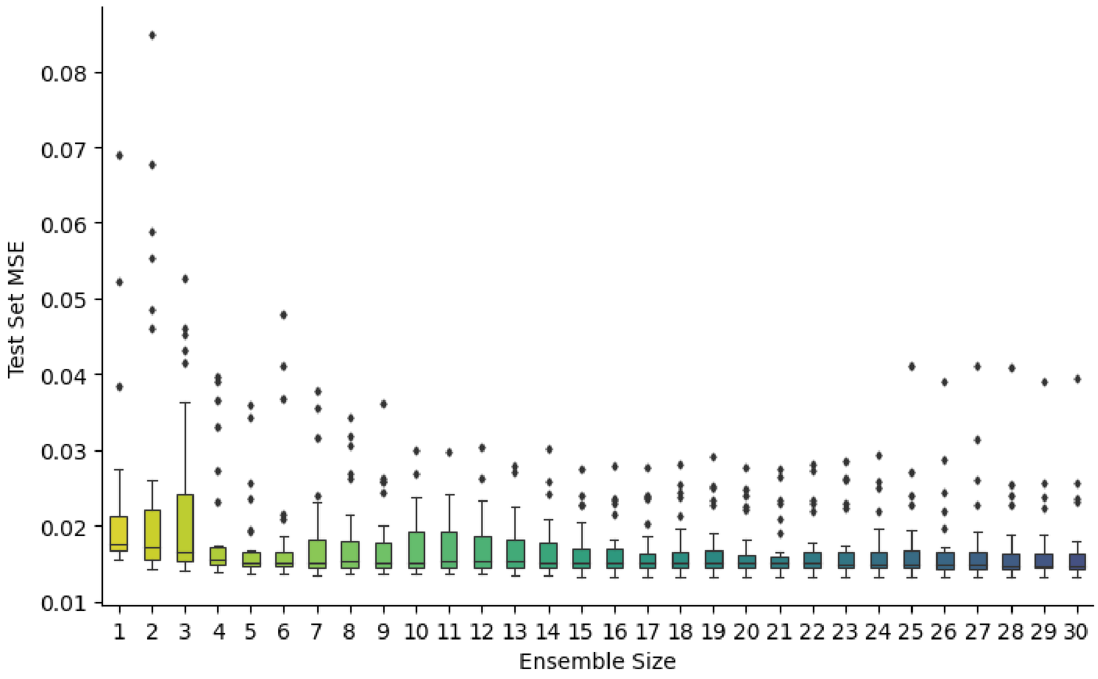

Figure 4.9: California Housing: MSE vs ensemble size of MTF.

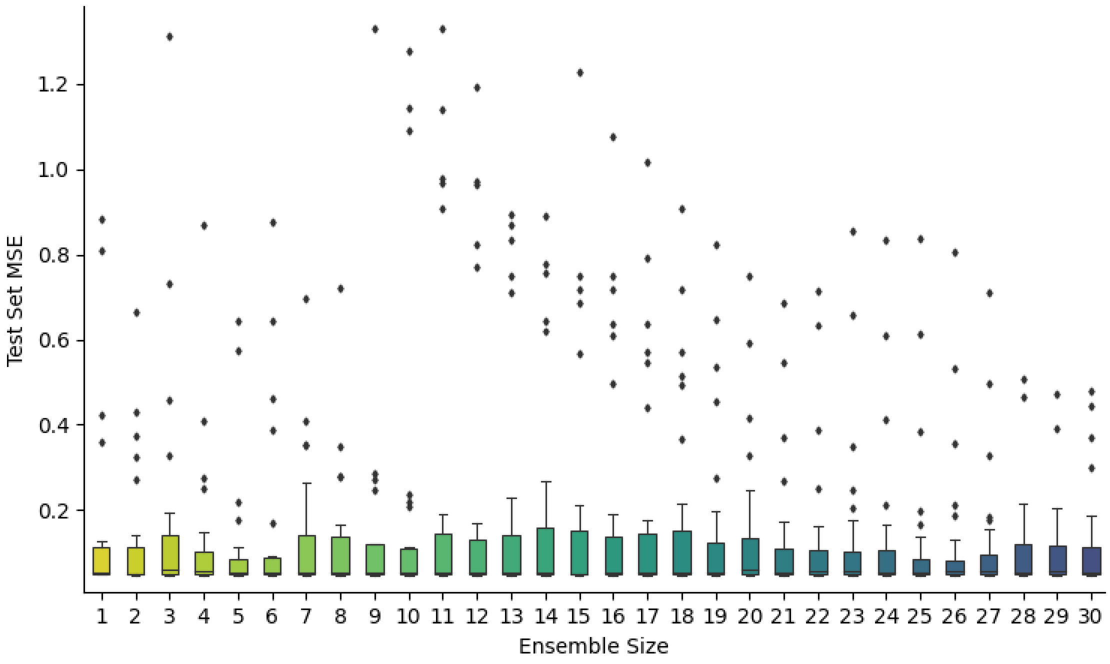

Figure 4.10: CASP: MSE vs ensemble size of MTF.

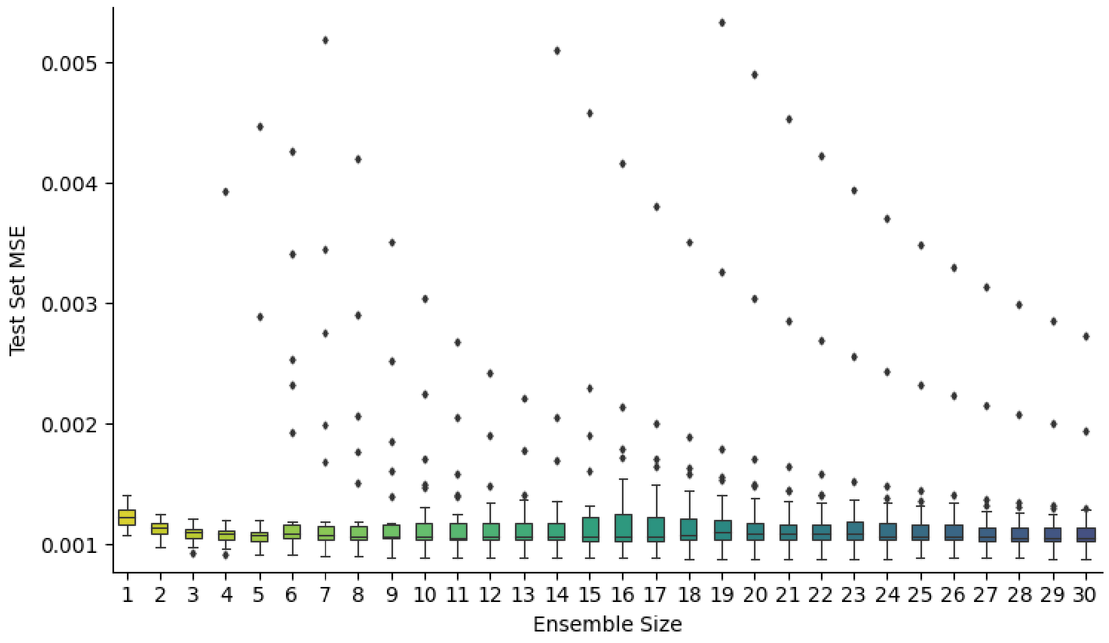

Figure 4.11: Elevators: MSE vs ensemble size of MTF.

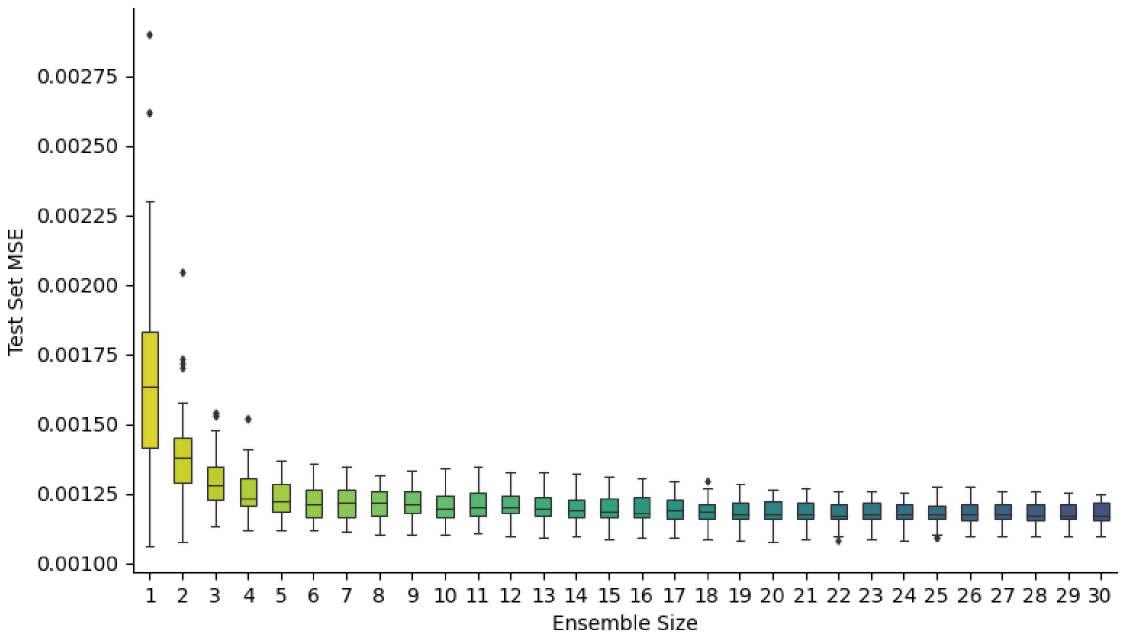

Figure 4.12: Friedman Artificial Domain: MSE vs ensemble size of MTF.

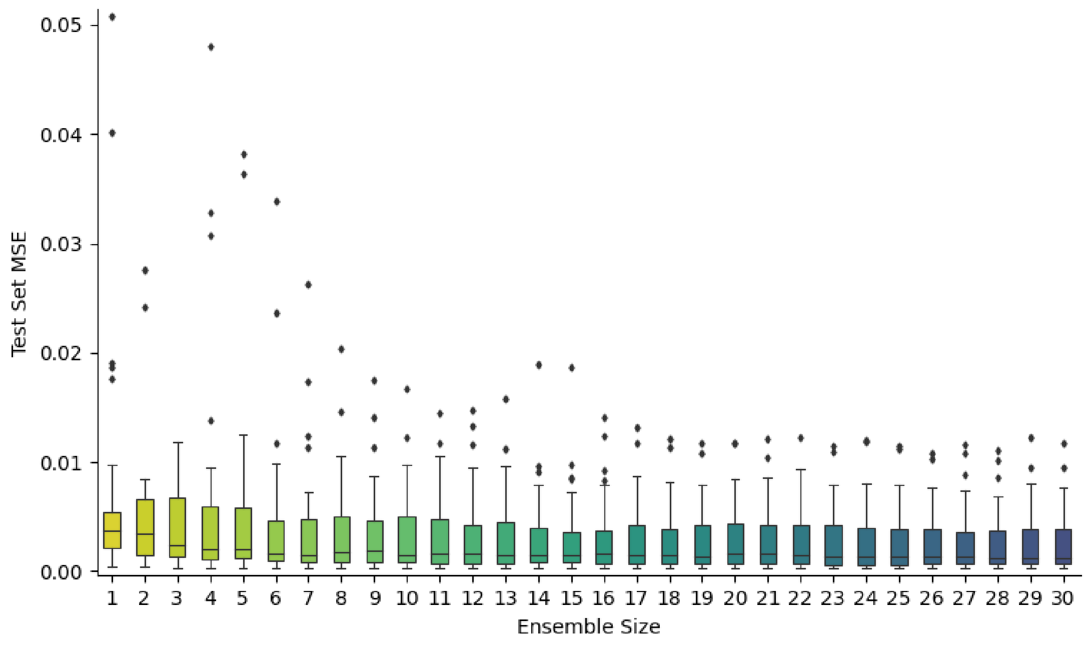

Figure 4.13: Machine CPU: MSE vs ensemble size of MTF.

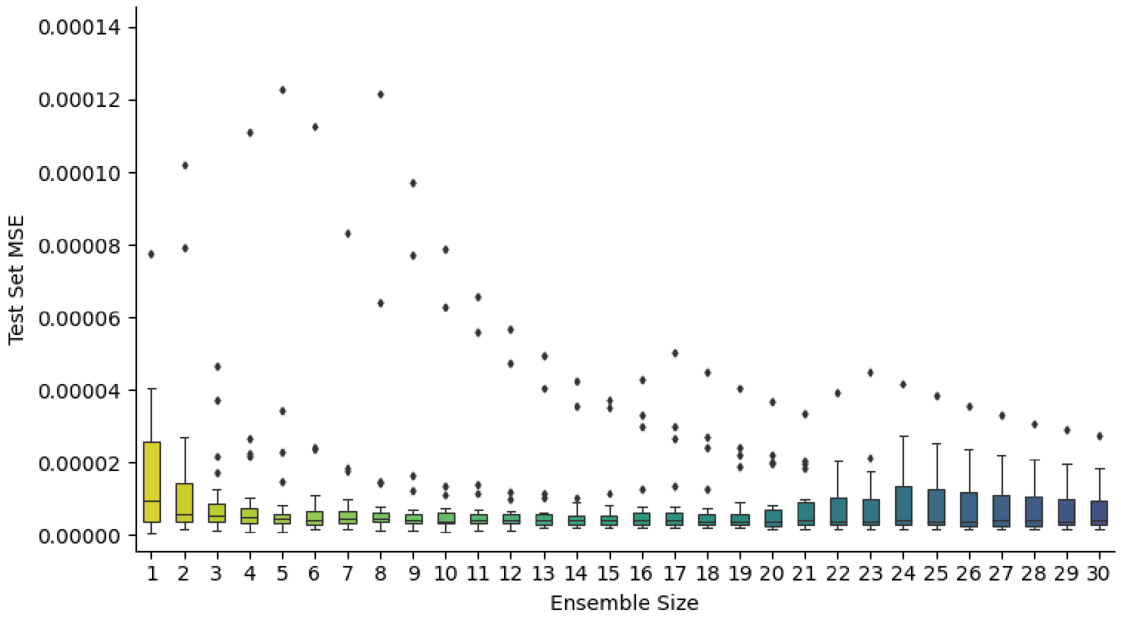

Figure 4.14: MV Artificial Domain: MSE vs ensemble size of MTF.

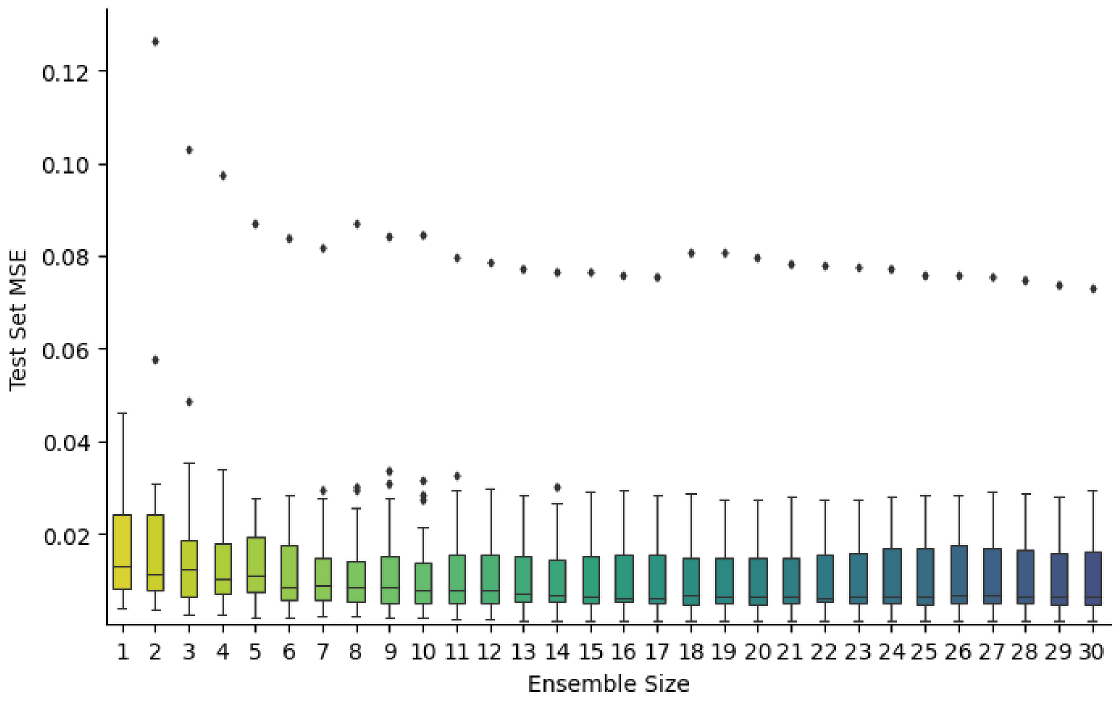

Figure 4.15: Servo: MSE vs ensemble size of MTF.

The results shown in this section confirm that the use of decorrelated model trees in an ensemble effectively reduces the high variance error of MT and produced a lower MSE as an ensemble. The ensemble size at which the MSE starts to converge is lower than initially anticipated, compared to random forest models which typically start with a minimum ensemble size of 100. The error in prediction for the majority of datasets plateaus off by an ensemble size of 20, excluding the outlier results that are handled through ensemble pruning.

The reasons hypothesised for the smaller required ensemble size compared to other decision tree-based ensembles such as random forest can be explained through the bias and variance dilemma. The base learners of random forest, which are regression trees with constant values within a leaf node, exhibit higher bias errors compared to model trees due to the reduced complexity. Therefore, a larger number of base learners are required to produce a good fit of the data that tends to be non-linear in its composition. Model trees, which exhibit extremely low bias errors, when ensembled start with a lower combined bias error and therefore converge quicker with each additional base learner in the ensemble. The number of model trees required to significantly reduce the high variance error is minimal in comparison to the number of regression trees required to reduce a bias error together with the variance error. Decorrelation of decision trees in an ensemble is an extremely effective method to reduce a high variance error. A single model tree already houses enough complexity to adequately model the majority of the datasets, however, multiple model trees are still required to help reduce the variance error.

In the conceptualisation of bagging predictors, Breiman suggested for a decision tree ensemble that makes use of bagging to perform regression, the ensemble size is optimal at a value around 25 [5]. After this number the advantages of bagging started to diminish, which is confirmed by the results in this section.

4.3. Conclusion

This chapter conceptualised the entire induction algorithm of MTF as well as defined and optimised each applicable hyperparameter of MTF. The best performing hyperparameter values for MTF on each of the ten benchmark datasets are listed in Table 4.2 together with the attributes of the dataset.

Table 4.2: Chosen hyperparameter values of MTF for each benchmark dataset.

Dataset	Maximum Polynomial Order	Maximum Tree Depth	Number of features	Number of instances
Abalone	2	3	1N 7C	4,177
Auto-MPG	3	2	3N 4C	398
Boston housing	3	2	0N 13C	506
California housing	2	4	0N 8C	20,460
CASP	2	2	0N 9C	45,730
Elevators	2	6	0N 18C	16,559
Friedman artificial domain	2	6	0N 10C	40,768
Machine CPU	1	3	0N 6C	209
MV artificial domain	2	6	3N 7C	40,768
Servo	3	2	4N 0C	167

Model trees that are confined to a maximum tree depth of two are referred to as stumps. In the case of datasets that are relatively small in size, i.e. less than a thousand instances, it is clear that MTF favours stumps for its base learners. The only exception to this is for Machine CPU where the maximum tree depth that produces the best result is only one greater. For datasets with few training instances, it seems that partitioning the feature space through too many splits result in degraded performance. It is hypothesised that the reason for this is the likeliness of decision trees to overfit data. For larger datasets, there are more training instances to generalise for during induction, which allows for deeper trees to be grown without these consequences. The exception to this is tree stumps being favoured for CASP, possibly due to an increase in noise over other large datasets.

Chapter 5

Experimental Results

In this chapter, MTF is compared against five state-of-the-art regression models on ten benchmarking datasets. The results provide insight into the potential and flexibility of MTF to produce good accuracy on different problems. The chapter is outlined as follows. Section 5.1 discusses the empirical method used, the selection and tuning of competing models as well as the selection of the datasets on which testing is performed. The hyperparameters of each model are listed and tuned for to ensure the models perform to the best of their ability. Next, the test results are shown in Section 5.2. Multiple error metrics are presented to provide conclusive results as to which model performed best in regards to different criteria. This section is concluded with the statistical significance of the findings through statistical tests. Finally, the conclusions this chapter brings forth regarding the performance of MTF are discussed in Section 5.3.

5.1. Empirical method

This section discusses the series of experiments designed and followed to evaluate the accuracy of MTF against other established regression techniques in terms of their predictive accuracy. The datasets used for evaluation are discussed in Section 5.1.1. Thereafter the selection and tuning of competing models are discussed in Section 5.1.2. MTF does not require any further tuning because this was already discussed in the previous chapter. The empirical method used for the testing of MTF strives to be as elaborate as possible through repetition and variation.

5.1.1. Datasets

To ensure the testing of MTF is thorough, ten datasets each with a unique composition are obtained from the UCI machine learning repository and the L. Torgo Repository [25]. Six datasets from the original testing of GPMCC are selected and an additional four datasets are chosen to expose MTF to big data problems. All datasets contain a single numerical target feature that a given regression model is assigned with predicting based on a set of input feature that may be nominal or continuous.

Large datasets are defined here as datasets comprising more than 10,000 instances. In the original testing of GPMCC, only one large dataset was present from the UCI Machine Learning Repository, namely Elevators. The other two large datasets were artificially generated. At the time, there was a lack of sufficient large databases covered by the UCI Machine Learning Repository [18]. For the testing of MTF, there are additional large benchmarking datasets available namely Physicochemical Properties of Protein Tertiary Structure (CASP) and California housing. Two large artificial datasets are also used in the testing of MTF which are the MV artificial domain and Friedman artificial domain. The first was used by Torgo in comparing the performance of PLT and MARS, two favourable regression techniques at the time [24]. The second artificial dataset was used by Friedman in the conceptualisation of MARS as well as the evaluation of bagging predictors [5, 10].

The ten datasets were chosen to ensure all degrees of dimensionality are covered during testing. The number of features ranges from a minimum of 4 to a maximum of 18. Decision tree-based methods are expected to have the advantage of embedded feature selection on the higher dimensional datasets. The datasets have varying degrees of linearity, as shown in the previous chapter through the tuning of the maximum polynomial order of MTF. The difference in the linearity of the datasets ensures the ability of MTF to adapt to varying degrees of complexity and dimensionality of data is evaluated. The ten datasets are listed below in Table 5.1 with their size and characteristics.

Table 5.1: Datasets used for the comparison of models.

Dataset	Number of features (N = Nominal, C = Continuous)	Number of instances
Abalone	1N 7C	4,177
Auto-MPG	3N 4C	398
Boston housing	0N 13C	506
California housing	0N 8C	20,460
CASP	0N 9C	45,730
Elevators	0N 18C	16,559
Friedman artificial domain	0N 10C	40,768
Machine CPU	0N 6C	209
MV artificial domain	3N 7C	40,768
Servo	4N 0C	167

5.1.2. Selection and optimisation of each model

The focus during evaluation is on the comparison of decision tree-based methods and how the introduction of ensembling and decorrelation of base learners can produce improved performance. However, the models used for comparison are not limited to decision tree-based methods. There are several questions that motivate the choice of models against which the performance of MTF is evaluated:

- Does ensembling a model tree help reduce the problematic high variance error it exhibits?
- Can the decorrelation of model trees within an ensemble further reduce the high variance error?

- Is the complexity of MTF unfavourable for datasets that have linear relationships between their input and target features?
- Is MTF able to outperform competing state-of-the-art regression techniques which are specifically catered towards non-linear problems?

The first question is addressed through a baseline M5 model tree as well as the M5 Ensemble (M5E). The accuracy of MTF is directly compared to, amongst other models, a baseline model tree and an ensemble thereof to illustrate the effectiveness of ensembling model trees with the intent of improving their accuracy. The second question is also answered through the use of the M5 and M5E models because M5E incorporates a simple bagging ensemble technique where trees are not decorrelated. This stand opposed to MTF where the base learners in the ensemble are decorrelated through the use of randomised splitting feature sets. The third question is addressed by the addition of random forest (RF) as well as an artificial feed-forward neural network (NN). Both these models produce favourable results in varying degrees of data complexity if tuned for properly. Neural networks can be tuned by adding or removing single nodes or layers of nodes to increase or decrease their complexity to suit the predictive task at hand. For the final question, a support vector regression model is added to the list of models. An SVR incorporates a Gaussian kernel function to effectively model non-linear problems. Due to the availability of the model itself, GPMCC is omitted.

Each model requires thorough tuning to ensure it performs to the best of its ability under each predictive problem. Therefore, similar to MTF in the previous chapter the hyperparameters of each model are tuned for each dataset prior to being evaluated. Each model is trained through a k-fold cross-validation approach per dataset. This ensures that both MTF and the remainder of the models are tuned for under the same set of circumstances i.e. the dataset as a whole before evaluation. Each model is therefore exposed to the same inductive biases of the same training instances. Recall from Chapter 4 that MTF was trained on 80% of the training instances, chosen by random, during tuning for 30 independent runs. If the value of k is chosen as five for the cross-validation, each model is likewise trained on 80% of the training instances and also exposed to the dataset in its entirety before evaluation. It is important to note that this does not affect the generalisation ability of the model because during evaluation a portion of the dataset is still held out to expose each model to unseen data. Table 5.2 lists each model and their applicable hyperparameters.

Of the five models, M5 is the only model without any hyperparameters applicable for tuning. M5 is implemented through the Cubist package. Additionally, Cubist is also used to implement the ensemble of bagged M5 trees. The size of the ensemble is referred to as the number of committees. Cubist improves the predictive accuracy of M5E by combining a nearest-neighbour technique to the output calculation. This brings rise to the second parameter, neighbours, which also requires tuning. The possible values of neighbours are 1, 3, 5, 7 and 9. The number of committees may range from 1 to 100. Since the two hyperparameters of M5 have a very limited range of values, grid-search optimisation was used without exceeding computational limitations. Grid-search optimisation ensures that the best possible set of hyperparameter values

Table 5.2: The hyperparameters of each model.

Model	Hyperparameters
M5	None
M5 Ensemble	Neighbours Committees
Neural network	Learning rate Batch size Hidden layer size
Random forest	Ensemble size Minimum number of leaf instances Maximum depth Splitting features
Support vector regression	C Gamma

are obtained, because every possible combination is evaluated. The remaining hyperparameters of the models are all tuned using Bayesian optimisation as the search space is too large to cover through grid-search optimisation.

The next model for discussion is the NN. A simple feed-forward neural network with a single hidden layer is used. The size of the hidden layer is a product of the complexity of the problem at hand and is tuned for each dataset separately. For the activation function, a leaky rectified linear unit is implemented. A leaky ReLU activation function improves the likelihood that the NN converges with each training sequence. The NN is trained through Stochastic Gradient Descent (SGD), which requires the specification of a learning rate. Finally, the batch size used for training the NN also influences the quality of the model. To train the NN as best possible, varying learning rates, batch sizes and hidden layer sizes are tuned using Bayesian optimisation. With each training epoch, the error metric on both the training set as well as validation set is measured. Once the error metric converges or overfitting is detected, training is halted. The NN is deemed to overfit once the error on the validation set stops decreasing whilst the error on the training set continues to decrease.

The final tree-based model used for comparison, RF, has the highest number of hyperparameters to tune for. The hyperparameters are ensemble size, minimum number of leaf instances, maximum tree depth, splitting features. All of which are also present in MTF and discussed in Chapter 4. Finally, the parameters of the SVR model are the values for C and gamma, similar to the evaluation of GASOPE in Chapter 3. The hyperparameters of RF and SVR are both tuned using Bayesian optimisation. Further discussion on the hyperparameters is superfluous to the evaluation of MTF.

5.2. Experimental Results

The results of evaluation are listed and discussed in this section. For each of the six models, two error metrics are compared on the training and test set of each dataset. The error metrics are root mean square error (RMSE) and MAE. The choice of error metrics and the results thereof are discussed in Section 5.2.1. Thereafter, Section 5.2.2 discusses the statistical significance of the results through the non-parametric Friedman test together with the post-hoc pairwise Bonferroni-Dunn test.

5.2.1. Evaluating the accuracy of each model

The datasets are first processed before evaluation or tuning takes place. Missing values are all dropped, only California housing and Abalone comprised missing values. Feature values are scaled into a range of $[0; 1]$. After the tuning of model hyperparameters, the generalisation ability of the models are evaluated. The dataset is shuffled randomly and divided into three sets, the training set, validation set and test set in an 80:10:10 ratio. This is repeated a total of 30 independent times per dataset and each model is tested under this configuration.

The training set was used to train each model. The validation set was only utilised by the NN and MTF. The NN employs the validation set for overfit detection during training whilst MTF utilises the validation set after training to prune the ensemble as a whole. The error metrics used for the evaluation of the performance of a given model are RMSE and MAE. Although RMSE is the favoured metric for model evaluation, MAE provides valuable insights into the performance of models, without penalising outlier results as heavily. For each independent run the RMSE and MAE values are computed on both the training and test set. Comparing both the training and test set error metrics allows for the identification of overfitting. Models with a relatively low training set error and higher test set error are likely to overfit the data at hand.

Tables 5.3 and 5.4 lists the results of all six models on every dataset over the 30 independent tests through the median of the error metric values. The median values are listed instead of mean values due to a minority of outlier results heavily skewing the mean values thereby degrading the interpretability. The mean values are available in Appendix D in Tables D.1 through D.4. It is important to note that the use of median values instead of mean values for the portrayal of the test results does not influence of the outcomes of the statistical tests. The statistical tests take the results of each independent run into account.

Comparing the accuracy of each model according to the RMSE and MAE scores shows that there is a large discrepancy between the two error metrics for decision tree-based models. M5 and M5E are shown producing the worst accuracy by a considerable margin according to RMSE. However, evaluating the models according to their MAE scores, both M5 and M5E are considerably more competitive. This is explained through the poor extrapolation qualities that model trees exhibit [18]. RMSE penalises outlier results more severely than MAE, that leads to the poorer RMSE scores for M5 and M5E compared to the other models which extrapolate better.

The the poor extrapolation qualities of the model tree methods are considerably reduced in MTF. MTF can produce competitive scores on both MAE as well as RMSE. Furthermore, the evaluation of the RMSE scores shows that RF is the best performing model for six out of the ten datasets. It is reinforced through these results that RF does not suffer from the same extrapolation problems as model trees because outlier values are quarantined into leaf nodes during induction. This is possible as RF can have a minimum leaf value of one, whereas model trees require multiple instances within a leaf node to properly fit a multivariate model describing the output of the leaf node. The base learners of RF thereby efficiently isolates the outlier values without degrading the accuracy of the ensemble model.

Table 5.3: Comparison of all six models on the first five datasets.

Dataset	Model	Training median		Test median	
		RMSE	MAE	RMSE	MAE
Abalone	M5	0.074835	0.052176	0.076114	0.053630
	M5E	0.074961	0.052110	0.075983	0.053379
	MTF	0.005510	0.052189	0.005676	0.053613
	NN	0.005487	0.052538	0.005629	0.053534
	RF	0.004102	0.044790	0.005744	0.053495
	SVR	0.005241	0.056161	0.006326	0.059169
Auto-MPG	M5	0.070832	0.050789	0.081180	0.058785
	M5E	0.065755	0.047523	0.077815	0.057379
	MTF	0.003760	0.044383	0.004644	0.051011
	NN	0.004668	0.050355	0.005193	0.052833
	RF	0.000737	0.018788	0.004832	0.050543
	SVR	0.004764	0.052498	0.004990	0.054921
Boston housing	M5	0.059977	0.042526	0.076849	0.054649
	M5E	0.051886	0.037964	0.066695	0.047304
	MTF	0.005374	0.044690	0.006150	0.051419
	NN	0.004325	0.047758	0.006021	0.052548
	RF	0.000686	0.017692	0.004069	0.044799
	SVR	0.028366	0.114317	0.029819	0.113600
California housing	M5	0.089878	0.057831	0.102522	0.064730
	M5E	0.082529	0.052641	0.093324	0.058811
	MTF	0.014213	0.082872	0.014836	0.084378
	NN	0.014873	0.085670	0.014858	0.086167
	RF	0.001409	0.024932	0.010467	0.068102
	SVR	0.012889	0.079686	0.013704	0.081421
CASP	M5	0.196568	0.136587	0.208861	0.144950
	M5E	0.175114	0.123580	0.187242	0.131827
	MTF	0.054299	0.190272	0.054908	0.190900
	NN	0.049117	0.174477	0.049652	0.175320
	RF	0.003776	0.041792	0.027135	0.113007
	SVR	0.015286	0.092911	0.031738	0.128393

Table 5.4: Comparison of all six models on the second five datasets.

Dataset	Model	Training median		Test median	
		RMSE	MAE	RMSE	MAE
Elevators	M5	0.031972	0.023461	0.033125	0.024294
	M5E	0.031422	0.023088	0.032382	0.023529
	MTF	0.001831	0.022883	0.003405	0.025486
	NN	0.000934	0.022519	0.000950	0.022596
	RF	0.000229	0.010387	0.001589	0.027721
	SVR	0.008210	0.081129	0.012114	0.093229
Friedman artificial domain	M5	0.032618	0.025897	0.033605	0.026728
	M5E	0.031495	0.025049	0.032159	0.025617
	MTF	0.001074	0.025992	0.001110	0.026485
	NN	0.001089	0.026271	0.001105	0.026423
	RF	0.000306	0.013420	0.001614	0.031792
	SVR	0.010444	0.088321	0.024795	0.128195
Machine	M5	0.027888	0.017556	0.044771	0.028120
	M5E	0.025303	0.016318	0.040548	0.025280
	MTF	0.000744	0.015702	0.001402	0.024449
	NN	0.001706	0.031165	0.002045	0.030528
	RF	0.000408	0.009469	0.000702	0.017116
	SVR	0.014072	0.082980	0.006432	0.075289
MV artificial domain	M5	3.003e-04	1.333e-04	3.337e-04	1.367e-04
	M5E	2.257e-04	1.222e-04	2.470e-04	1.243e-04
	MTF	1.999e-06	4.061e-04	2.732e-06	4.295e-04
	NN	6.220e-07	6.629e-04	6.449e-07	6.669e-04
	RF	4.036e-07	2.830e-04	1.535e-06	6.789e-04
	SVR	1.805e-03	3.520e-02	1.826e-03	3.529e-02
Servo	M5	0.045259	0.025987	0.055805	0.037230
	M5E	0.045259	0.025987	0.055805	0.037230
	MTF	0.003817	0.034379	0.004534	0.042299
	NN	0.008128	0.065783	0.006947	0.067827
	RF	0.000772	0.012659	0.003838	0.031874
	SVR	0.009689	0.071009	0.006620	0.066440

5.2.2. Statistical significance of the results

Statistical tests are performed on the test results to determine which differences in performance are considered significant. The null-hypothesis is that all models are equal in their performance based on the results If the null-hypothesis is rejected, pairwise tests are performed to determine which models produced results that are statically dissimilar. The Friedman test is used to test the null-hypothesis. Thereafter, the post-hoc test is the Bonferroni-Dunn test.

To perform the Friedman test, each independent test run out of the total 30 are ranked twice. Once according to RMSE scores and once more according to MAE scores. This is performed individually for each dataset as well as all ten datasets combined. At a significance level of 5%, each of the eleven Friedman tests resulted in a rejection of the null-hypothesis and post-hoc tests performed accordingly.

The results of the post-hoc tests are presented by Figures 5.1 through 5.11. The critical diagrams are interpreted as follows, each model is placed on a scale of one to six according to their average performing rank over the 30 tests. The black bars group models which are **not** considered statistically dissimilar. For example, Figure 5.1 shows that on average, NN was ranked the best performing model whilst SVR was the worst on the Abalone dataset. Furthermore, NN, MTF and RF are considered to produce results that do not sufficiently distinguish them. The same applies to SVR, M5 and M5E. However, MTF, NN and RF are considered to be statistically more accurate models than SVR, M5 and M5E. For the remaining

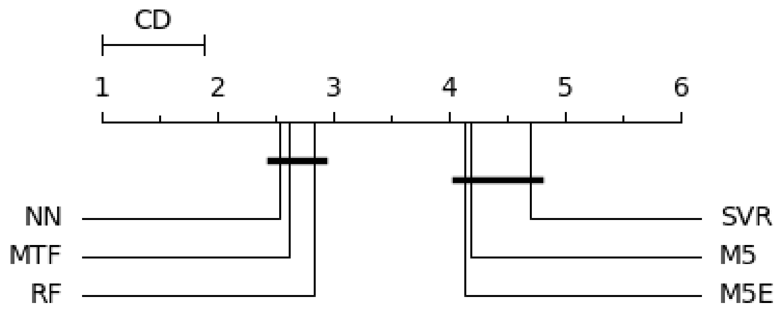

Figure 5.1: Critical difference diagram on Abalone.

critical diagrams, notice the difference in the performance of MTF compared to the more simple model tree ensemble of M5E. MTF is shown to produce a similar or better rank over M5E for eight out of the ten datasets, four of which are statistically better. Statistically, RF produced a best-ranked result for eight of the ten datasets. The RF inspired modifications brought into MTF to improve its performance over a single model tree and bagged ensemble of model trees are shown to produce a significantly increase in accuracy. However, RF still matches or often outperforms MTF for the majority of cases. The only case where MTF outperforms RF is on the Friedman artificial domain dataset, which is a large dataset with non-linear relationships between the input and output features. RF outperforms MTF on Boston housing, California housing, CASP and Servo. It is worth noting that MTF produced very competitive results on Machine CPU, a piecewise linear dataset on which GPMCC did not have favourable results [18].

This portrays the flexibility of MTF to produce adequate results on both linear as well as non-linear data, given that it is properly tuned to the problem at hand.

As expected, M5E is shown to either match the performance of a single M5 model tree or considerably increase its accuracy for all cases. This illustrates that the flaws of model trees, which include their tendency to overfit, are addressed through the use of a bootstrap-aggregated ensemble. Other flaws, such as poor extrapolation, are further improved on by the use of decorrelated base learners in an ensemble.

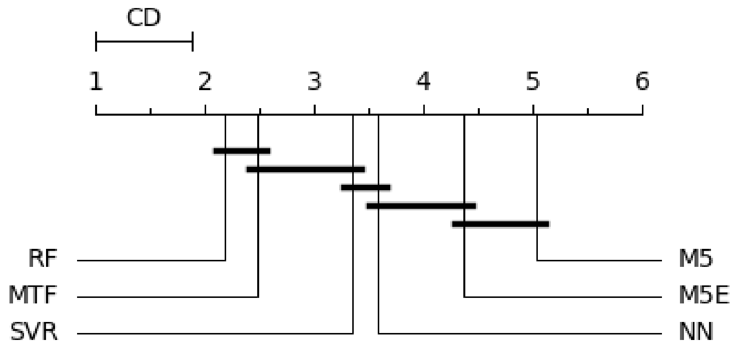

Figure 5.2: Critical difference diagram of Auto-MPG.

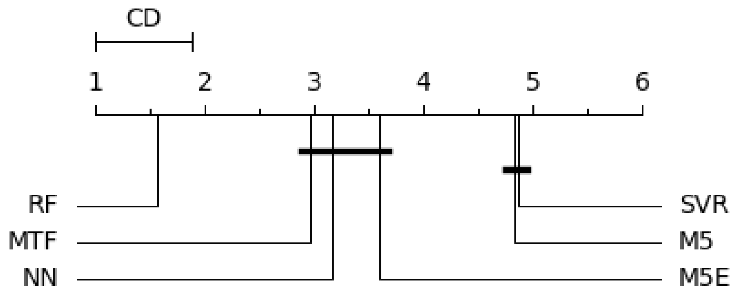

Figure 5.3: Critical difference diagram of Boston housing.

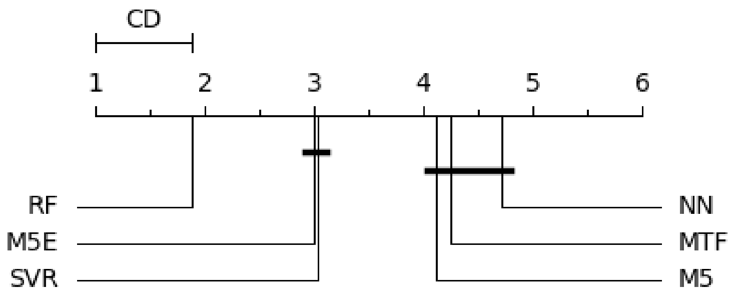

Figure 5.4: Critical difference diagram of California housing.

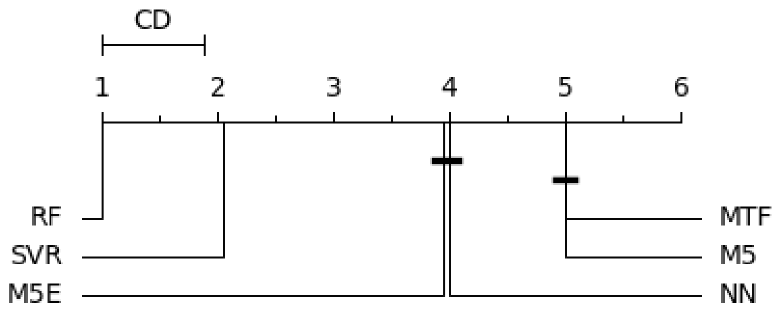

Figure 5.5: Critical difference diagram of CASP.

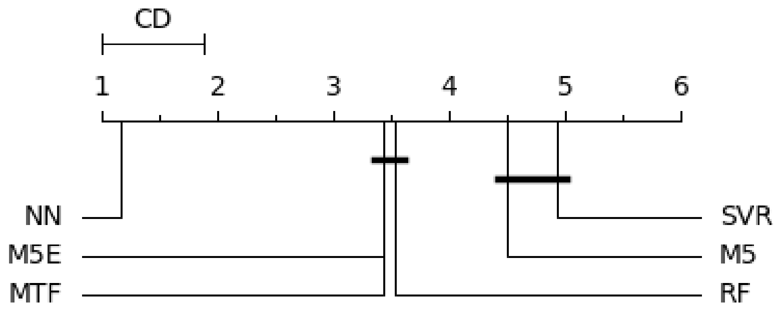

Figure 5.6: Critical difference diagram of Elevators.

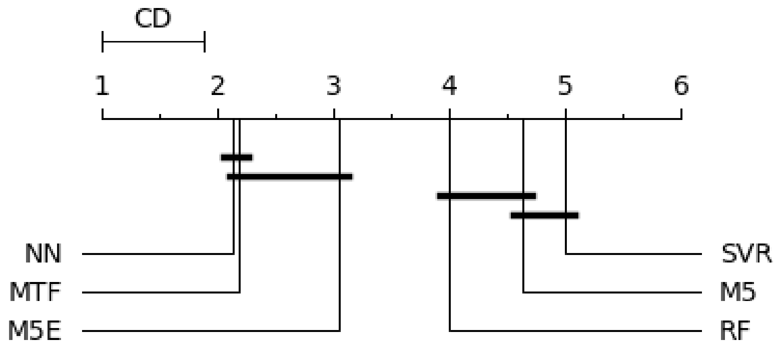

Figure 5.7: Critical difference diagram of Friedman artificial domain.

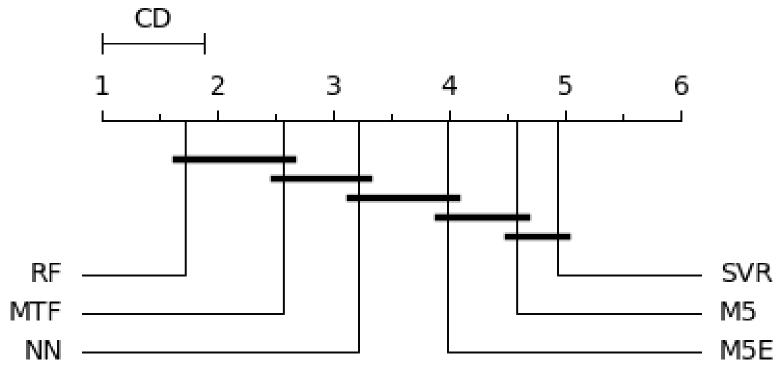

Figure 5.8: Critical difference diagram of Machine CPU.

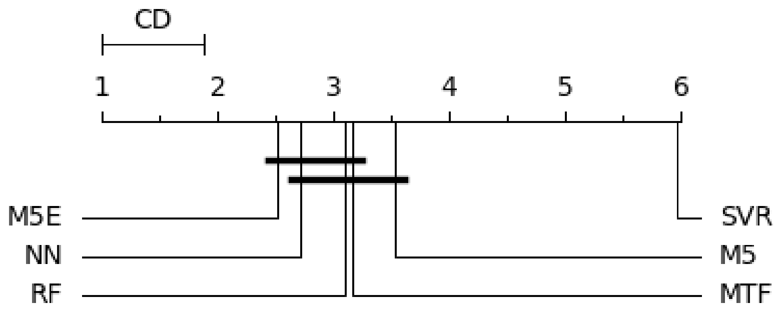

Figure 5.9: Critical difference diagram of MV artificial domain.

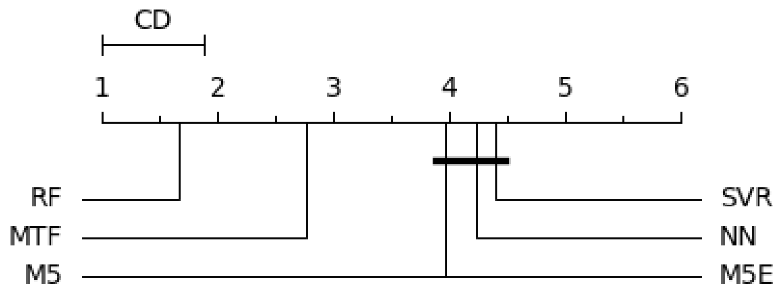

Figure 5.10: Critical difference diagram of Servo.

The three datasets which comprise more non-linear relationships mappings are Auto-MPG, Boston housing and Servo, as shown through the tuning of MTF in Section 4.2.2. All three of these datasets are considered small datasets. For Auto-MPG and Boston housing, MTF was tied for the best-ranked model. For Servo, MTF was ranked second best. Compared to NN and SVR, which are very popular solutions to non-linear problems, MTF outperformed them significantly four out of the six possible times and statistically matched them for the remainder.

Finally, Figure 5.11 shows the combined ranking for all ten datasets. MTF and NN produced very comparable results across all test cases. RF was a clear best performer, whilst SVR failed to improve on the results a single model tree achieved.

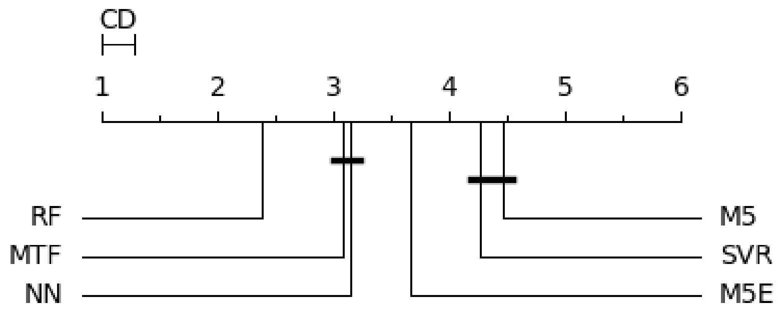

Figure 5.11: Critical difference diagram on the combined testing runs of all ten datasets.

The test results brought fourth insights into the ideal configuration of a model tree depending on the problem at hand. In the case of small datasets, model trees with a single split, i.e. stumps, as base learners in an ensemble tended to perform better than the competing tree-based models which incorporated deeper trees. Recall that MTF was tuned to induce stumps for Auto-MPG, Boston housing and Servo. In smaller sized datasets, there are fewer possible splits for decision tree-based approaches to follow. For model trees, the number of splits is even less due to the higher number of minimum leaf instances required to constitute a split. By inducing deeper trees on a smaller pool of viable splits, decision trees are expected to overfit the dataset. After consecutively reducing the number of instances in a node through splitting, the leaf node is left with fewer observations to induce the output model on, making it more susceptible to overfitting the noise present in these training instances. MTF solves this issue through the use of stumps, minimising the splits required to describe the relationships of the dataset and ensuring there are a larger number of instances in a given leaf node. Additionally, due to the increased complexity of the higher-order polynomial output functions within the leaf nodes of MTF, MTF can divide the feature space a single time and still adequately model the intricate patterns within the data.

For large datasets where MTF was given the freedom of inducing deep trees, namely Friedman artificial domain and MV artificial domain, MTF was tied for the best performing model. With each consecutive split, the likelihood of a node containing a large number of instances is higher than in the case of a small dataset. Thereby the higher-order polynomial functions in the leaf nodes of the model tree are given sufficient training instances to model the output off of. In addition to this, the feature space of the data is divided in such a manner that different relationships within the data are distinguishable and modelled separately from each other. Whereas with stumps, the feature space is only divided a single time per base learner in the ensemble. The two large datasets, California housing and CASP, where MTF produced poor results are cases where the maximum tree depth was limited to four and two respectively. It is hypothesised that these two datasets have a significant increase in noise over the other large datasets which MTF is unable to handle as effectively as the models used for comparison. This would explain the tuning results in the previous chapter, which showed deeper trees producing error metrics with exceptionally large variability. Furthermore, the models that are less complex in their composition, i.e. RF and SVR, as opposed to MTF, M5E and NN were the considerably best ranking models on these datasets. The other two large datasets where MTF produced competitive performance are artificially induced and as a result, have significantly less noise compared to California housing and CASP. The linear base models of MTF were expected to improve performance in cases with noise, but additional measurements are required to increase the robustness of MTF to noise. MTF is highly complex due to the higher-order polynomial functions used to predict the output. Therefore, it is recommended that noisy data be pre-processed before MTF is exposed to it.

5.3. Conclusion

This chapter aimed to empirically investigate the advantages ensemble learning can offer model trees. Additionally, the performance of model trees and model tree ensembles are placed into perspective against other state-of-the-art regression techniques. Recall the questions posed in Section 5.1.2. It was showed that the bagging of M5 models guarantees an improvement in the performance of the base learner, a model tree. Furthermore, the decorrelation of the base learners within MTF significantly increased the robustness of MTF to some of the flaws which model trees and previous ensembles thereof exhibited. These flaws included poor extrapolation and a tendency to overfit data as evident through the high variance error these models inherit from their decision tree structure. The incorporation of RF inspired techniques within an ensemble of model trees resulted in MTF being able to compete with NN and outperform SVR. Finally, MTF was also shown producing competitive performance on data that had linear relationships between the input and target features. This proved that the advantages of model trees are not limited to applications on non-linear data. However, the model must be thoroughly tuned to the problem at hand.

Chapter 6

Conclusion

This chapter concludes the thesis through a summary in Section 6.1, followed by a discussion of the possible avenues for future research regarding the topic of model tree ensembles in Section 6.2.

6.1. Summary

The main goal of this thesis was to thoroughly research, design and implement the use of a model tree comprising higher-order polynomials output functions within an ensemble. To achieve this, Chapter 2 started with the introduction of decision trees and the existing ensemble methods that can be applied to reduce the high variance error decision trees tend to exhibit. It was also shown that model trees that comprise linear output functions have been used within an ensemble to successfully combat the high variance error. However, the only two model trees with non-linear output functions, PLT and GPMCC, were never tested within an ensemble [18, 24]. Model trees comprising higher-order polynomial output functions were shown to outperform their linear output function counterparts. A disadvantage of PLT and GPMCC is the computational demand associated with the induction of non-linear output functions. Therefore, to successfully implement MTF, the tree structure in which GASOPE was employed to produce higher-order output functions, required a less computationally expensive induction algorithm.

In Chapter 3 GASOPE was redesigned with the increased computational power available today, as opposed to when it was first conceptualised. It was also found that GPMCC clearly produced an overfitted approximation of the Abalone dataset. This accentuates the need for the optimisation of such a complex regression model as GASOPE as well as any model tree that employs it. With proper optimisation of the applicable hyperparameters, GASOPE produced adequate results to justify the implementation thereof within MTF.

Next, Chapter 4 presented the decision tree structure as well as the ensemble method which was employed to induce MTF. The greedy induction of the base learners of MTF and the decorrelation thereof within an ensemble provided the following benefits: the computational cost of inducing a single model tree was lenient enough for the application within an ensemble. The decorrelation of the base learners would theoretically reduce the observed variance error of MTF. The ensemble would be more robust to overfitting, which a single model tree was susceptible to. The importance of the optimisation of the hyperparameters were once again critical to the success of MTF. It was found that the application of model trees within an ensemble on small datasets preferred the use of stumps for base learners. For big datasets, allowing the base learners to be grown deeper, produced the best results.

The penultimate Chapter 5 compared the accuracy of MTF against five state-of-the-art regression models on a set of ten benchmarking datasets. MTF was shown producing competitive performance on both non-linear as well as linear problems. MTF produced similar results to a NN whilst outperforming M5E, M5 model tree and SVR. RF produced the best results when comparing the accuracy of all ten datasets together. The decorrelation of the base learners within MTF effectively increased the robustness of MTF to the flaws that model trees exhibited. The flaws were poor extrapolation and the tendency to overfit data due to the high variance error that model trees are prone to exhibit.

6.2. Future Research

Throughout the conceptualisation of MTF, several design aspects were considered but not yet implemented. These possible ideas are reserved for future research and are:

Boosting. Boosting is an alternative ensemble technique to bootstrap aggregation which is employed in MTF; the difference being that boosting induces base learners sequentially with the aim of reducing the net error at every step. Boosting favours the use of weak learners as base learners. In Section 2.2.4, boosting was discussed as a popular ensemble method for decision tree stumps. Although it was hypothesised that bagging would better suit the application of model trees within an ensemble, the implementation of boosting may also produce good results. Bagging was chose as the preferred ensemble method due to the notion that MTF would incorporate base learners that are deep in nature. However, it was shown in Section 4.2.3 that smaller datasets preferred the use of decision tree stumps. Therefore, boosting may produce improved results over bagging in the case of smaller datasets.

Hybrid model trees. The next idea, hybrid model trees, refers to the base learners of MTF. One big disadvantage of model trees are their inability to isolate outliers into a separate leaf node. Due to the output functions of model trees, leaf nodes have a minimum number of instances hyperparameter which has to be satisfied during induction. Therefore, outliers are grouped with other observations within a leaf node. As a results, the output function produces a weak fit of the data subset characterised by the leaf node. The proposed hybrid model tree comprises leaf nodes of both constant value and polynomial equations for the functions of the decision tree. Thereby, the need for a minimum number of instances within a leaf node is dropped and outliers allowed to be isolated within their own leaf nodes. It is worth noting that such a decision tree would require quite a deep tree structure to allow for the use of leaf nodes with constant values.

Data extraction. By implementing model trees in a decorrelated manner within an ensemble, the initial interpretability of decision trees are lost. Interpretability is one of the biggest advantages decision trees have over other models. However, there are steps that can be implemented to extract information from MTF. One such step is the process of variable importance extraction. By measuring the frequency of the unique feature splits within the base learners of the ensemble, underlying relationships that determine which variable has the most discriminative power within the dataset are uncovered. Although this would not directly increase the performance of the model, it does restore the advantage that model trees offer through interpretability, whilst allowing for the use thereof within an ensemble.

Bibliography

[1] D. Aleksovski, J. Kocijan, and S. Džeroski, "Model-tree ensembles for noise-tolerant system identification," *Advanced Engineering Informatics*, vol. 29, no. 1, pp. 1–15, 2015.

[2] R. C. Barros, D. D. Ruiz, and M. P. Basgalupp, "Evolutionary model trees for handling continuous classes in machine learning," *Information Sciences*, vol. 181, no. 5, pp. 954 – 971, 2011. [Online]. Available: http://www.sciencedirect.com/science/article/pii/S0020025510005554

[3] A. Blumer, A. Ehrenfeucht, D. Haussler, and M. K. Warmuth, "Occam's razor," *Information Processing Letters*, vol. 24, no. 6, pp. 377 – 380, 1987. [Online]. Available: http://www.sciencedirect.com/science/article/pii/0020019087901141

[4] L. Breiman, J. H. Friedman, R. A. Olshen, and C. J. Stone, *Classification and Regression Trees*. Monterey, CA: Wadsworth and Brooks, 1984.

[5] L. Breiman, "Bagging predictors," *Machine learning*, vol. 24, no. 2, pp. 123–140, 1996.

[6] ——, "Random forests," *Machine learning*, vol. 45, no. 1, pp. 5–32, 2001.

[7] T. Chai and R. R. Draxler, "Root mean square error (rmse) or mean absolute error (mae)?–arguments against avoiding rmse in the literature," *Geoscientific model development*, vol. 7, no. 3, pp. 1247–1250, 2014.

[8] H. Chen, J. Periaux, and A. Ecer, "Domain decomposition methods using gas and game theory for the parallel solution of cfd problems," in *Parallel Computational Fluid Dynamics 2000*, C. Jenssen, H. Andersson, A. Ecer, N. Satofuka, T. Kvamsdal, B. Pettersen, J. Periaux, and P. Fox, Eds. Amsterdam: North-Holland, 2001, pp. 341 – 348. [Online]. Available: http://www.sciencedirect.com/science/article/pii/B978044450673350110X

[9] J. Demšar, "Statistical comparisons of classifiers over multiple data sets," *Journal of Machine learning research*, vol. 7, no. Jan, pp. 1–30, 2006.

[10] J. H. Friedman, "Multivariate Adaptive Regression Splines," *The Annals of Statistics*, vol. 19, no. 1, pp. 1 – 67, 1991. [Online]. Available: https://doi.org/10.1214/aos/1176347963

[11] P. Geurts, "Contributions to decision tree induction: bias/variance tradeoff and time series classification," Ph.D. dissertation, University of Liège Belgium, 2002.

[12] T. Hastie, R. Tibshirani, and J. Friedman, *The Elements of Statistical Learning: Data Mining, Inference, and Prediction*, ser. Springer Series in Statistics. Springer New York, 2013. [Online]. Available: https://books.google.co.za/books?id=yPfZBwAAQBAJ

[13] O. Kisi and K. S. Parmar, “Application of least square support vector machine and multivariate adaptive regression spline models in long term prediction of river water pollution,” *Journal of Hydrology*, vol. 534, pp. 104–112, 2016.

[14] G. Louppe, “Understanding random forests: From theory to practice,” *arXiv preprint arXiv:1407.7502*, 2014.

[15] G. Moisen, “Classification and regression trees,” *In: Jørgensen, Sven Erik; Fath, Brian D.(Editor-in-Chief). Encyclopedia of Ecology, volume 1. Oxford, UK: Elsevier. p. 582-588.*, pp. 582–588, 2008.

[16] B. Pfahringer, “Semi-random model tree ensembles: An effective and scalable regression method,” in *Australasian Joint Conference on Artificial Intelligence.* Springer, 2011, pp. 231–240.

[17] G. Potgieter and A. Engelbrecht, “Genetic algorithms for the structural optimisation of learned polynomial expressions,” *Applied Mathematics and Computation*, vol. 186, no. 2, pp. 1441 – 1466, 2007. [Online]. Available: http://www.sciencedirect.com/science/article/pii/S0096300306010708

[18] G. Potgieter and A. P. Engelbrecht, “Evolving model trees for mining data sets with continuous-valued classes,” *Expert Systems with Applications*, vol. 35, no. 4, pp. 1513 – 1532, 2008. [Online]. Available: http://www.sciencedirect.com/science/article/pii/S0957417407003673

[19] J. R. Quinlan *et al.*, “Learning with continuous classes,” in *5th Australian Joint Conference on Artificial Intelligence*, vol. 92. World Scientific Press, 1992, pp. 343–348.

[20] M. Sattari, M. Pal, R. Mirabbasi, and J. Abraham, “Ensemble of m5 model tree based modelling of sodium adsorption ratio,” *Journal of AI and Data Mining*, vol. 6, no. 1, pp. 69–78, 2018.

[21] D. J. Sheskin, *Handbook of parametric and nonparametric statistical procedures.* Chapman and Hall/CRC, 2003.

[22] S. Singh, “Understanding the Bias-Variance Tradeoff,” 2018. [Online]. Available: https://towardsdatascience.com/understanding-the-bias-variance-tradeoff-165e6942b229. [Accessed: 22- Mar- 2020].

[23] J. Snoek, H. Larochelle, and R. P. Adams, “Practical bayesian optimization of machine learning algorithms,” in *Advances in Neural Information Processing Systems 25*, F. Pereira, C. J. C. Burges, L. Bottou, and K. Q. Weinberger, Eds. Curran Associates, Inc., 2012, pp. 2951–2959. [Online]. Available: http://papers.nips.cc/paper/4522-practical-bayesian-optimization-of-machine-learning-algorithms.pdf

[24] L. Torgo, "Partial linear trees." in *International Conference on Machine Learning*, 2000, pp. 1007–1014.

[25] ——, "Regression datasets," [Online]. Available: https://www.dcc.fc.up.pt/~ltorgo/Regression/DataSets.html. [Accessed: 15- Aug- 2020].

[26] ——, "Functional models for regression tree leaves," in *International Conference on Machine Learning*, vol. 97, 1997, pp. 385–393.

[27] Y. Wang and I. Witten, "Induction of model trees for predicting continuous classes," *Induction of Model Trees for Predicting Continuous Classes*, 1997.

Appendix A

Dataset linearity estimation via GASOPE

Table A.1 lists the tuning results of the maximum polynomial order hyperparameter in full. $\overline{TMSE}$ refers to the mean squared error on the training set, $\overline{GMSE}$ refers to the mean squared error on the generalisation set, σ indicates the standard deviation and $\bar{t}$ is the average simulation completion time in seconds.

Table A.1: Tuning results of GASOPE for varying maximum polynomial orders on each dataset.

Dataset	Order	$\overline{TMSE}$	σ_{TMSE}	$\overline{GMSE}$	σ_{GMSE}	$\bar{t}$
	1	5.945e-03	1.959e-08	6.237e-03	2.659e-07	15.06
Abalone	2	5.718e-03	1.492e-08	7.750e-03	4.450e-05	21.10
	3	5.827e-03	3.535e-08	8.432e-02	1.361e-01	66.85
	1	5.390e-03	1.508e-07	6.307e-03	1.413e-06	5.455
Auto MPG	2	4.794e-03	1.045e-07	5.750e-03	1.485e-06	6.274
	3	4.802e-03	1.041e-07	5.743e-03	1.459e-06	8.012
	1	7.726e-03	1.135e-06	1.013e-02	2.226e-05	8.442
Boston Housing	2	6.106e-03	5.772e-07	8.938e-03	1.166e-05	12.02
	3	6.211e-03	4.155e-07	9.117e-03	2.059e-05	21.09
	1	1.967e-02	1.065e-07	1.976e-02	6.810e-07	58.18
California Housing	2	1.935e-02	2.956e-07	2.057e-02	9.817e-06	88.87
	3	2.003e-02	8.046e-07	2.081e-02	4.441e-06	389.4
	1	5.961e-02	2.673e-07	5.955e-02	9.002e-07	152.2
CASP	2	5.771e-02	1.681e-07	5.764e-02	1.062e-06	240.5
	3	5.839e-02	3.028e-07	5.841e-02	5.956e-07	1089
	1	1.439e-03	6.562e-10	1.475e-03	6.150e-09	101.3
Elevators	2	1.353e-03	2.664e-09	1.386e-03	7.509e-09	136.5
	3	1.413e-03	4.727e-09	1.439e-03	8.932e-09	571.2
	1	6.862e-03	7.178e-10	6.871e-03	1.161e-08	73.95
Friedman Artificial Domain	2	2.882e-03	6.531e-07	2.877e-03	6.371e-07	128.8
	3	3.101e-03	6.495e-07	3.115e-03	6.606e-07	707.9
	1	9.247e-04	3.028e-08	4.762e-03	5.160e-05	4.408
Machine CPU	2	7.023e-04	2.122e-08	1.313e-02	5.458e-04	5.729
	3	6.972e-04	1.334e-08	1.306e-01	3.897e-01	8.072
	1	1.413e-03	4.426e-06	1.418e-03	4.553e-06	92.00
MV Artificial Domain	2	2.533e-04	1.614e-08	2.530e-04	1.626e-08	128.2
	3	3.856e-04	2.773e-07	3.803e-04	2.538e-07	703.6
	1	1.808e-02	8.123e-06	2.415e-02	7.287e-05	9.630
Servo	2	8.770e-03	2.556e-06	1.391e-02	3.795e-05	15.32
	3	8.514e-03	2.474e-06	1.409e-02	3.852e-05	16.95

Appendix B

Complete tuning results for maximum tree depth

Tables B.1 through B.10 lists the mean tuning results of the maximum tree depth hyperparameter in full, σ indicates the standard deviation.

Table B.1: Tuning results of MT for varying tree depth on Abalone.

Baseline comparison	Depth	$\overline{TMSE}$	σ_{TMSE}	$\overline{GMSE}$	σ_{GMSE}	$\bar{t}$
	2	5.506e-03	1.060e-04	9.780e-03	1.713e-02	30.90
	3	5.413e-03	1.006e-04	1.292e-02	2.363e-02	41.16
	4	5.246e-03	1.038e-04	1.734e-02	3.813e-02	57.30
	5	5.007e-03	9.336e-05	2.801e-01	1.460e+00	85.74
Disabled	6	4.606e-03	1.084e-04	2.620e-02	1.042e-01	125.8
	7	4.173e-03	1.129e-04	9.535e-02	4.691e-01	180.1
	8	3.690e-03	1.223e-04	2.786e-01	1.460e+00	246.1
	9	3.255e-03	1.301e-04	3.237e-01	1.663e+00	314.3
	10	2.985e-03	1.387e-04	1.241e+00	4.020e+00	366.3
	2	5.505e-03	1.044e-04	1.255e-02	3.436e-02	31.33
	3	5.392e-03	9.197e-05	1.044e-02	2.224e-02	41.75
	4	5.223e-03	9.516e-05	1.675e-02	5.850e-02	57.58
	5	5.009e-03	1.030e-04	9.728e-02	4.108e-01	85.57
Enabled	6	4.640e-03	9.666e-05	4.151e-02	1.650e-01	128.7
	7	4.239e-03	1.338e-04	9.124e-03	7.163e-03	183.2
	8	3.759e-03	1.422e-04	1.346e-02	2.198e-02	248.9
	9	3.359e-03	1.591e-04	1.635e-02	2.225e-02	315.9
	10	3.144e-03	1.228e-04	1.936e-02	2.361e-02	366.6

Table B.2: Tuning results of MT for varying tree depth on Auto-MPG.

Baseline comparison	Depth	$\overline{TMSE}$	σ_{TMSE}	$\overline{GMSE}$	σ_{GMSE}	$\bar{t}$
Disabled	2	4.123e-03	3.176e-04	6.480e-03	1.711e-03	11.77
	3	3.615e-03	3.054e-04	8.555e-03	4.047e-03	16.24
	4	2.684e-03	2.612e-04	9.941e+00	3.321e+01	27.25
	5	2.240e-03	2.300e-04	1.048e+02	3.292e+02	36.73
	6	2.220e-03	2.488e-04	9.508e+01	3.299e+02	37.49
	7	2.243e-03	2.636e-04	5.313e+01	2.696e+02	37.85
	8	2.169e-03	2.386e-04	9.978e+01	3.293e+02	37.94
	9	2.179e-03	2.959e-04	6.564e+01	2.698e+02	37.89
	10	2.202e-03	2.547e-04	9.381e+01	3.302e+02	37.55
Enabled	2	4.187e-03	3.071e-04	6.062e-03	1.441e-03	11.89
	3	3.642e-03	3.732e-04	7.256e-03	2.384e-03	16.37
	4	2.739e-03	3.173e-04	7.903e-03	3.251e-03	27.47
	5	2.308e-03	3.040e-04	9.544e-03	7.038e-03	36.81
	6	2.219e-03	3.046e-04	1.082e-02	7.357e-03	38.18
	7	2.228e-03	2.804e-04	2.316e-02	6.684e-02	38.39
	8	2.239e-03	2.950e-04	1.162e-02	9.239e-03	38.30
	9	2.214e-03	3.579e-04	1.863e-02	3.455e-02	38.44
	10	2.234e-03	3.070e-04	2.664e-02	9.646e-02	38.24

Table B.3: Tuning results of MT for varying tree depth on Boston housing.

Baseline comparison	Depth	$\overline{TMSE}$	σ_{TMSE}	$\overline{GMSE}$	σ_{GMSE}	$\bar{t}$
Disabled	2	3.729e-03	4.277e-04	2.052e+01	1.123e+02	25.94
	3	2.851e-03	2.197e-04	4.656e+04	2.550e+05	36.51
	4	2.020e-03	2.475e-04	1.525e+01	5.375e+01	71.06
	5	1.420e-03	2.102e-04	1.173e+03	6.175e+03	117.6
	6	1.129e-03	2.018e-04	7.848e+02	3.913e+03	195.6
	7	1.034e-03	2.030e-04	3.957e+04	2.163e+05	223.3
	8	1.061e-03	2.307e-04	2.313e+02	6.416e+02	232.7
	9	1.044e-03	2.205e-04	1.193e+03	6.295e+03	212.2
	10	1.051e-03	2.037e-04	1.074e+06	5.881e+06	220.5
Enabled	2	3.677e-03	5.035e-04	2.252e-02	6.581e-02	27.60
	3	2.873e-03	2.888e-04	3.615e+02	1.569e+03	31.77
	4	2.001e-03	2.832e-04	2.507e+04	1.365e+05	80.01
	5	1.504e-03	2.639e-04	2.782e+04	1.523e+05	133.6
	6	1.325e-03	2.551e-04	1.229e+06	6.729e+06	180.4
	7	1.202e-03	2.388e-04	3.669e+02	1.711e+03	235.9
	8	1.240e-03	2.265e-04	1.191e+02	5.671e+02	231.0
	9	1.190e-03	2.150e-04	1.712e+04	7.744e+04	236.9
	10	1.234e-03	2.486e-04	2.049e+01	6.088e+01	250.1

Table B.4: Tuning results of MT for varying tree depth on California housing.

Baseline comparison	Depth	$\overline{TMSE}$	σ_{TMSE}	$\overline{GMSE}$	σ_{GMSE}	$\bar{t}$
	2	1.750e-02	3.490e-04	1.797e-02	1.202e-03	192.0
	3	1.675e-02	3.012e-04	2.357e-02	2.990e-02	260.9
	4	1.552e-02	2.946e-04	1.793e-02	4.749e-03	322.0
	5	1.461e-02	1.596e-04	3.462e-01	1.732e+00	388.3
Disabled	6	1.317e-02	2.327e-04	1.927e-01	5.807e-01	475.4
	7	1.155e-02	1.818e-04	5.193e-02	1.062e-01	593.7
	8	9.990e-03	1.476e-04	1.377e-01	3.264e-01	770.1
	9	8.395e-03	1.656e-04	4.740e-01	1.105e+00	985.5
	10	7.050e-03	1.921e-04	1.382e-01	5.039e-01	1235
	2	1.769e-02	4.936e-04	1.899e-02	5.300e-03	205.0
	3	1.667e-02	2.925e-04	1.903e-02	4.239e-03	284.1
	4	1.551e-02	1.837e-04	1.888e-02	5.160e-03	338.8
	5	1.462e-02	2.061e-04	1.908e-01	9.237e-01	409.4
Enabled	6	1.323e-02	2.353e-04	8.328e-02	2.368e-01	496.6
	7	1.158e-02	1.982e-04	7.381e-02	1.645e-01	615.6
	8	9.992e-03	1.946e-04	1.346e-01	2.438e-01	782.7
	9	8.463e-03	1.671e-04	3.064e-01	8.081e-01	995.1
	10	7.220e-03	1.806e-04	9.248e-02	1.647e-01	1241

Table B.5: Tuning results of MT for varying tree depth on CASP.

Baseline comparison	Depth	$\overline{TMSE}$	σ_{TMSE}	$\overline{GMSE}$	σ_{GMSE}	$\bar{t}$
	2	5.634e-02	4.317e-04	5.665e-02	1.367e-03	729.3
	3	5.350e-02	6.796e-04	5.432e-02	1.814e-03	1058
	4	5.068e-02	5.662e-04	5.846e-02	2.968e-02	1280
	5	4.803e-02	4.786e-04	1.478e-01	2.784e-01	1415
Disabled	6	4.541e-02	4.044e-04	1.478e+01	3.532e+01	1554
	7	4.206e-02	3.906e-04	3.521e+00	6.675e+00	1748
	8	3.897e-02	3.720e-04	1.024e+01	2.375e+01	1988
	9	3.528e-02	4.532e-04	7.447e+00	1.711e+01	2339
	10	3.146e-02	5.529e-04	1.367e+02	5.207e+02	2778
	2	5.631e-02	5.115e-04	5.638e-02	8.936e-04	982.8
	3	5.358e-02	5.591e-04	5.873e-02	1.773e-02	1606
	4	5.057e-02	4.347e-04	2.274e-01	7.066e-01	1822
	5	4.782e-02	5.241e-04	1.343e+00	5.481e+00	1930
Enabled	6	4.521e-02	4.826e-04	1.550e+00	4.711e+00	2032
	7	4.219e-02	5.274e-04	8.545e+00	2.967e+01	2160
	8	3.900e-02	5.348e-04	1.017e+04	5.564e+04	2334
	9	3.553e-02	5.290e-04	6.643e+01	2.149e+02	2617
	10	3.199e-02	7.173e-04	6.812e+04	2.754e+05	3050

Table B.6: Tuning results of MT for varying tree depth on Elevators.

Baseline comparison	Depth	$\overline{TMSE}$	σ_{TMSE}	$\overline{GMSE}$	σ_{GMSE}	$\bar{t}$
Disabled	2	1.301e-03	3.115e-05	1.182e+02	6.477e+02	773.9
	3	1.156e-03	3.586e-05	2.529e-03	7.415e-03	898.3
	4	1.103e-03	2.578e-05	1.145e-03	5.774e-05	932.7
	5	1.021e-03	1.863e-05	8.159e-03	2.480e-02	998.2
	6	9.606e-04	1.594e-05	1.077e-01	3.710e-01	1108
	7	8.615e-04	1.301e-05	5.085e-01	1.187e+00	1296
	8	7.508e-04	1.451e-05	7.457e-01	1.081e+00	1563
	9	6.479e-04	1.406e-05	1.952e+00	1.767e+00	1923
	10	5.515e-04	1.412e-05	3.487e+00	2.006e+00	2360
Enabled	2	1.313e-03	3.851e-05	1.339e-03	7.128e-05	784.1
	3	1.158e-03	4.272e-05	1.192e-03	6.441e-05	960.0
	4	1.102e-03	2.722e-05	1.157e-03	4.344e-05	993.0
	5	1.024e-03	1.846e-05	1.117e-03	5.167e-05	1045
	6	9.608e-04	1.366e-05	1.115e-03	4.691e-05	1172
	7	8.757e-04	1.174e-05	1.588e-03	2.387e-03	1327
	8	7.839e-04	1.252e-05	2.088e-03	3.051e-03	1614
	9	7.012e-04	1.603e-05	2.524e-03	3.279e-03	1946
	10	6.245e-04	1.549e-05	3.229e-03	4.649e-03	2397

Table B.7: Tuning results of MT for varying tree depth on Friedman artificial domain.

Baseline comparison	Depth	$\overline{TMSE}$	σ_{TMSE}	$\overline{GMSE}$	σ_{GMSE}	$\bar{t}$
Disabled	2	3.078e-03	4.716e-04	3.079e-03	4.816e-04	577.8
	3	1.965e-03	3.284e-04	1.976e-03	3.324e-04	848.5
	4	1.400e-03	2.623e-04	1.408e-03	2.695e-04	1028
	5	1.336e-03	1.492e-04	1.352e-03	1.527e-04	1158
	6	1.277e-03	1.183e-04	1.309e-03	1.245e-04	1298
	7	1.204e-03	7.137e-05	1.272e-03	7.356e-05	1502
	8	1.132e-03	4.402e-05	1.296e-03	4.749e-05	1823
	9	1.050e-03	4.036e-05	1.410e-03	5.247e-05	2286
	10	9.777e-04	2.149e-05	1.628e-03	4.409e-05	2892
Enabled	2	3.175e-03	5.443e-04	3.181e-03	5.556e-04	799.3
	3	1.807e-03	3.202e-04	1.804e-03	3.162e-04	1224
	4	1.496e-03	3.405e-04	1.506e-03	3.450e-04	1499
	5	1.386e-03	2.073e-04	1.403e-03	2.016e-04	1626
	6	1.246e-03	8.520e-05	1.281e-03	9.509e-05	1724
	7	1.233e-03	7.704e-05	1.315e-03	7.173e-05	1871
	8	1.150e-03	5.687e-05	1.321e-03	5.749e-05	2145
	9	1.067e-03	4.219e-05	1.431e-03	5.755e-05	2552
	10	9.793e-04	2.179e-05	1.634e-03	5.213e-05	3153

Table B.8: Tuning results of MT for varying tree depth on Machine CPU.

Baseline comparison	Depth	$\overline{TMSE}$	σ_{TMSE}	$\overline{GMSE}$	σ_{GMSE}	$\bar{t}$
	2	6.026e-04	9.361e-05	9.390e-03	2.212e-02	7.683
	3	5.810e-04	1.355e-04	7.829e-03	1.986e-02	10.64
	4	5.716e-04	1.407e-04	7.551e-03	1.956e-02	13.66
	5	5.554e-04	1.362e-04	4.273e-01	2.291e+00	18.23
Disabled	6	5.571e-04	1.174e-04	4.223e-01	2.292e+00	18.68
	7	5.484e-04	1.213e-04	4.221e-01	2.292e+00	18.69
	8	5.562e-04	1.162e-04	4.226e-01	2.292e+00	18.41
	9	5.481e-04	1.378e-04	4.227e-01	2.292e+00	18.57
	10	5.361e-04	1.238e-04	4.219e-01	2.292e+00	18.73
	2	6.512e-04	1.253e-04	3.506e-03	5.197e-03	7.731
	3	5.780e-04	1.273e-04	4.126e-03	8.305e-03	10.86
	4	5.849e-04	1.195e-04	4.260e-03	8.707e-03	13.81
	5	5.669e-04	1.707e-04	4.607e-03	8.222e-03	18.37
Enabled	6	5.519e-04	1.203e-04	5.220e-03	8.165e-03	19.28
	7	5.625e-04	1.137e-04	4.994e-03	8.366e-03	19.32
	8	5.671e-04	1.637e-04	5.989e-03	1.180e-02	19.43
	9	5.562e-04	1.312e-04	4.480e-03	8.186e-03	19.31
	10	5.655e-04	1.368e-04	4.728e-03	7.767e-03	19.17

Table B.9: Tuning results of MT for varying tree depth on MV artificial domain.

Baseline comparison	Depth	$\overline{TMSE}$	σ_{TMSE}	$\overline{GMSE}$	σ_{GMSE}	$\bar{t}$
	2	5.506e-03	1.060e-04	9.780e-03	1.713e-02	30.90
	3	5.413e-03	1.006e-04	1.292e-02	2.363e-02	41.16
	4	5.246e-03	1.038e-04	1.734e-02	3.813e-02	57.30
	5	5.007e-03	9.336e-05	2.801e-01	1.460e+00	85.74
Disabled	6	4.606e-03	1.084e-04	2.620e-02	1.042e-01	125.8
	7	4.173e-03	1.129e-04	9.535e-02	4.691e-01	180.1
	8	3.690e-03	1.223e-04	2.786e-01	1.460e+00	246.1
	9	3.255e-03	1.301e-04	3.237e-01	1.663e+00	314.3
	10	2.985e-03	1.387e-04	1.241e+00	4.020e+00	366.3
	2	5.505e-03	1.044e-04	1.255e-02	3.436e-02	31.33
	3	5.392e-03	9.197e-05	1.044e-02	2.224e-02	41.75
	4	5.223e-03	9.516e-05	1.675e-02	5.850e-02	57.58
	5	5.009e-03	1.030e-04	9.728e-02	4.108e-01	85.57
Enabled	6	4.640e-03	9.666e-05	4.151e-02	1.650e-01	128.7
	7	4.239e-03	1.338e-04	9.124e-03	7.163e-03	183.2
	8	3.759e-03	1.422e-04	1.346e-02	2.198e-02	248.9
	9	3.359e-03	1.591e-04	1.635e-02	2.225e-02	315.9
	10	3.144e-03	1.228e-04	1.936e-02	2.361e-02	366.6

Table B.10: Tuning results of MT for varying tree depth on Servo.

Baseline comparison	Depth	$\overline{TMSE}$	σ_{TMSE}	$\overline{GMSE}$	σ_{GMSE}	$\bar{t}$
	2	4.078e-03	1.095e-03	8.603e-03	5.128e-03	8.685
	3	4.159e-03	1.215e-03	1.254e-02	9.328e-03	12.12
	4	4.078e-03	1.199e-03	1.115e-02	5.915e-03	15.26
	5	4.077e-03	1.121e-03	1.151e-02	6.450e-03	14.99
Disabled	6	4.173e-03	1.297e-03	1.227e-02	9.013e-03	14.86
	7	4.092e-03	1.296e-03	1.163e-02	6.847e-03	14.83
	8	4.280e-03	1.070e-03	1.119e-02	6.258e-03	15.04
	9	4.055e-03	1.253e-03	1.091e-02	6.089e-03	15.12
	10	4.099e-03	1.220e-03	1.123e-02	6.389e-03	14.86
	2	4.234e-03	1.362e-03	8.808e-03	7.529e-03	8.977
	3	4.235e-03	1.307e-03	1.235e-02	1.156e-02	12.09
	4	4.448e-03	1.171e-03	1.112e-02	8.168e-03	15.10
	5	4.162e-03	1.165e-03	1.353e-02	1.273e-02	15.42
Enabled	6	4.273e-03	1.258e-03	1.095e-02	9.716e-03	15.40
	7	4.424e-03	1.275e-03	1.181e-02	9.668e-03	15.39
	8	4.096e-03	1.180e-03	1.162e-02	9.248e-03	15.69
	9	4.232e-03	1.175e-03	1.246e-02	9.169e-03	15.64
	10	4.293e-03	1.037e-03	1.158e-02	1.006e-02	15.50

Appendix C

Complete results for ensemble size tuning of MTF

Tables C.1 through C.10 lists the tuning results of the ensemble size hyperparameter in full. $\overline{TMSE}$ refers to the mean squared error on the training set, $\overline{GMSE}$ refers to the mean squared error on the generalisation set and σ indicates the standard deviation.

Table C.1: Tuning results of varying ensemble size for MTF on Abalone.

Ensemble size	$\overline{TMSE}$	σ_{TMSE}	$\overline{GMSE}$	σ_{GMSE}
1	6.636e-03	2.660e-03	7.542e-03	9.630e-03
2	6.106e-03	8.084e-04	6.169e-03	2.463e-03
3	6.052e-03	8.801e-04	7.022e-03	5.713e-03
4	7.151e-03	5.392e-03	7.198e-03	6.311e-03
5	6.625e-03	3.447e-03	6.836e-03	4.740e-03
6	6.353e-03	2.407e-03	6.539e-03	3.699e-03
7	6.171e-03	1.885e-03	7.569e-03	7.471e-03
8	6.105e-03	1.491e-03	6.453e-03	3.281e-03
9	6.236e-03	1.995e-03	6.439e-03	3.355e-03
10	6.158e-03	1.619e-03	6.168e-03	2.564e-03
11	6.066e-03	1.291e-03	6.050e-03	2.124e-03
12	5.980e-03	1.073e-03	5.879e-03	1.465e-03
13	5.957e-03	9.348e-04	6.098e-03	2.122e-03
14	5.947e-03	8.078e-04	6.016e-03	1.814e-03
15	5.905e-03	7.591e-04	5.961e-03	1.627e-03
16	5.933e-03	8.061e-04	5.956e-03	1.572e-03
17	5.876e-03	7.114e-04	5.911e-03	1.420e-03
18	5.840e-03	6.412e-04	5.935e-03	1.537e-03
19	5.845e-03	6.413e-04	6.076e-03	2.245e-03
20	5.797e-03	5.809e-04	6.035e-03	2.320e-03
21	5.735e-03	5.208e-04	6.027e-03	2.174e-03
22	5.727e-03	5.106e-04	6.101e-03	2.439e-03
23	5.707e-03	4.645e-04	6.137e-03	2.404e-03
24	5.707e-03	4.733e-04	6.191e-03	2.624e-03
25	5.704e-03	4.518e-04	6.145e-03	2.449e-03
26	5.683e-03	4.229e-04	6.111e-03	2.224e-03
27	5.682e-03	3.972e-04	6.115e-03	2.178e-03
28	5.665e-03	3.728e-04	6.103e-03	2.062e-03
29	5.663e-03	3.695e-04	6.064e-03	1.921e-03
30	5.666e-03	3.951e-04	6.139e-03	2.132e-03

Table C.2: Tuning results of varying ensemble size for MTF on Auto-MPG.

Ensemble size	$\overline{TMSE}$	σ_{TMSE}	$\overline{GMSE}$	σ_{GMSE}
1	2.098e-02	7.727e-02	7.792e-03	4.987e-03
2	8.826e-03	1.859e-02	1.836e-02	6.745e-02
3	6.338e-03	8.167e-03	1.146e-02	3.115e-02
4	5.883e-03	5.328e-03	9.019e-03	1.783e-02
5	5.316e-03	3.401e-03	7.865e-03	1.191e-02
6	4.970e-03	2.412e-03	6.793e-03	8.405e-03
7	4.738e-03	1.751e-03	6.401e-03	6.514e-03
8	4.588e-03	1.393e-03	6.128e-03	5.236e-03
9	4.505e-03	1.144e-03	5.946e-03	4.442e-03
10	4.390e-03	9.037e-04	5.701e-03	3.777e-03
11	4.328e-03	7.212e-04	5.513e-03	3.344e-03
12	4.274e-03	6.619e-04	5.351e-03	3.056e-03
13	4.237e-03	5.923e-04	5.231e-03	2.855e-03
14	4.205e-03	5.356e-04	5.160e-03	2.668e-03
15	4.168e-03	4.810e-04	5.109e-03	2.513e-03
16	4.145e-03	4.376e-04	5.059e-03	2.379e-03
17	4.123e-03	4.056e-04	5.024e-03	2.302e-03
18	4.113e-03	3.773e-04	5.015e-03	2.266e-03
19	4.086e-03	3.572e-04	4.934e-03	2.184e-03
20	4.063e-03	3.348e-04	4.884e-03	2.158e-03
21	4.047e-03	3.207e-04	4.862e-03	2.100e-03
22	4.034e-03	3.065e-04	4.862e-03	2.063e-03
23	4.035e-03	3.007e-04	4.834e-03	2.020e-03
24	4.018e-03	2.836e-04	4.813e-03	1.986e-03
25	4.014e-03	2.824e-04	4.813e-03	1.966e-03
26	4.009e-03	2.733e-04	4.770e-03	1.981e-03
27	4.002e-03	2.710e-04	4.760e-03	1.949e-03
28	3.996e-03	2.676e-04	4.748e-03	1.950e-03
29	3.993e-03	2.592e-04	4.736e-03	1.960e-03
30	4.005e-03	2.705e-04	4.727e-03	1.946e-03
31	4.003e-03	2.652e-04	4.713e-03	1.908e-03
32	4.000e-03	2.636e-04	4.699e-03	1.902e-03
33	3.993e-03	2.606e-04	4.687e-03	1.874e-03
34	3.985e-03	2.581e-04	4.671e-03	1.854e-03
35	3.984e-03	2.566e-04	4.669e-03	1.846e-03
36	3.979e-03	2.573e-04	4.663e-03	1.847e-03
37	4.023e-03	3.305e-04	4.777e-03	1.961e-03
38	4.014e-03	3.229e-04	4.763e-03	1.942e-03
39	4.011e-03	3.146e-04	4.898e-03	2.069e-03
40	4.007e-03	3.053e-04	4.882e-03	2.044e-03

Table C.3: Tuning results of varying ensemble size for MTF on Boston Housing.

Ensemble size	$\overline{TMSE}$	σ_{TMSE}	$\overline{GMSE}$	σ_{GMSE}
1	5.625e-01	3.025e+00	1.059e-02	5.311e-03
2	7.917e-01	2.390e+00	1.720e+00	6.587e+00
3	3.592e-01	1.058e+00	7.615e-01	2.897e+00
4	2.320e-01	6.180e-01	4.302e-01	1.621e+00
5	1.518e-01	3.951e-01	2.771e-01	1.036e+00
6	1.193e-01	2.773e-01	1.948e-01	7.213e-01
7	1.460e-01	3.495e-01	1.586e-01	5.314e-01
8	1.931e-01	5.402e-01	1.228e-01	4.068e-01
9	2.788e-01	7.831e-01	9.820e-02	3.205e-01
10	2.260e-01	6.322e-01	8.029e-02	2.577e-01
11	1.919e-01	5.215e-01	7.062e-02	2.111e-01
12	1.637e-01	4.378e-01	6.080e-02	1.777e-01
13	1.412e-01	3.731e-01	5.282e-02	1.501e-01
14	1.610e+00	8.116e+00	4.666e-02	1.286e-01
15	1.036e+01	4.918e+01	1.367e-01	5.284e-01
16	9.105e+00	4.324e+01	1.209e-01	4.646e-01
17	8.062e+00	3.831e+01	1.080e-01	4.117e-01
18	7.201e+00	3.417e+01	9.714e-02	3.671e-01
19	6.476e+00	3.067e+01	8.762e-02	3.295e-01
20	5.845e+00	2.768e+01	7.955e-02	2.972e-01
21	1.079e+01	3.840e+01	8.090e-02	2.717e-01
22	9.967e+00	3.496e+01	7.393e-02	2.471e-01
23	9.120e+00	3.198e+01	6.816e-02	2.263e-01
24	8.385e+00	2.940e+01	6.332e-02	2.079e-01
25	7.550e+00	2.651e+01	5.878e-02	1.916e-01
26	9.510e+00	2.750e+01	5.484e-02	1.772e-01
27	8.818e+00	2.549e+01	5.121e-02	1.645e-01
28	8.206e+00	2.370e+01	4.879e-02	1.529e-01
29	1.562e+01	4.759e+01	4.546e-02	1.425e-01
30	1.460e+01	4.447e+01	4.283e-02	1.332e-01
31	1.367e+01	4.164e+01	4.056e-02	1.247e-01
32	1.284e+01	3.908e+01	6.197e-02	1.700e-01
33	1.208e+01	3.675e+01	6.284e-02	1.605e-01
34	1.138e+01	3.462e+01	5.958e-02	1.512e-01
35	1.525e+01	3.972e+01	5.536e-02	1.421e-01
36	1.442e+01	3.754e+01	5.255e-02	1.341e-01
37	1.357e+01	3.548e+01	5.010e-02	1.269e-01
38	1.282e+01	3.364e+01	5.013e-02	1.216e-01
39	1.235e+01	3.186e+01	4.773e-02	1.153e-01
40	1.174e+01	3.028e+01	4.618e-02	1.095e-01

Table C.4: Tuning results of varying ensemble size for MTF on California Housing.

Ensemble size	$\overline{TMSE}$	σ_{TMSE}	$\overline{GMSE}$	σ_{GMSE}
1	1.759e-02	3.331e-03	2.212e-02	1.165e-02
2	2.039e-02	2.039e-02	2.594e-02	1.864e-02
3	1.739e-02	9.006e-03	2.244e-02	1.179e-02
4	1.636e-02	5.009e-03	1.889e-02	7.794e-03
5	1.599e-02	3.485e-03	1.726e-02	5.565e-03
6	1.581e-02	2.559e-03	1.827e-02	8.359e-03
7	1.544e-02	1.808e-03	1.789e-02	6.445e-03
8	1.522e-02	1.363e-03	1.783e-02	5.902e-03
9	1.503e-02	1.058e-03	1.738e-02	5.255e-03
10	1.489e-02	8.582e-04	1.709e-02	4.301e-03
11	1.482e-02	8.349e-04	1.683e-02	3.825e-03
12	1.472e-02	6.919e-04	1.700e-02	4.074e-03
13	1.471e-02	6.047e-04	1.678e-02	3.792e-03
14	1.464e-02	5.331e-04	1.678e-02	3.998e-03
15	1.461e-02	5.900e-04	1.649e-02	3.515e-03
16	1.458e-02	5.426e-04	1.654e-02	3.655e-03
17	1.457e-02	4.952e-04	1.645e-02	3.673e-03
18	1.447e-02	4.120e-04	1.667e-02	3.944e-03
19	1.448e-02	4.014e-04	1.670e-02	4.133e-03
20	1.446e-02	3.896e-04	1.643e-02	3.768e-03
21	1.444e-02	3.884e-04	1.642e-02	3.855e-03
22	1.446e-02	3.459e-04	1.651e-02	3.965e-03
23	1.457e-02	7.220e-04	1.660e-02	4.140e-03
24	1.456e-02	6.810e-04	1.648e-02	3.963e-03
25	1.456e-02	6.708e-04	1.691e-02	5.606e-03
26	1.454e-02	5.547e-04	1.688e-02	5.409e-03
27	1.451e-02	5.251e-04	1.710e-02	5.983e-03
28	1.512e-02	3.549e-03	1.685e-02	5.468e-03
29	1.505e-02	3.301e-03	1.678e-02	5.155e-03
30	1.498e-02	3.085e-03	1.678e-02	5.257e-03

Table C.5: Tuning results of varying ensemble size for MTF on CASP.

Ensemble size	$\overline{TMSE}$	σ_{TMSE}	$\overline{GMSE}$	σ_{GMSE}
1	3.664e-01	5.559e-01	2.627e+00	1.285e+01
2	2.583e-01	3.228e-01	6.190e-01	2.738e+00
3	3.631e-01	4.483e-01	5.605e-01	2.206e+00
4	4.197e-01	6.132e-01	3.445e-01	1.247e+00
5	3.118e-01	4.071e-01	3.066e-01	8.451e-01
6	2.565e-01	2.964e-01	2.342e-01	5.738e-01
7	2.191e-01	2.339e-01	1.982e-01	4.206e-01
8	2.048e-01	2.026e-01	2.528e-01	5.468e-01
9	1.686e-01	1.574e-01	2.859e-01	5.314e-01
10	1.574e-01	1.577e-01	2.409e-01	4.307e-01
11	1.415e-01	1.299e-01	2.383e-01	3.832e-01
12	1.269e-01	1.075e-01	2.159e-01	3.387e-01
13	1.217e-01	9.179e-02	1.961e-01	2.844e-01
14	1.152e-01	7.773e-02	1.861e-01	2.592e-01
15	1.074e-01	6.801e-02	1.933e-01	2.908e-01
16	1.032e-01	6.254e-02	1.965e-01	2.777e-01
17	9.743e-02	5.618e-02	1.891e-01	2.599e-01
18	9.461e-02	5.073e-02	1.773e-01	2.299e-01
19	8.960e-02	4.622e-02	1.503e-01	1.991e-01
20	9.031e-02	4.714e-02	1.400e-01	1.701e-01
21	8.428e-02	3.803e-02	1.242e-01	1.529e-01
22	8.317e-02	3.578e-02	1.271e-01	1.654e-01
23	7.965e-02	3.276e-02	1.351e-01	1.849e-01
24	8.004e-02	3.633e-02	1.293e-01	1.799e-01
25	8.103e-02	3.551e-02	1.241e-01	1.793e-01
26	7.876e-02	3.245e-02	1.214e-01	1.661e-01
27	7.814e-02	2.862e-02	1.178e-01	1.478e-01
28	7.763e-02	2.729e-02	1.083e-01	1.145e-01
29	7.530e-02	2.510e-02	1.007e-01	1.010e-01
30	7.381e-02	2.328e-02	1.142e-01	1.220e-01

Table C.6: Tuning results of varying ensemble size for MTF on Elevators.

Ensemble size	$\overline{TMSE}$	σ_{TMSE}	$\overline{GMSE}$	σ_{GMSE}
1	2.006e-03	2.727e-03	1.230e-03	8.217e-05
2	5.563e-03	2.093e-02	1.132e-03	6.643e-05
3	5.802e-03	1.703e-02	1.092e-03	6.779e-05
4	3.897e-03	9.556e-03	1.168e-03	5.258e-04
5	3.013e-03	6.076e-03	1.393e-03	1.068e-03
6	2.440e-03	4.223e-03	1.555e-03	1.245e-03
7	2.395e-03	3.432e-03	1.918e-03	3.025e-03
8	2.501e-03	3.011e-03	1.742e-03	2.531e-03
9	2.487e-03	2.515e-03	1.593e-03	2.003e-03
10	2.420e-03	2.249e-03	1.500e-03	1.619e-03
11	2.261e-03	1.917e-03	1.417e-03	1.336e-03
12	2.112e-03	1.635e-03	1.363e-03	1.123e-03
13	1.924e-03	1.371e-03	1.324e-03	9.568e-04
14	1.790e-03	1.181e-03	1.272e-03	7.613e-04
15	1.743e-03	1.023e-03	1.281e-03	6.910e-04
16	1.653e-03	8.947e-04	1.282e-03	6.160e-04
17	1.643e-03	8.459e-04	1.253e-03	5.470e-04
18	1.591e-03	7.547e-04	1.239e-03	4.856e-04
19	1.695e-03	8.764e-04	1.361e-03	8.680e-04
20	1.741e-03	1.240e-03	1.328e-03	7.819e-04
21	1.696e-03	1.116e-03	1.300e-03	7.090e-04
22	1.700e-03	1.010e-03	1.275e-03	6.468e-04
23	1.640e-03	9.218e-04	1.255e-03	5.921e-04
24	1.590e-03	8.441e-04	1.237e-03	5.451e-04
25	1.527e-03	7.645e-04	1.220e-03	5.024e-04
26	1.484e-03	7.057e-04	1.201e-03	4.647e-04
27	1.461e-03	6.618e-04	1.186e-03	4.320e-04
28	1.423e-03	6.150e-04	1.174e-03	4.022e-04
29	1.391e-03	5.728e-04	1.163e-03	3.759e-04
30	1.363e-03	5.340e-04	1.154e-03	3.525e-04

Table C.7: Tuning results of varying ensemble size for MTF on Friedman artificial domain.

Ensemble size	$\overline{TMSE}$	σ_{TMSE}	$\overline{GMSE}$	σ_{GMSE}
1	1.615e-03	3.828e-04	1.664e-03	4.212e-04
2	1.367e-03	1.830e-04	1.401e-03	2.047e-04
3	1.268e-03	9.960e-05	1.298e-03	1.074e-04
4	1.230e-03	8.186e-05	1.260e-03	8.765e-05
5	1.209e-03	6.644e-05	1.236e-03	7.432e-05
6	1.196e-03	6.262e-05	1.223e-03	6.789e-05
7	1.195e-03	6.114e-05	1.221e-03	6.659e-05
8	1.190e-03	5.435e-05	1.216e-03	6.106e-05
9	1.191e-03	5.347e-05	1.217e-03	5.972e-05
10	1.184e-03	5.204e-05	1.210e-03	6.185e-05
11	1.186e-03	5.005e-05	1.212e-03	6.093e-05
12	1.181e-03	4.578e-05	1.207e-03	5.687e-05
13	1.176e-03	4.540e-05	1.202e-03	5.770e-05
14	1.172e-03	4.223e-05	1.198e-03	5.398e-05
15	1.169e-03	4.077e-05	1.194e-03	5.307e-05
16	1.169e-03	4.031e-05	1.195e-03	5.216e-05
17	1.167e-03	3.863e-05	1.192e-03	5.016e-05
18	1.162e-03	3.739e-05	1.187e-03	4.893e-05
19	1.160e-03	3.595e-05	1.185e-03	4.694e-05
20	1.159e-03	3.405e-05	1.184e-03	4.499e-05
21	1.159e-03	3.197e-05	1.184e-03	4.322e-05
22	1.156e-03	3.298e-05	1.180e-03	4.266e-05
23	1.157e-03	3.179e-05	1.181e-03	4.016e-05
24	1.156e-03	3.024e-05	1.180e-03	3.791e-05
25	1.157e-03	3.148e-05	1.181e-03	3.911e-05
26	1.157e-03	3.152e-05	1.180e-03	3.928e-05
27	1.158e-03	3.145e-05	1.181e-03	4.031e-05
28	1.158e-03	3.017e-05	1.181e-03	3.921e-05
29	1.158e-03	2.911e-05	1.181e-03	3.800e-05
30	1.157e-03	2.945e-05	1.180e-03	3.892e-05

Table C.8: Tuning results of varying ensemble size for MTF on Machine CPU.

Ensemble size	$\overline{TMSE}$	σ_{TMSE}	$\overline{GMSE}$	σ_{GMSE}
1	9.193e-02	4.622e-01	7.587e-03	1.155e-02
2	2.557e-02	1.155e-01	1.242e-02	2.916e-02
3	1.215e-02	5.137e-02	7.721e-03	1.545e-02
4	7.641e-03	2.886e-02	6.539e-03	1.113e-02
5	5.677e-03	1.846e-02	5.746e-03	9.243e-03
6	4.360e-03	1.283e-02	4.777e-03	7.272e-03
7	3.565e-03	9.413e-03	4.252e-03	5.802e-03
8	2.878e-03	7.247e-03	3.992e-03	4.754e-03
9	2.479e-03	5.732e-03	3.746e-03	4.371e-03
10	2.261e-03	4.698e-03	3.658e-03	4.198e-03
11	2.053e-03	3.886e-03	3.520e-03	3.974e-03
12	1.968e-03	3.320e-03	3.635e-03	4.250e-03
13	1.807e-03	2.870e-03	3.445e-03	3.977e-03
14	1.712e-03	2.477e-03	3.217e-03	4.065e-03
15	1.641e-03	2.152e-03	3.168e-03	3.996e-03
16	1.533e-03	1.884e-03	3.115e-03	3.685e-03
17	1.473e-03	1.675e-03	3.057e-03	3.486e-03
18	1.405e-03	1.495e-03	2.931e-03	3.257e-03
19	1.333e-03	1.353e-03	2.915e-03	3.170e-03
20	1.291e-03	1.223e-03	2.969e-03	3.283e-03
21	1.370e-03	1.234e-03	2.897e-03	3.167e-03
22	1.302e-03	1.126e-03	2.783e-03	3.069e-03
23	1.257e-03	1.025e-03	2.740e-03	3.104e-03
24	1.237e-03	9.364e-04	2.759e-03	3.243e-03
25	7.040e-03	3.187e-02	2.641e-03	3.099e-03
26	6.556e-03	2.946e-02	2.566e-03	2.920e-03
27	6.163e-03	2.734e-02	2.639e-03	3.128e-03
28	5.792e-03	2.542e-02	2.566e-03	2.984e-03
29	5.477e-03	2.367e-02	2.582e-03	3.022e-03
30	5.171e-03	2.214e-02	2.557e-03	2.954e-03
31	4.904e-03	2.074e-02	2.521e-03	2.911e-03
32	4.660e-03	1.947e-02	2.477e-03	2.793e-03
33	4.441e-03	1.832e-02	2.490e-03	2.779e-03
34	4.228e-03	1.725e-02	2.500e-03	2.756e-03
35	4.038e-03	1.625e-02	2.481e-03	2.686e-03
36	3.883e-03	1.536e-02	2.511e-03	2.749e-03
37	3.717e-03	1.456e-02	2.500e-03	2.708e-03
38	3.587e-03	1.388e-02	2.546e-03	2.795e-03
39	3.556e-03	1.317e-02	2.566e-03	2.765e-03
40	3.439e-03	1.251e-02	2.553e-03	2.675e-03

Table C.9: Tuning results of varying ensemble size for MTF on MV artificial domain.

Ensemble size	$\overline{TMSE}$	σ_{TMSE}	$\overline{GMSE}$	σ_{GMSE}
1	9.820e-05	4.318e-04	2.615e-05	4.432e-05
2	1.083e-04	3.657e-04	2.010e-05	4.160e-05
3	6.084e-05	1.693e-04	1.507e-05	3.540e-05
4	3.562e-05	9.526e-05	2.388e-03	1.302e-02
5	3.036e-05	6.751e-05	1.532e-03	8.333e-03
6	2.353e-05	4.686e-05	1.073e-03	5.785e-03
7	1.853e-05	3.449e-05	7.893e-04	4.250e-03
8	1.511e-05	2.659e-05	6.026e-04	3.239e-03
9	1.262e-05	2.114e-05	4.777e-04	2.559e-03
10	5.069e-04	2.716e-03	2.734e-03	1.492e-02
11	4.201e-04	2.244e-03	2.260e-03	1.233e-02
12	4.932e-04	2.014e-03	1.900e-03	1.036e-02
13	4.208e-04	1.716e-03	1.620e-03	8.831e-03
14	1.203e-02	5.998e-02	1.397e-03	7.614e-03
15	1.048e-02	5.225e-02	1.217e-03	6.633e-03
16	9.208e-03	4.592e-02	1.072e-03	5.829e-03
17	8.142e-03	4.068e-02	9.502e-04	5.163e-03
18	7.268e-03	3.628e-02	8.479e-04	4.605e-03
19	7.299e-03	3.262e-02	3.540e-03	1.563e-02
20	6.588e-03	2.944e-02	3.195e-03	1.411e-02
21	6.181e-03	2.668e-02	2.910e-03	1.279e-02
22	5.632e-03	2.431e-02	2.652e-03	1.166e-02
23	5.175e-03	2.224e-02	2.427e-03	1.067e-02
24	4.753e-03	2.043e-02	2.230e-03	9.796e-03
25	4.381e-03	1.883e-02	2.056e-03	9.028e-03
26	4.053e-03	1.740e-02	1.901e-03	8.347e-03
27	3.759e-03	1.614e-02	1.763e-03	7.740e-03
28	3.495e-03	1.501e-02	1.640e-03	7.197e-03
29	3.259e-03	1.399e-02	1.529e-03	6.709e-03
30	3.328e-03	1.310e-02	1.429e-03	6.269e-03

Table C.10: Tuning results of varying ensemble size for MTF on Servo.

Ensemble size	$\overline{TMSE}$	σ_{TMSE}	$\overline{GMSE}$	σ_{GMSE}
1	1.224e-02	7.994e-03	6.367e-02	2.255e-01
2	8.217e-03	2.808e-03	2.913e-02	5.965e-02
3	7.993e-03	5.595e-03	1.788e-02	1.950e-02
4	6.943e-03	3.314e-03	1.632e-02	1.757e-02
5	1.088e-02	2.572e-02	1.489e-02	1.560e-02
6	9.059e-03	1.788e-02	1.356e-02	1.517e-02
7	7.865e-03	1.330e-02	1.348e-02	1.491e-02
8	7.152e-03	1.013e-02	1.335e-02	1.587e-02
9	6.590e-03	8.284e-03	1.321e-02	1.580e-02
10	6.112e-03	6.671e-03	1.294e-02	1.569e-02
11	5.905e-03	5.564e-03	1.272e-02	1.498e-02
12	5.655e-03	4.734e-03	1.235e-02	1.472e-02
13	5.536e-03	4.046e-03	1.223e-02	1.442e-02
14	5.365e-03	3.522e-03	1.217e-02	1.446e-02
15	5.231e-03	3.101e-03	1.220e-02	1.451e-02
16	5.097e-03	2.726e-03	1.214e-02	1.441e-02
17	4.972e-03	2.471e-03	1.202e-02	1.435e-02
18	4.919e-03	2.266e-03	1.199e-02	1.510e-02
19	4.820e-03	2.081e-03	1.169e-02	1.497e-02
20	4.764e-03	1.926e-03	1.159e-02	1.475e-02
21	4.830e-03	1.853e-03	1.173e-02	1.456e-02
22	4.749e-03	1.692e-03	1.166e-02	1.444e-02
23	4.706e-03	1.594e-03	1.171e-02	1.440e-02
24	3.389e-02	1.598e-01	1.186e-02	1.442e-02
25	3.163e-02	1.473e-01	1.176e-02	1.422e-02
26	2.958e-02	1.364e-01	1.194e-02	1.429e-02
27	2.779e-02	1.267e-01	1.176e-02	1.416e-02
28	2.615e-02	1.178e-01	1.166e-02	1.399e-02
29	2.473e-02	1.102e-01	1.157e-02	1.381e-02
30	2.336e-02	1.029e-01	1.162e-02	1.376e-02
31	2.213e-02	9.644e-02	1.160e-02	1.366e-02
32	2.111e-02	9.093e-02	1.156e-02	1.363e-02
33	2.010e-02	8.552e-02	1.160e-02	1.362e-02
34	1.916e-02	8.060e-02	1.162e-02	1.392e-02
35	1.832e-02	7.608e-02	1.156e-02	1.384e-02
36	1.756e-02	7.189e-02	1.150e-02	1.377e-02
37	1.697e-02	6.863e-02	1.154e-02	1.382e-02
38	1.629e-02	6.508e-02	1.140e-02	1.370e-02
39	1.571e-02	6.187e-02	1.139e-02	1.376e-02
40	1.512e-02	5.878e-02	1.142e-02	1.408e-02

Appendix D

Mean results for the comparative tests of MTF

Tables D.1 through D.4 lists the tuning results of the ensemble size hyperparameter in full. $\overline{TMSE}$ refers to the mean squared error on the training set, $\overline{GMSE}$ refers to the mean squared error on the generalisation set and σ indicates the standard deviation.

Table D.1: Comparison of RMSE scores of all six models on the first five datasets.

		Training set		Test set	
Dataset	Model	$\overline{RMSE}$	σ_{RMSE}	$\overline{RMSE}$	σ_{RMSE}
Abalone	M5	7.487e-02	7.439e-04	7.655e-02	4.053e-03
	M5E	7.497e-02	6.412e-04	7.638e-02	3.951e-03
	MTF	5.716e-03	5.872e-04	7.967e-03	7.312e-03
	NN	5.521e-03	2.383e-04	5.687e-03	6.901e-04
	RF	4.110e-03	7.358e-05	5.750e-03	6.201e-04
	SVR	5.245e-03	9.294e-05	6.242e-03	5.103e-04
Auto-MPG	M5	6.969e-02	4.315e-03	8.265e-02	1.538e-02
	M5E	6.717e-02	3.143e-03	7.931e-02	1.313e-02
	MTF	3.727e-03	3.145e-04	5.334e-03	2.256e-03
	NN	4.668e-03	5.110e-04	5.649e-03	1.740e-03
	RF	7.234e-04	5.819e-05	5.130e-03	2.328e-03
	SVR	4.714e-03	3.182e-04	5.452e-03	1.955e-03
Boston housing	M5	6.126e-02	7.321e-03	8.553e-02	2.507e-02
	M5E	5.285e-02	2.909e-03	7.295e-02	1.975e-02
	MTF	2.325e+00	1.041e+01	2.053e+00	7.667e+00
	NN	4.795e-03	1.745e-03	7.327e-03	4.759e-03
	RF	6.921e-04	4.475e-05	4.765e-03	2.173e-03
	SVR	2.843e-02	1.141e-03	2.792e-02	7.549e-03
California housing	M5	8.994e-02	8.781e-04	1.027e-01	3.937e-03
	M5E	8.256e-02	5.523e-04	9.378e-02	3.744e-03
	MTF	1.425e-02	3.474e-04	1.562e-02	3.743e-03
	NN	1.474e-02	5.709e-04	1.502e-02	8.810e-04
	RF	1.411e-03	1.571e-05	1.043e-02	7.687e-04
	SVR	1.287e-02	1.397e-04	1.382e-02	9.041e-04
CASP	M5	1.964e-01	7.460e-04	2.083e-01	2.600e-03
	M5E	1.751e-01	5.113e-04	1.873e-01	2.092e-03
	MTF	5.467e-02	9.813e-04	5.509e-02	1.827e-03
	NN	4.927e-02	1.092e-03	4.988e-02	1.719e-03
	RF	3.778e-03	2.425e-05	2.711e-02	8.643e-04
	SVR	1.528e-02	8.673e-05	3.162e-02	9.892e-04

Table D.2: Comparison of RMSE scores of all six models on the second five datasets.

		Training set		Test set	
Dataset	Model	$\overline{RMSE}$	σ_{RMSE}	$\overline{RMSE}$	σ_{RMSE}
Elevators	M5	3.202e-02	4.119e-04	3.356e-02	1.241e-03
	M5E	3.144e-02	2.533e-04	3.250e-02	9.241e-04
	MTF	2.789e-03	2.625e-03	8.441e-03	1.492e-02
	NN	9.488e-04	6.544e-05	9.688e-04	8.033e-05
	RF	2.288e-04	2.842e-06	1.598e-03	1.171e-04
	SVR	8.208e-03	4.832e-05	1.211e-02	5.740e-04
Friedman artificial domain	M5	3.264e-02	1.635e-04	3.352e-02	2.892e-04
	M5E	3.148e-02	1.272e-04	3.214e-02	3.339e-04
	MTF	1.074e-03	1.808e-05	1.114e-03	3.768e-05
	NN	1.100e-03	4.336e-05	1.111e-03	5.084e-05
	RF	3.063e-04	1.647e-06	1.623e-03	4.707e-05
	SVR	1.045e-02	2.861e-05	2.471e-02	4.413e-04
Machine	M5	2.884e-02	5.599e-03	5.565e-02	3.267e-02
	M5E	2.515e-02	2.403e-03	4.656e-02	2.191e-02
	MTF	1.651e-02	6.284e-02	1.985e-01	1.072e+00
	NN	1.707e-03	5.629e-04	2.708e-03	2.510e-03
	RF	4.056e-04	6.040e-05	1.794e-03	2.780e-03
	SVR	1.303e-02	1.796e-03	1.179e-02	1.315e-02
MV artificial domain	M5	3.036e-04	1.534e-05	3.425e-04	6.922e-05
	M5E	2.270e-04	1.576e-05	2.504e-04	3.419e-05
	MTF	1.674e-04	6.898e-04	1.845e-03	8.016e-03
	NN	2.426e-06	3.992e-06	2.435e-06	4.001e-06
	RF	4.078e-07	6.813e-08	1.821e-06	8.785e-07
	SVR	1.808e-03	2.984e-05	1.820e-03	3.893e-05
Servo	M5	4.667e-02	1.423e-02	6.216e-02	2.263e-02
	M5E	4.667e-02	1.423e-02	6.216e-02	2.263e-02
	MTF	3.802e-03	7.877e-04	8.851e-03	1.094e-02
	NN	7.742e-03	1.821e-03	1.055e-02	9.743e-03
	RF	7.555e-04	1.177e-04	5.824e-03	6.729e-03
	SVR	9.512e-03	1.352e-03	1.101e-02	1.021e-02

Table D.3: Comparison of MAE scores of all six models on the first five datasets.

		Training set		Test set	
Dataset	Model	$\overline{MAE}$	σ_{RMSE}	$\overline{MAE}$	σ_{RMSE}
Abalone	M5	5.219e-02	5.356e-04	5.362e-02	2.982e-03
	M5E	5.213e-02	4.366e-04	5.336e-02	2.863e-03
	MTF	5.226e-02	5.886e-04	5.441e-02	3.696e-03
	NN	5.285e-02	1.163e-03	5.372e-02	2.687e-03
	RF	4.479e-02	3.839e-04	5.367e-02	1.995e-03
	SVR	5.623e-02	5.492e-04	5.952e-02	1.973e-03
Auto-MPG	M5	5.036e-02	2.912e-03	5.928e-02	1.098e-02
	M5E	4.806e-02	1.981e-03	5.609e-02	8.850e-03
	MTF	4.417e-02	1.608e-03	5.087e-02	8.830e-03
	NN	4.994e-02	2.678e-03	5.431e-02	8.388e-03
	RF	1.881e-02	6.244e-04	4.885e-02	9.064e-03
	SVR	5.264e-02	1.327e-03	5.546e-02	8.823e-03
Boston housing	M5	4.335e-02	3.814e-03	5.615e-02	9.564e-03
	M5E	3.819e-02	1.625e-03	4.852e-02	8.228e-03
	MTF	7.043e-02	7.255e-02	1.107e-01	2.004e-01
	NN	4.911e-02	8.328e-03	5.710e-02	1.202e-02
	RF	1.771e-02	4.883e-04	4.622e-02	7.893e-03
	SVR	1.142e-01	2.200e-03	1.157e-01	1.311e-02
California housing	M5	5.789e-02	4.628e-04	6.507e-02	1.809e-03
	M5E	5.262e-02	3.429e-04	5.895e-02	1.770e-03
	MTF	8.292e-02	6.408e-04	8.427e-02	2.005e-03
	NN	8.547e-02	2.272e-03	8.618e-02	2.198e-03
	RF	2.497e-02	1.359e-04	6.774e-02	1.806e-03
	SVR	7.969e-02	3.699e-04	8.170e-02	1.794e-03
CASP	M5	1.367e-01	9.483e-04	1.448e-01	1.921e-03
	M5E	1.236e-01	4.015e-04	1.319e-01	1.531e-03
	MTF	1.904e-01	7.091e-04	1.910e-01	1.991e-03
	NN	1.750e-01	3.913e-03	1.759e-01	4.199e-03
	RF	4.178e-02	1.414e-04	1.129e-01	1.960e-03
	SVR	9.292e-02	2.236e-04	1.283e-01	2.022e-03

Table D.4: Comparison of MAE scores of all six models on the second five datasets.

		Training set		Test set	
Dataset	Model	$\overline{MAE}$	σ_{RMSE}	$\overline{MAE}$	σ_{RMSE}
Elevators	M5	2.352e-02	2.097e-04	2.443e-02	5.393e-04
	M5E	2.305e-02	1.801e-04	2.370e-02	5.343e-04
	MTF	2.296e-02	4.652e-04	2.601e-02	2.240e-03
	NN	2.278e-02	1.025e-03	2.299e-02	1.148e-03
	RF	1.038e-02	5.122e-05	2.774e-02	7.475e-04
	SVR	8.113e-02	1.756e-04	9.329e-02	1.475e-03
Friedman artificial domain	M5	2.590e-02	1.281e-04	2.668e-02	2.380e-04
	M5E	2.503e-02	1.070e-04	2.558e-02	2.829e-04
	MTF	2.602e-02	2.043e-04	2.651e-02	4.477e-04
	NN	2.640e-02	5.235e-04	2.654e-02	6.117e-04
	RF	1.342e-02	4.193e-05	3.177e-02	4.490e-04
	SVR	8.831e-02	1.119e-04	1.280e-01	1.322e-03
Machine	M5	1.785e-02	2.572e-03	3.031e-02	1.275e-02
	M5E	1.629e-02	1.218e-03	2.661e-02	9.131e-03
	MTF	2.046e-02	1.862e-02	4.924e-02	1.361e-01
	NN	2.860e-02	5.488e-03	3.194e-02	1.060e-02
	RF	9.362e-03	6.196e-04	2.075e-02	9.790e-03
	SVR	8.210e-02	3.151e-03	8.145e-02	2.035e-02
MV artificial domain	M5	1.340e-04	2.736e-06	1.366e-04	4.974e-06
	M5E	1.214e-04	3.275e-06	1.239e-04	4.322e-06
	MTF	4.290e-04	1.163e-04	6.569e-04	8.871e-04
	NN	1.017e-03	1.033e-03	1.019e-03	1.034e-03
	RF	2.836e-04	2.629e-06	6.775e-04	1.805e-05
	SVR	3.523e-02	3.504e-04	3.525e-02	4.152e-04
Servo	M5	2.782e-02	7.868e-03	3.854e-02	1.061e-02
	M5E	2.782e-02	7.868e-03	3.854e-02	1.061e-02
	MTF	3.428e-02	3.759e-03	4.676e-02	1.521e-02
	NN	6.096e-02	9.931e-03	6.972e-02	1.851e-02
	RF	1.240e-02	1.130e-03	3.419e-02	1.482e-02
	SVR	7.038e-02	2.739e-03	7.271e-02	1.615e-02